APPLICATION OF UNMODIFIED ACTIVATED CARBON FOR REMOVAL OF ODOR FROM WASTEWATER TREATMENT FACILITIES

By

FOAD ADIB

A dissertation submitted to Graduate Faculty in Engineering in partial fulfillment of the requirements for the degree of Doctor of Philosophy, The City University of New York

Year 2000

Bell & Howell Information and Learning Company
300 North Zeeb Road
P.O. Box 1346
Ann Arbor, MI 48106-1346

This manuscript has been read and accepted for the Graduate Faculty in Engineering in satisfaction of the dissertation requirement for the degree of Doctor of Philosophy.

9/12/2000
Date

Professor Reza Khanbilvardi
Chairman of Examining Committee

9/12/2000
Date

Dean Mumtaz Kassir
Executive Officer

Dr. Teresa Bandosz

Dr. Amos Turk

Dr. John Fillos

Dr. Richard Birchwood

Supervisory Committee

THE CITY UNIVERSITY OF NEW YORK

Abstract

Application of Unmodified Activated Carbon for Removal of Odor from Wastewater Treatment Facilities

By

Foad Adib

Advisor: Professor Reza M. Khanbilvardi, Department of Civil Engineering, CUNY

Co-Advisor: Professor Teresa J. Bandosz, Department of Chemistry, CCNY and GCCUNY

Unmodified activated carbons (UAC) can be used to effectively remove H_2S, as the leading malodorant, from the air streams at the wastewater treatment facilities. Upon adsorption in pores of UAC, H_2S is immobilized through oxidation by oxygen to more stable elemental sulfur or sulfuric acid, which deposit in the pores of carbon. The general mechanism for the process includes initial chemisorption of both oxygen and hydrogen sulfide on the surface of carbon and the following surface reaction between the adsorbed species. Presence of a high level of humidity in the influent is a necessary condition for the process. The reactions take place in a thin film of water that forms inside the pores of carbon and serves as the reaction medium.

The surface pH of carbon has a dominant effect on the process. Unlike molecular H_2S, hydrosulfide ion can be easily oxidized. A pH value around 4.5, which is only high enough for mild dissociation of H_2S, is sufficient for its effective removal. The effect of

pore structure is not as vivid as surface chemistry in the performance of carbons, but carbons with higher pore volume, especially microporous volume, provide more removal capacity.

Oxidized carbons, despite their lower capacities, show a higher selectivity toward formation of sulfuric acid than UACs. Similar effect is observed when nitrogen is incorporated into the carbon. Nearly all of sulfuric acid and a lot of sulfur radical content can be removed by washing at ambient temperature. Oxidized carbons provide a benefit of oxidation-during-washing of the sulfur radicals whereas UACs generally give way to the formation of bulky insoluble polysulfides. The latter will permanently deposit in the pores and can not be removed by simple methods.

A rate expression is provided for the process based on the Langmuir-Hinshelwood surface reaction model. Sulfur deposition is introduced to the rate expression as the fouling factor and an expression is derived based on the initial rate of the reaction and the square of available sites. The model can effectively predict the performance of carbon and can be used to design a bed of carbon to withstand a certain situation.

Acknowledgements

My first and foremost gratitude has to be offered to my wife Marzie and my son Dara for eagerly coping with what must have seemed my middle-aged endless preoccupation with THE DOCTRATE!

I must acknowledge with deep appreciation the support and encouragement of my advisor Professor Reza M. Khanbilvardi. His good nature and generosity in providing every request for the necessities of my work are not forgettable.

I will always remain indebted to my co-advisor Professor Teresa J. Bandosz for her guidance and materialization of this effort. She outlined the methodology and repeatedly examined every step of the work including every note in this dissertation.

My gratitude is also presented to Professor Amos Turk for his continuous encouragement and scientific discussions. I am honored to have continued his pioneer work on this subject.

I thank Professor John Fillos, chairman of Civil Engineering Department for his support and assistance throughout my study. The participation of Professor Richard Birchwood in my graduation committee is appreciated.

I specially appreciate the scientific environment of activated carbon laboratory of Chemistry Department, which brought this research into reality. Every discussion in this study was concluded after hours of scientific discourse with Dr. Andrey Bagreev. The assistance from my lab co-workers Ms. Anna Kleyman and Mr. Issa Salame is appreciated.

Table of Contents

List of Tables

List of Figures

List of Figures (continued)

List of Figures (continued)

CHAPTER 1

INTRODUCTION

Problems associated with the removal of odors from air have become controversial issues in urban areas. The control of odor emitted from wastewater treatment facilities, especially in warmer seasons, constitutes a formidable technical and scientific challenge for engineers. One of the leading malodorants arising from sewage treatment facilities is hydrogen sulfide (H_2S) [1].

According to an air analysis performed by McGinley on 36 wastewater treatment plants, the odor and hydrogen sulfide data showed a good correlation over the range of air samples collected [2] (Figure 1). Statistical analysis of linear regression of the data showed correlation coefficients as high as 0.99. Other major components of odor include mercaptans (R-S-H) which share close chemical structures with H_2S. Hence, H_2S can be considered as a characterizing component of odor. Figure 2 presents a plot of ambient H_2S levels for a treatment plant measured on a grid system format. The resulting contour lines of H_2S concentration identify the most odorous processes of the treatment plant under study.

At concentrations as low as 8 parts per billion (ppb), H_2S can be detected by human nose. In parts-per-million (ppm) concentrations, H_2S is known to cause eye irritation, nausea and respiratory problems [2]. According to OSHA Regulations for Toxic and Hazardous Substances no measurable weighted average concentration of H_2S is allowed for an 8-hour shift. However, a once only exposure to a ceiling concentration

of 20 ppm with a maximum peak of 50 ppm above that is acceptable for a maximum of 10 minutes provided no other measurable exposure occurs [3]. The air quality regulations at most of the localities require the enforcement of the odor levels at the boundary of industry and sewage treatment plants effectively at a zero tolerance level (No odor detectable by an enforcement officer) [2].

Activated carbons are widely used as adsorbents for removing contaminants and pollutants from gaseous and liquid streams. Among the desirable properties of these materials are (a) a high surface area, which is the result of their microporosity, (b) strongly adsorbing surfaces, a result of the high density of carbon atoms on the surface and (c) the tailored catalytic activities due to the possibility of modifying the surface chemistry of these materials [4, 5].

One of the main environmental applications of activated carbons is sorption of H_2S and other odorous compounds from sewage systems [6-8]. Carbons impregnated with various reactive materials have been used for this purpose. H_2S can be fixed on the carbon surface as an insoluble sulfide by impregnating the carbon with the salt of a heavy metal such as copper sulfate or lead acetate. The presence of a toxic metal residue on the exhausted carbon, however, makes it a hazardous waste. Carbons impregnated with potassium iodide are also used for the purpose of odor removal. Another treatment includes impregnation of carbons with certain nitrogen compounds such as urea followed by calcination at high temperature [9], which incorporates basic nitrogen sites into a carbon matrix. Traditionally, caustic carbons have been widely used as H_2S adsorbents. Impregnation with sodium or potassium hydroxide enhances the kinetics of adsorption process for slightly acidic gases such as H_2S. The produced sulfide (S^{2-}) is then converted

to various oxidized compounds by interaction with oxygen in air [10]. The concurrent injection of a gaseous base such as ammonia into the polluted air stream is found to enhance the capacity of activated carbons for immobilization of H_2S and is currently used in New York City wastewater treatment facilities [6].

Activated carbons used for removal of H_2S from sewage treatment plants of New York City are generally impregnated with caustic materials such as NaOH or KOH [7]. Air currents around odor generating facilities are initially washed with chemicals in scrubbers, during which they intake high levels of humidity, and are then blown through activated carbon vessels. The residual H_2S quickly reacts with caustic and is immobilized. The presence of humidity facilitates the reaction [11, 12]. The fast kinetics of acid-base reactions promises the effective removal of H_2S and prevention of any leakages due to channeling effects.

Despite their efficiency and high capacity for removal of H_2S, caustic impregnated carbons have increasingly drawn major objections due to their disadvantages. The highly energetic reactions of caustic with carbon dioxide and water in the air lower the carbon's self-ignition temperature and increase the risk of *in situ* fire [8]. The dominance of fast acid-base reaction in the overall adsorption process does not allow for slower oxidation process. Hence, the oxidation of H_2S can only proceed to elemental sulfur [7, 13] rather than sulfates, which are not hazardous and may be washed away from the carbon surface. Consequently when the carbon is exhausted, it can not be regenerated by simple methods and should be removed and discarded or reactivated off-site. Economic aspects of production and handling caustic carbon should be added to these technical disadvantages.

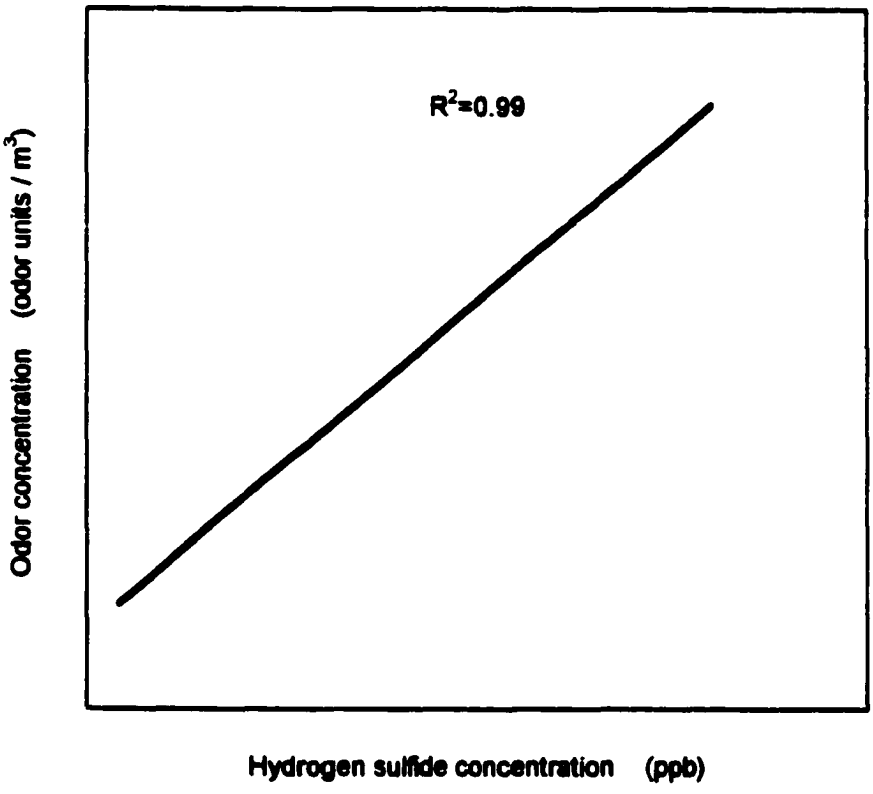

Figure 1. Correlation of hydrogen sulfide and odor for a typical wastewater treatment plant.
Source: McGinly, C.M. [2], With permission from author.

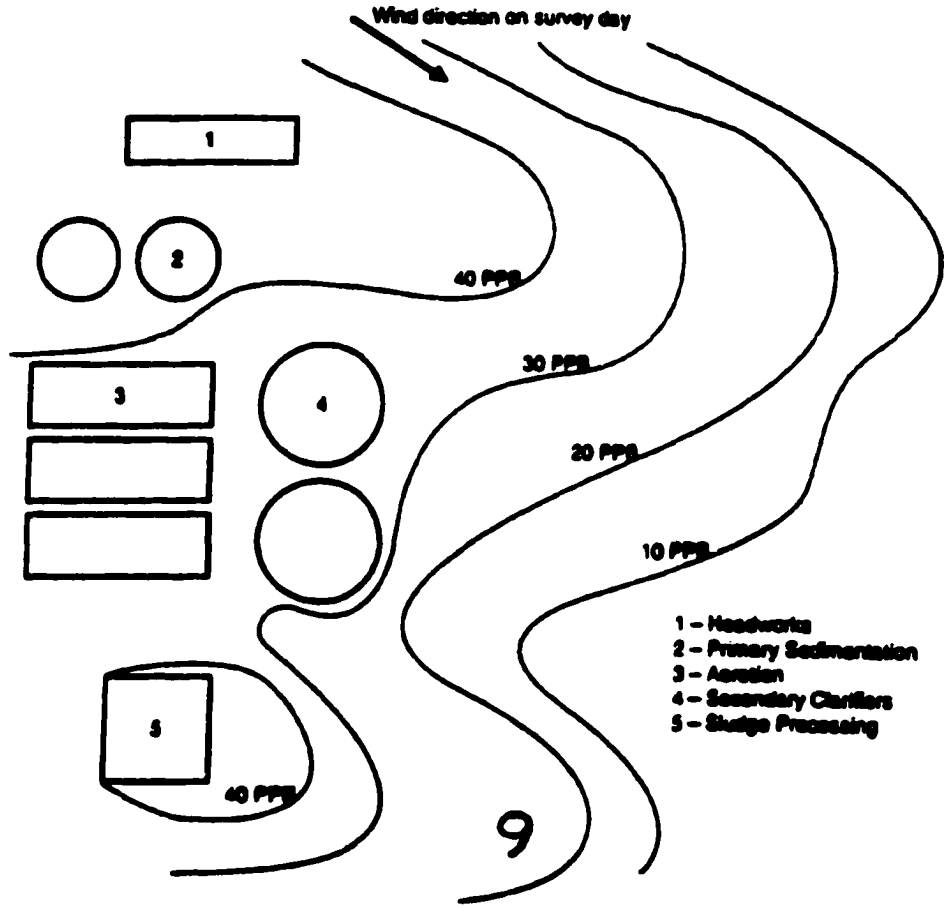

Figure 2. Ambient H_2S levels for a wastewater treatment plant.

Source: McGinly, C.M. [2], With permission from author.

In response to these concerns, attention was directed towards the application of unmodified activated carbon (UAC) for the removal of H_2S [9, 12]. UAC has the following advantages over the caustic and other impregnated materials [14, 15]:

1. Cost per pound is much lower since untreated carbons are less expensive than chemically modified.
2. Their capacity for physical sorption is high. Considerable volume of micropores is occupied by impregnants in caustic and other impregnated carbons rendering these micropores unavailable for physical adsorption.
3. Activated carbon can facilitate chemical transformations due to their unique surface features. These features include a high content of elemental sp^2-hybridized carbon exhibiting at least two-dimensional order; the ease with which they combine with other elements to form a variety of surface complexes; and the transient nature of their surface properties [5]. Clean carbon surfaces consist of (at least) two chemically different kinds of sites (i.e., basal and edge carbon atoms). Edge sites are very reactive, especially toward oxygen, since they contain single unpaired electrons. The schematic structure of activated carbon is shown in Figure 3. It is widely assumed that pores of activated carbons are created between parallel oriented graphite-like crystallites (slit-shape pores). At the edges of these crystallites, atoms other than carbon can be built into the activated carbon matrix [5, 16-18]. The most common heteroatoms are oxygen, hydrogen, nitrogen, and phosphorus [19]. Those atoms are arranged in the forms of common organic functional groups. The surface of UAC can contain at least five different types of surface oxygen groups (i.e., carboxylic, lactonic, phenolic, carbonyl, and etheric) [17, 18] (Figure 4). These groups provide

for coexistence of acidic and basic features as well as electron receiver and donor sites in a carbon, which can facilitate an extended spectrum of chemical reactions. Hence, the surface of UAC with incorporated heteroatoms can act as a catalyst for oxidation of H_2S.

4. The deposition of other compounds like inorganic salts , besides sulfur or sulfur acids, is limited. UAC provides a higher selectivity toward the formation of sulfur oxides [19, 20].
5. Sulfur acids are highly hydrophilic and may be washed away while sulfur deposits may be removed by desorption at a moderate temperature in an effort to regenerate the exhausted carbon [20, 21].

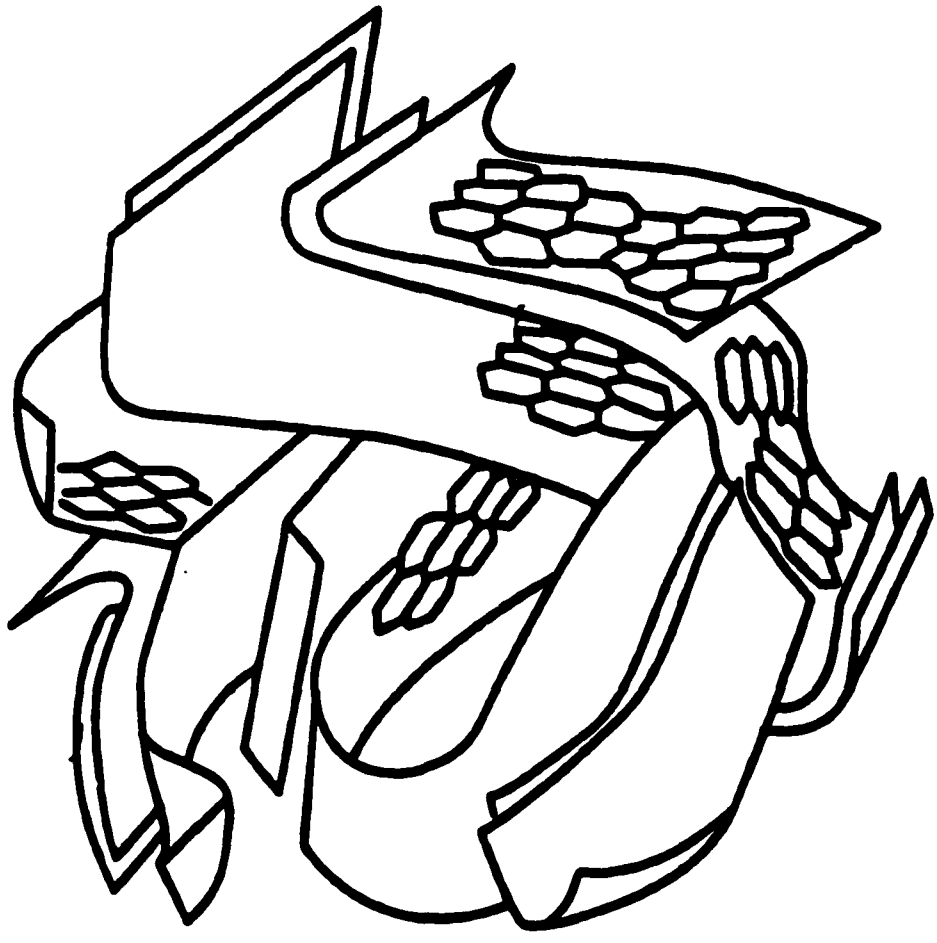

Figure 3. Schematic structure of activated carbon.

Source: J. B. Donnet et al., The Observation of Activated Carbons by Scanning Microscopy *Carbon* 1994, 32, 183

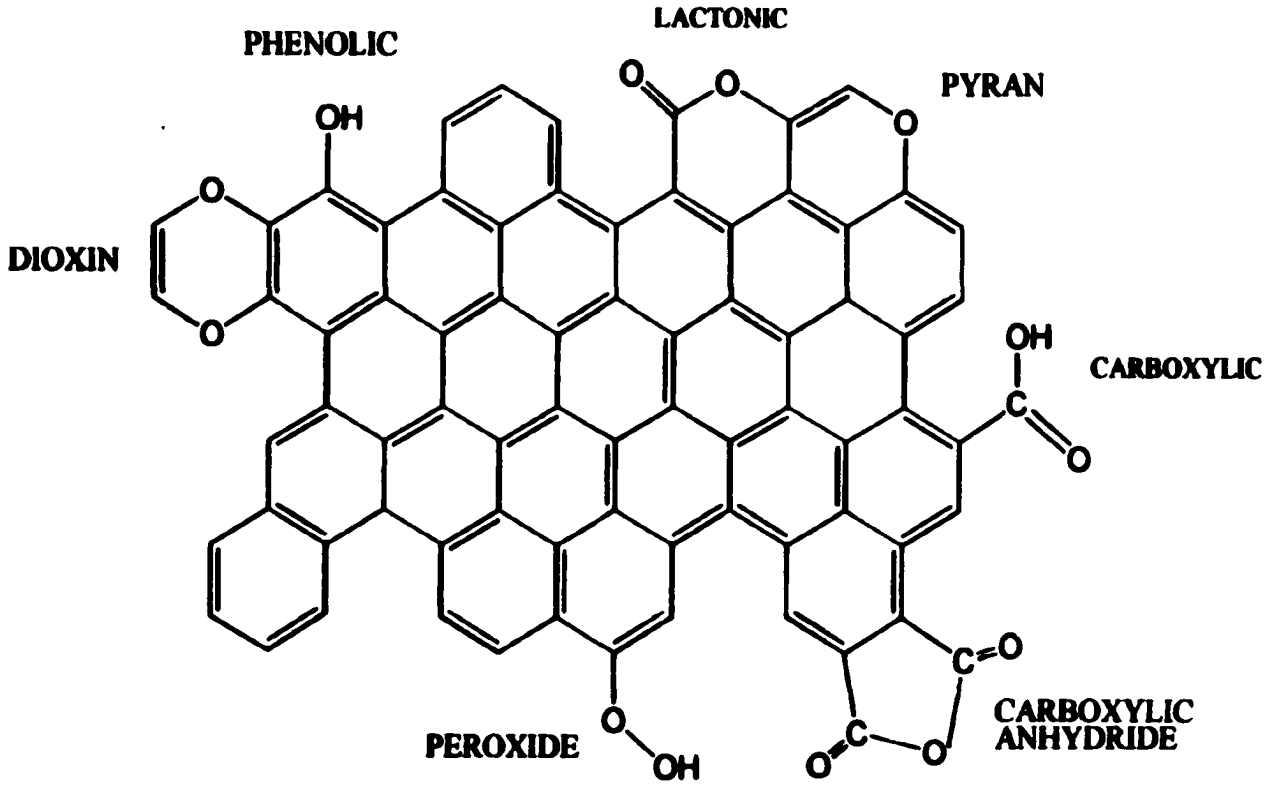

Figure 4. Main Types of oxygen surface groups in activated carbon.

The application of UAC for removal of H_2S from air has been investigated as early as the 1960s [22-29]. Hydrogen sulfide in natural gas is usually extracted in a sweetening plant and converted to elemental sulfur by the Claus process [21]. When the concentration of H_2S in the gas is below 10 % the Claus process is not economical. In that case, very low concentrations of H_2S (i.e., 300-3000 ppm), were usually extracted and flared as sulfur dioxide to the atmosphere [22, 30]. The tightening of the regulations with respect to sulfur dioxide emissions and the search for more efficient sulfur recovery techniques [31] led to major research in this field. An alternative method for removal of relatively low concentrations of H_2S from sour natural gas using direct oxidation by the oxygen in the air in the presence of catalysts such as activated carbon was introduce in the late 60s [32].

Considerable removal capacities have been reported for carbons at temperatures ranging from 20 to above 300 °C and with H_2S concentration varying from 2 to 20000 ppm. Most researchers agree that below 100 °C the effect of humidity is crucial [14, 22]. Above 100 °C the physical adsorption of water is insignificant owing to its very low partial pressure. The reactions, therefore, in most cases may be assumed to take place under dry conditions. According to Steijn and Mars [22] who performed series of experiments in the temperature range 130-200 °C, the selectivity towards sulfur was more than 90 %: the formation of sulfur dioxide and sulfate on the catalyst was negligible. Addition of excess water to the feed did not change the conversion of H_2S on an activated carbon catalyst at 150 °C. Their proposed reaction for the conversion is [22]:

$$2\,H_2S + O_2 \rightarrow \tfrac{1}{4}\,S_8 + 2\,H_2O \qquad (1.1)$$

The authors emphasized that the radical pathways are responsible for the oxidation process. They claimed that sulfur trapped in the micropores acts as a catalyst for further oxidation of H_2S; the catalytic activity of carbon is closely related to the degree of micropore filling; and materials containing pores with a radius close to 10 Å are considered as efficient catalysts. Steijns and Mars proposed, based on the work of other investigators [33, 34], that sulfur in micropores of the size 4 to 10 Å is present as long-chain biradicals that can catalyze cracking reactions as well as the oxidation of H_2S. It is noteworthy that in their earlier work [22] they only considered the effect of microporosity and did not attribute any role to the chemical features of the carbon surface [i.e., surface functional groups]. One reason for that may be the dry condition of the experiments, which renders these groups inactive. Other researchers, however on the contrary, suggested that, in the same temperature regions, the surface oxygen groups of activated carbon are the active sites where the oxidation proceeds while the size of the pores plays an important (but secondary) role in the process [35]. Contrary to the findings of Steijns and Mars, it was reported that the sulfur deposited in coconut-shells based activated carbon had no catalytic activity [36].

Continuing the study of H_2S removal, Steijns et al. performed a series of experiments using several catalysts including activated carbon for oxidation of H_2S in the temperature range 20-250 °C under dry condition [37, 38]. They provided further evidence through electron spin resonance studies for their earlier claim that radical pathways were the main conduits of the process and sulfur biradicals were the active species in the transformations. Two new factors were added to the analysis based on the

work of other researchers [39]. It was proposed that H_2S and molecular oxygen are initially *dissociatively chemisorbed* and then interact on the carbon surface. Although this proposition might suggest that some degree of surface chemical features of activated carbon is involved in the chemisorption process, only the formation of radicals is intended. Steijns and co-workers suggest that the dissociation and chemisorption is strictly the result of the interaction of molecular species with the sulfur biradicals already present in the micropores and not the product of interaction with the carbon surface. In another study based on the results of experiments performed in the temperature range 20-150 °C, Steijns et al. concluded that in the mechanism of H_2S oxidation on activated carbons, carbon radicals do not play an important role [38]. The issue of surface chemistry and the role of water were addressed when series of experiments were carried out at 200 °C and in the presence of varying amount of humidity in the feed. In these experiments activated carbon as well as other materials such as zeolite, silica, alumina, and several metal oxides were used as adsorbents [40]. It was reported that admixing of water led to a decrease of activity and selectivity (for sulfur) especially in the case of wide-pore (>10 Å) alumina and silica. This effect was small in microporous activated carbon and zeolite. It was also observed that the activity of alumina was always higher than that of silica, even when silica with a small average pore diameter was used. This difference in sulfur adsorption behavior was attributed to the presence of Lewis acid sites at the surface of the alumina and their absence on silica. It was concluded that the adsorption of sulfur was enhanced by the interaction between the *Lewis base sulfur* [radical] and the *Lewis acid centers*, i.e., aluminum ions at the surface. As for the water effect they suggested that in the microporous materials such as activated carbons and

zeolites the strong adsorption of sulfur was especially caused by the small average pore diameter. Hence, water had only a small effect on the rate because the chemical composition of the surface was only a secondary factor in the sulfur adsorption. Although the investigation of Steijns and co-workers was limited to certain conditions of the process it, undoubtedly, summarized more than a decade of research on the subject and opened up new lines of work.

By early 1980s, the capability of activated carbon for immobilization of H_2S; the importance of small micropores (pores under 10 Å); and the general mechanism leading to the formation of elemental sulfur in the H_2S adsorption/oxidation process were well established. But the fundamental issue of the role of carbon surface chemistry in the process was not considered yet and contradictory views existed on the effect of water. Little was known with certainty about the mechanism of the H_2S oxidation in air on activated carbon surface in the presence of humidity and in ambient temperature [22]. Parallel to the further tightening of the odor regulations, research on the application of adsorbents for odor removal became an independent branch. Previously, environmental applications of H_2S adsorbents were largely shadowed by the industrial usage primarily for recovery of sulfur from natural gas. Such a usage predetermined the conditions and the directions of research. For example, prior to 1980, small attention was focused on the application of activated carbons for removal of H_2S in air at ambient temperature and humid conditions, typical of odorous air at wastewater treatment plants.

Coskun and Tollefson [41] performed a series of experiments using activated carbon for removal of H_2S from air in the temperature range 24-200 °C. Although they used the conditions of experiments for purifying natural gas (high concentration of H_2S

and high temperature), their work was unique in using air as the feed. Prior to that most workers used a mixture of H_2S, oxygen and an inert gas for feed. It was suggested that at temperatures below 100 °C, the water produced during the oxidation reaction would deposit on the carbon active sites and contribute to the fouling of the catalyst and lowering the activity. Hence, it was concluded that the activity of the carbon depends strongly upon the temperature and the sulfur loading. These findings were in contradiction with earlier analysis by Steijns and Mars [22] based on the work of Storp [42]. Steijns and Mars had suggested that "the oxidation of H_2S may proceed in the liquid phase (water). An indication of this is the fact that below 50 °C a complete exhaustion of the H_2S by active carbon is only possible if the introduced gas has a relative humidity of at least 60%".

Kaliva and Smith [11] studied the performance of UAC for the removal/oxidation of low concentration of H_2S in air with varying humidity at room temperature. They suggested that the presence of water vapor, under the experiment conditions, enhances the oxidation of H_2S by air. In an effort to model the oxidation process they assumed that the only reaction occurring in the temperature range 20-50 °C is the formation of elemental sulfur according to Equation 1.1, and catalyst fouling results from the depletion of the carbon active sites by sulfur deposition. They did not consider the effect of carbon surface chemistry. They did however suggest, from their observation of the humidity effect, that there was the possibility of formation of a complex between adsorbed oxygen and water and the subsequent reaction between the complex and the adsorbed H_2S.

Klein and Henning [26] emphasized that the formation of a water film on the surface of the carbon at low temperatures is an essential condition for the proceeding of

the reaction. They reaffirmed the mechanism initially proposed by Hedden et. al. [27] for oxidation of H_2S in the water film on the surface of activated carbon:

$$O_2 \rightarrow O + O \qquad (1.2)$$

$$H_2S \rightarrow HS^{\cdot} + H^{\cdot} \qquad (1.3)$$

$$HS^{\cdot} + O \rightarrow S + OH^{\cdot} \qquad (1.4)$$

The produced sulfur is deposited in the activated carbon. Their work was new in that they pointed out the formation of *sulfuric acid* as a side reaction in the presence of humidity:

$$H_2S + 2\ O_2 \rightarrow H_2SO_4 \qquad (1.5)$$

Since no evidence of sulfur dioxide was observed and none of the researchers had reported its formation under similar conditions, the authors concluded that SO_2 acted as an intermediate product.

Thus, the application of activated carbon for removal of H_2S from gas streams was well researched for industrial uses at high temperatures. Effort was underway to model the process rate and activity of carbons. Ghosh and Tollefson [27, 43] studying the results obtained for the oxidation of H_2S over activated carbon in the temperature range 125-200 °C, developed a model based on the *Langmuir-Hinshelwood* surface reaction model. They used the general oxidation mechanism of H_2S proposed by Steijns and Mars [22](Equation 1.1) with several new assumptions. They assumed that the surface reaction

between the adsorbed H_2S and oxygen is the rate-limiting step. By this they excluded the physical effects such as adsorption, external mass transfer resistance, and intra-particle or pore diffusional resistance in the rate expression. They also assumed that the entire sulfur produced in the reaction at the unsteady state (fouling) deposits in pores causing deactivation of the catalyst. The effect of *residence time* was also addressed in their work. It was reported that an increase in conversion occurs with an increase in residence time. This finding was attributed to the fact that there could be more surface available per gas molecule providing an increased number of collisions of the molecules with the surface. This enhanced the rate of reaction of the molecules.

In their work, however, Tollefson and co-workers reiterated that the mechanism of the reaction in the presence of water, below 100 °C is not well established. Hence, the application of UAC could not be recommended for odor removal yet. The major difficulty seemed to lie with the fact that it was not known why carbons perform so differently for removal of H_2S in ambient temperature and what properties in activated carbon govern the reaction. In lieu of such a shortcome, impregnated activated carbons, in which catalysis was safely controlled by added materials, were adopted for odor removal applications and the use of UAC experienced a major setback. Consequently, research was diverted towards the use of impregnated carbons and methods of modification and several patents were granted for modified activated carbons used for odor removal purposes [9, 44-47].

Turk et al., proposed that side stream of ammonia injection enhances the capacity of UAC for H_2S and methyl mercaptan removal [6]. Their work included results of full-scale experiments performed at a New York City wastewater treatment plant in which

application of UAC (with ammonia side stream) was compared with a conventional caustic carbon. It was shown that UAC could adsorb 3 or more times H_2S more than caustic carbon. The end product was reported to be predominantly elemental sulfur in the case of UAC with ammonia while caustic carbon was suggested to have contained bulky alkali sulfides, sulfites, sulfates, and possibly carbonates. The difference in capacity was attributed to the filling of the pores with smaller elemental sulfur in UAC and bulky compounds in caustic carbon [6].

The surface chemistry of carbon could not play a role in the presence of dominant ammonia activity that would govern the mechanism. Nevertheless, following this work, the application of UAC in New York City wastewater treatment plants was adopted later. Based on the results provided from the full scale tests it was later shown that UAC is capable of competing with caustic carbons and may even perform superior in longer applications[48].

The work of Bandosz in 1999 [49] addresses the combined role of surface chemistry and porosity of UAC in removal of hydrogen sulfide. Material evidence on the effect of surface oxygen groups and the importance of water in the process was provided. The difference in activity of carbons and selectivity of oxidation products (elemental sulfur or sulfuric acid) were investigated.

The objectives of the present research may be summarized as follow:

1. To identify the surface features of unmodified activated carbons (UAC) of different origins that are important for their performance as adsorbents of hydrogen sulfide (H_2S).

2. To provide a mechanism for the adsorption/oxidation of H_2S based on the surface properties of UAC.
3. To investigate the possibility of in situ regeneration of the exhausted carbon by simple methods such as washing at close to ambient temperatures.
4. To predict the performance of UAC beds as adsorbents of H_2S.

CHAPTER 2

EXPERIMENTAL

2.1. Materials

Preparation: Activated carbons from three different origins were chosen for this study. The first sorbent, RB3, was a peat based, pellet shaped carbon, manufactured by Norit Americas Inc. The second, S208c, supplied by Waterlink Barnebey Sutcliffe, was a granular activated carbon obtained from coconut shell. Each carbon was washed in a Soxhlet apparatus to a constant pH of the leachate to remove the water-soluble impurities and then dried in oven at 120 °C. These initial samples were referred to as N (Norit) and S (Waterlink Barnebey Sutcliffe).

To broaden the spectrum of the materials to account for variation in surface chemistry and porosity, the initial samples were oxidized with 15M nitric acid with a ratio of 5 mL of acid per gram of carbon at room temperature. Then the carbons were washed, dried, and designated as N1 and S1. Two other oxidized samples were prepared using a saturated solution of ammonium persulfate as an oxidant in 1M sulfuric acid at a ratio of 10 mL per gram of carbon at room temperature. These samples were referred to as N2 and S2.

The third choice was wood based activated carbons. Three different carbons from the same origin were chosen to include the effect of variations in surface chemistry and pore structure. These were activated carbons manufactured by Westvaco (H_3PO_4

activation): Bax-1500, WVA-900, and WVA-1100. These carbons were washed and dried similarly and respectively designated as W1, W2, and W3.

Modification: Two samples of W1 were impregnated with urea (saturated solution) and heated in nitrogen at the rate of 10 °C /min, one sample to 450 °C and the other to 950 °C and maintained at these temperatures for 0.5 hour in order to introduce nitrogen groups. After modification the samples were water-washed to remove any excess of urea decomposition products. The modified carbons are referred to as W1u450 and W1u950. Another sample used for experiments is a commercial carbon modified with urea manufactured by Calgon Carbon, Centaur® [9, 46].

2.2. Methods

H_2S breakthrough capacity

Moist air (relative humidity 80 % at 25 °C) containing 0.3 % (3000 ppm) H_2S was passed through a column of carbon (length 370 mm, diameter 9 mm) at 0.5 L/min at room temperature (Figure 5). The column was widened at the top 60 mm to a diameter of 23 mm to minimize the wall effect. The total volume of the bed was 45.0 cm^3. The H_2S emission was monitored by an Interscan LD-17 H_2S continuous monitor system interfaced with a computer data acquisition program. The test was stopped at a breakthrough concentration of 500 ppm. The breakthrough capacity of carbon was then calculated using the integrated area above the breakthrough curve (difference between inlet 3000 ppm and breakthrough concentration curves), the mass of carbon and flow rate.

Figure 5. Schematics of the apparatus used for the breakthrough test.

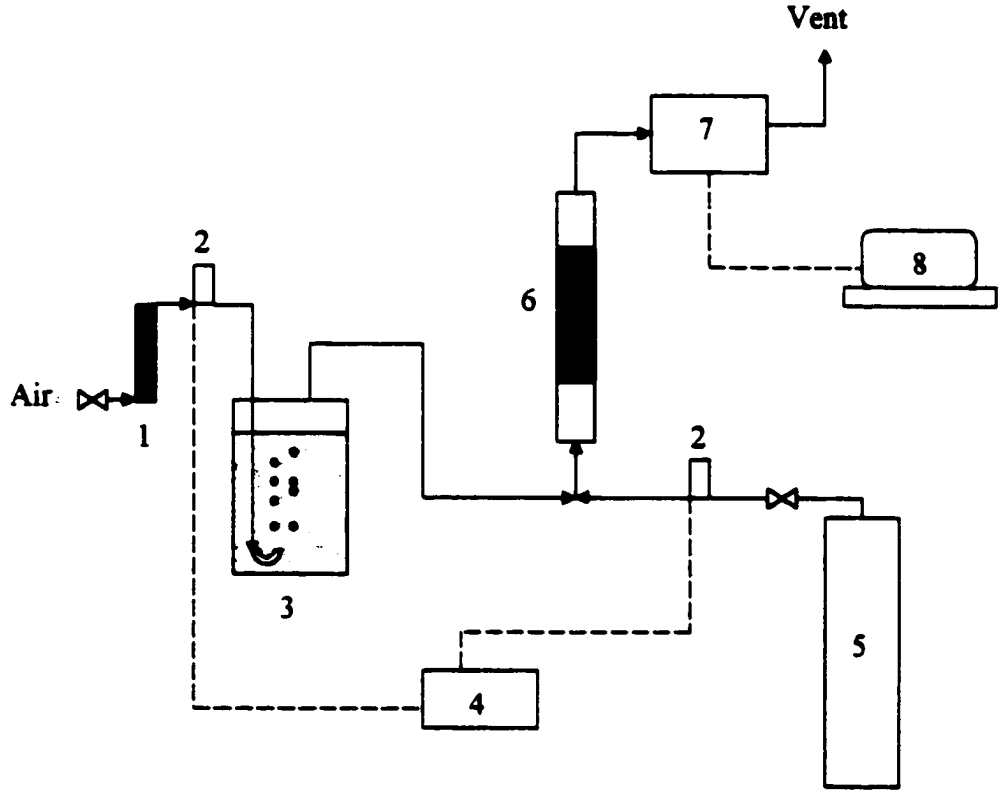

1. Air filter
2. Mass flowmeter
3. Bubbler (humidifier)
4. Flow controller
5. H_2S cylinder
6. Carbon column
7. H_2S concentration sensor
8. Computer (data acquisition)

→ Flow lines

-- Wire lines

⋈ Valve

The tests were repeated at least 3 times. The exhausted carbons (after adsorption of H_2S) were designated with addition of letter E to their names (e.g., SE, NE, or W1E).

Kinetic studies

Crushed carbon particles sieved in the range of 100-300 μm were used for kinetic studies. Carbon particles were placed in a 9 mm jacketed glass column between two thin layers of glass wool. The reaction temperature was maintained at 20± 0.1°C throughout the experiment using a water bath recirculating water in the jacket. Airflow of 100±1 mL/min containing varying concentration of H_2S was applied to the carbon to explore the effect of H_2S concentration on the rate of reaction. For the effect of residence time, the carbon's weight was varied while the flow was kept constant. The tests were stopped at a breakthrough concentration of 500 ppm. The rate of reaction was calculated as the amount of H_2S adsorbed per unit time in any time interval. The adsorbed amount of H_2S was calculated from the breakthrough curve, weight of carbon, and the flow rate.

Regeneration of exhausted carbons

3.0 grams of the exhausted carbons were washed in a Soxhlet appratus to a constant pH. These Soxhlet-regenerated carbons were defined with addition of letter S (e.g., SS, NS, or W1S). Alternatively, the same amount of W1E was heated up at 150 °C under an airflow of 100 mL/min for 5 hours for desorption of the deposited sulfur compounds. This heat treated sample was referred to as W1Eheated.

Boehm titration

The oxygenated surface groups were determined according to the method of Boehm [18] which includes series of consecutive back-titrations of carbon slurry in solutions with different acidic activities. One gram of carbon sample was placed in 50 mL of the following 0.05M solutions: sodium hydroxide, sodium carbonate, sodium bicarbonate and hydrochloric acid. The vials were sealed and shaken for 24 h and then 5 mL of each filtrate was pipetted and the excess of base or acid was titrated with HCl or NaOH. The numbers of acidic sites of various types were calculated under the assumption that NaOH neutralizes carboxyl, phenolic, and lactonic groups; Na_2CO_3 - carboxyl and lactonic; and $NaHCO_3$ only carboxyl groups. The number of surface basic sites was calculated from the amount of hydrochloric acid that reacted with the carbon.

Potentiometric titration

Potentiometric titration measurements were performed with a DMS Titrino 716 automatic titrator (Metrohm). The instrument was set at the mode when the equilibrium pH was collected. Subsamples of the carbons of about 0.100 g in 50 mL 0.01 M $NaNO_3$ were placed in a container maintained at 25 °C and equilibrated overnight with the electrolyte solution. To eliminate the influence of atmospheric CO_2, the suspension was continuously saturated with N_2. The carbon suspension was stirred throughout the measurements. Volumetric standard NaOH (0.1M) was used as titrant. The experiments were done in the pH range of 3-10. Each sample was titrated with base after acidifying the carbon suspension. The titration curves were then transformed into proton binding isotherms Q(pH), by using the proton balance equation [50]. It was assumed that the

system consists of acidic sites characterized by their acidity constants, K_a. The fraction of sites which are protonated at a certain pH, q(pH, pK_a), depends on their pK_a value according to the following form of the Langmuir equation

$$q(pH, pK_a) = [1 + 10^{(pH - pK_a)}]^{-1} \quad (2.1)$$

The population of sites can be described by a continuous pK_a distribution, $f(pK_a)$. The *proton binding isotherm*, Q(pH), incorporating the experimental results and representing the total amount of protonated sites is related to the pK_a distribution by the following integral equation

$$Q(pH) = \int_{-\infty}^{\infty} q(pH, pK_a) f(pK_a)\, dpK_a \quad (2.2)$$

The integral is solved numerically using SAIEUS procedure [51].

pH of carbon surface

A sample of 0.4 g of dry carbon powder was added to 20 mL of deionized water and the suspension was stirred overnight to reach equilibrium. Then the sample was filtered and the pH of the solution was measured.

Thermal analysis

Thermal analysis was carried out using TA Instruments Thermal Analyzer. The instrument settings were: heating rate 10 deg/min and either air or nitrogen atmosphere

with 50 mL/min flow rate. Three sets of data were collected with respect to temperature. These are weight (TG), derivative of weight (DTG), and temperature difference (DTA) between the sample and the blank scale. The latter provides information about the type of reaction (exothermic or endothermic) that is taking place at a specific temperature. Exothermic reactions appear in DTA curve as peaks whereas endothermic reactions appear as valleys.

Temperature Programmed Desorption

Temperature programmed desorption (TPD) was conducted on a Pulse ChemiSorb 2705 (Micromeritics) using helium as a carrier gas. The dried carbon samples of about 0.2 g were placed in a U-shaped quartz reactor and heated at 120 °C for 3 hours under a helium flow (40 mL/min). Then the flow was changed to 18 mL/min and after the baseline stabilized the temperature was raised to 1000 °C at a rate of 10 deg/min. The decomposition products of surface oxygen-containing groups (CO, CO_2, and H_2O) were measured by a thermo-conductivity detector. Three series of experiments were carried out for each carbon sample in order to distinguish the products of desorption. In the first step, the combined amount of CO, CO_2 and H_2O was determined. In the second step, the TPD curve for CO was measured using a cold trap with liquid nitrogen (-196 °C) located before the detector. Then the curve representing CO and CO_2 was recorded using a cold trap with dry ice (-78.5 °C). The instrument was calibrated by injection of precise volumes of the pure gases (CO and CO_2).

Sorption of nitrogen

Nitrogen isotherms were measured using an ASAP 2010 (Micromeritics) at −196 °C. Before the experiment the samples were heated at 120 °C and then outgased at this temperature under a vacuum of 10^{-5} torr to a constant pressure. The BET surface area was calculated from the isotherms by assuming a monolayer surface coverage, knowing the cross section of one molecule of nitrogen gas. The isotherms were used to calculate the specific surface area, S_{N2}, volume in pores smaller than 5Å, $V_{<5Å}$, volume in pores smaller than 10Å, $V_{<10Å}$, micropore volume, V_{mic}, volume of mesopores, V_{mes}, and total pore volume, V_t . All of the above parameters were calculated using Density Functional Theory (DFT) [52, 53]. This method is based on the assumption that the experimentally observed isotherm can be expressed as the sum of the convolution of a kernel function (local isotherm), representing the isotherm of an ideal homoporous adsorbent with a frequency distribution of pore sizes

$$X(p) = \sum_i x(p, H) f(H) \qquad (2.3)$$

Where X(p) is the experimental isotherm expressed as cm^3 STP g^{-1}, x(p, H) is expressed as cm^3 STP m^{-2} and $f(H)$ is the distribution of pore areas as a function of pore width H.

Sorption of water

Water sorption experiments were carried out at 20 °C using Micromeritics ASAP 2010 with a vapor sorption kit. The instrument was equipped with a home made thermostatted system controlled by a Fisher Scientific Isotemp Refrigerated Circulator.

Samples were first heated at 120 °C and outgased to 10^{-5} torr. HPLC grade water used as an adsorbate was free of any dissolved gases. Using ASAP 2010 one is able to measure water uptake starting from very low relative pressure ($p/p_o \sim 10^{-3}$) [12, 53, 54]. Each point of the isotherm was recorded after equilibrium was reached. The isotherms were measured to a relative pressure of about 0.3.

Ion chromotography

Approximately 3 grams of the exhausted sample was washed with 300 mL of distilled water in a Soxhlet apparatus for 24 hours. The concentration of sulfate ion in the leachate was measured by ion chromatography using a Dionex 4500I model with AS9-SC ion exchange resin column. Calibration was initially carried out by several standard solutions containing known concentrations of potassium sulfate. The leachate samples were diluted to render accuracy within ±1 mg/L range. Each reading was repeated at least once to establish the reproducibility of the results within ±1 mg/L range.

FTIR

IR spectra were collected using a Nicolet Impact 410 FT-IR spectrometer equipped with a diffuse reflectance unit. The instrument resolution was set at 4 cm^{-1}. Carbon powder was placed in a micro-sample holder. Before each measurement, the instrument was run to establish the background, which was then automatically subtracted from the sample spectrum. In each case at least three samples were run for comparison. The intensity was collected in Kubelka-Munk units.

Sulfur analysis

The content of sulfur in the initial, exhausted, and regenerated carbons was measured by Huffman and Galbraith Laboratories based on ASTM D-4239 Section 3.3 (high temperature combustion IR detection at 1350 °C).

Elemental analysis:

The content of carbon, hydrogen, and nitrogen was determined by Huffman Laboratories, Golden CO.

CHAPTER 3

RESULTS AND DISCUSSION

3.1. H_2S Breakthrough Capacity

The H_2S breakthrough curves for all nine carbons studied are shown in Figures 6-8 (A). Although the adsorbent volume was constant the tested samples varied in weight due to the variation in densities. H_2S adsorption isotherms showing the adsorption capacity (mg H_2S/g of carbon) against the emission concentration are collected in Figures 6-8 (B). Analysis of the H_2S capacities at emission concentration equal to 500 ppm (Table 1) reveals considerable differences in the performance of carbons. The N and S carbons show similar capacities (96±5 and 112±4 mg/g respectively) whereas W1 and W3 render much higher capacities (295±8 and 238±10 mg/g respectively). In the case of W1 carbon, 30 minutes of pre-humidification was necessary to fully develop the removal capability without which carbon showed negligible removal capacity. The capacities for S1 and S2 and W2 are the lowest (15±2, 12±1, and 16±1 mg/g respectively). It is evident that in N and S series of carbons, oxidation with either nitric acid or ammonium persulfate significantly reduces the capacity. This effect is more severe in S series. In both series, ammonium persulfate oxidation caused the most adverse effect on the capacity.

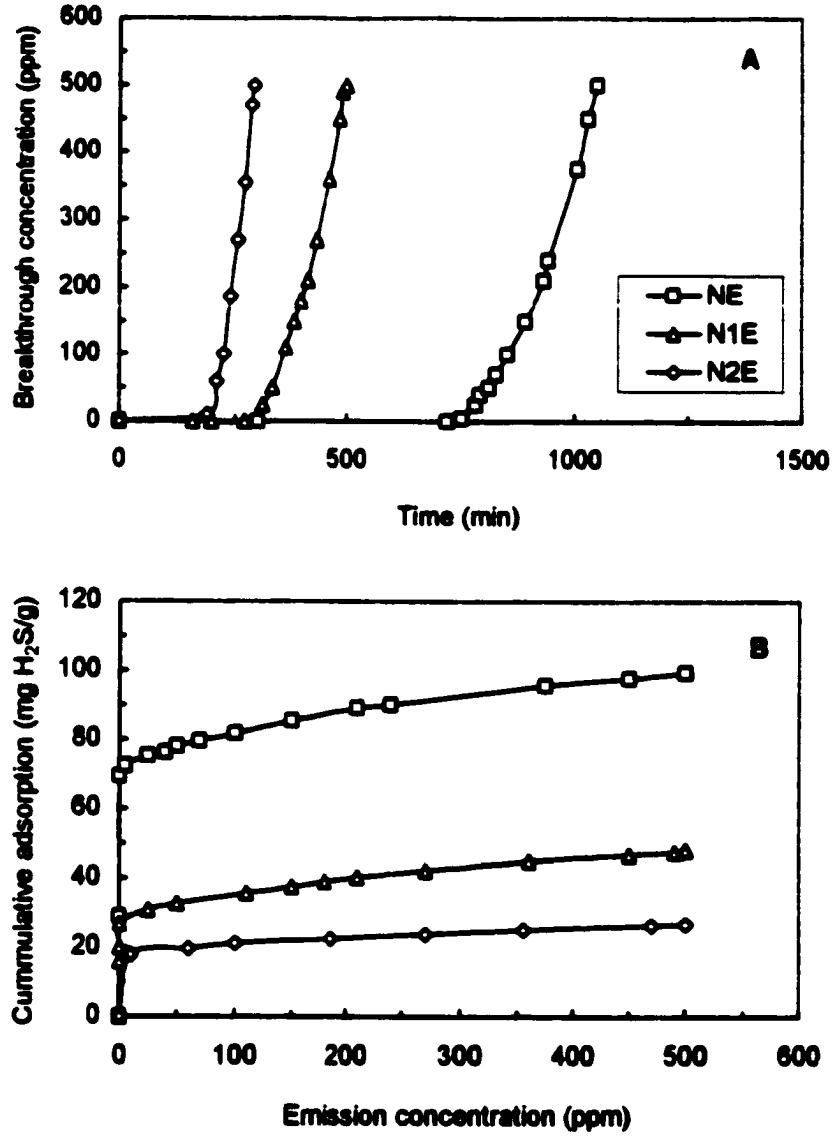

Figure 6. Breakthrough curve (A) and Adsorption curve (B) for N series.

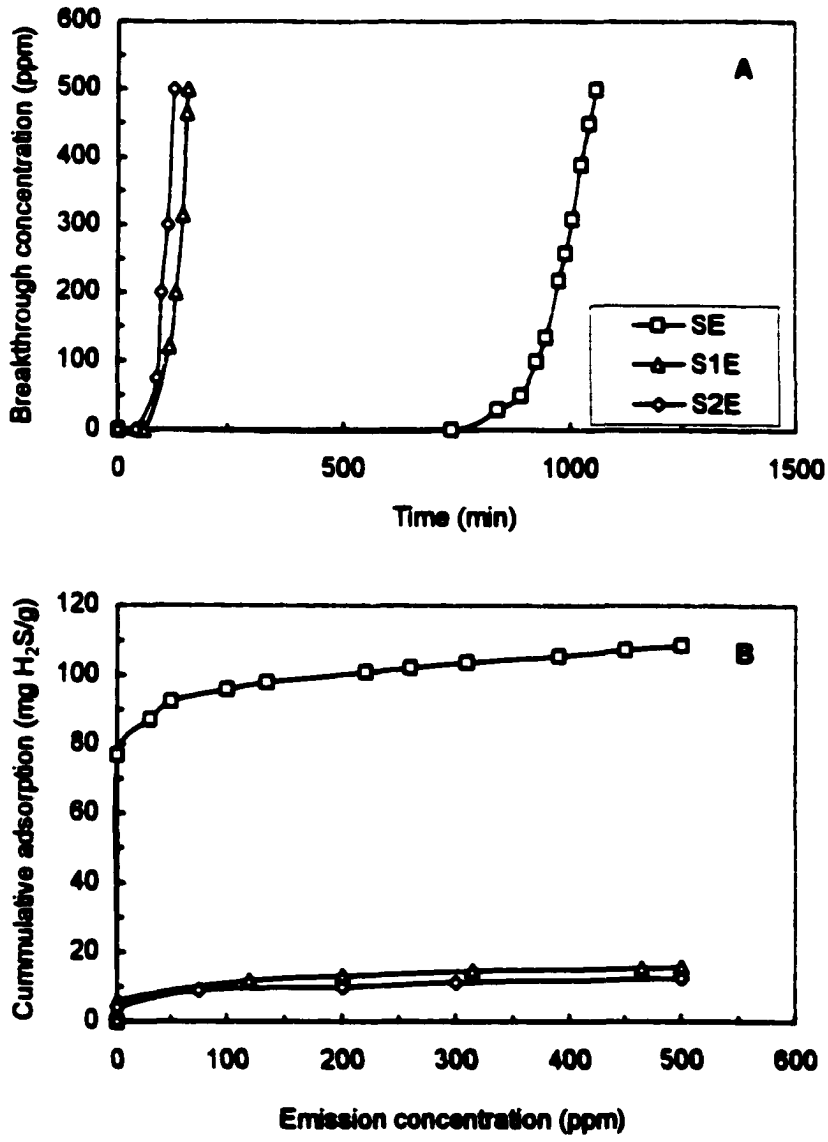

Figure 7. Breakthrough curve (A) and Adsorption curve (B) for S series.

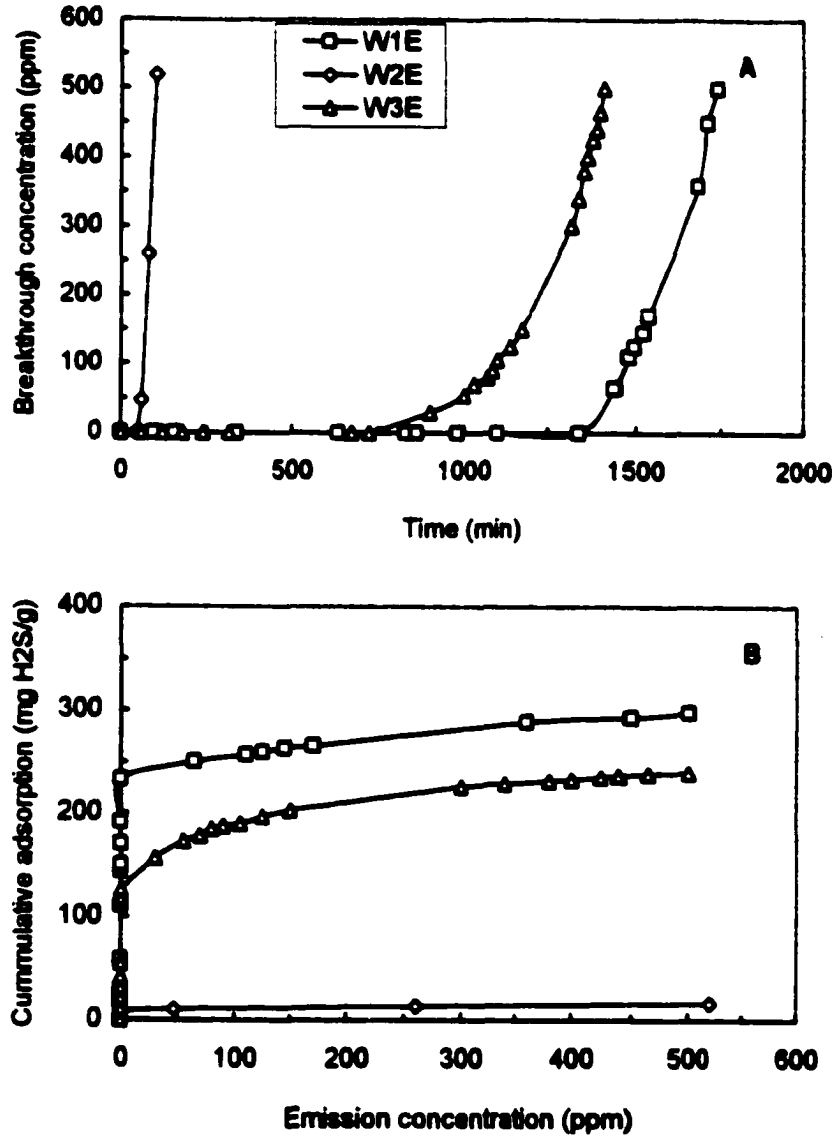

Figure 8. Breakthrough curve (A) and Adsorption curve (B) for W series.

Table 1. Results of Surface Chemistry Analysis and Breakthrough Capacity

Sample	H_2S Capacity	Functional Groups						Surface pH
		Carboxylic	Lactonic	Phenolic	Acidic	Basic	All	
	mg/g C	[meq /g]	[meq /g]	[meq /g]	[meq /g]	[meq /g]	[meq /g]	
N	96±5	0.000	0.125	0.000	0.125	1.000	1.125	7.72
N1	48±1	0.315	0.410	0.325	1.050	0.450	1.500	4.47
N2	28±2	0.557	0.808	0.334	1.699	0.490	2.189	3.59
S	112±4	0.175	0.025	0.125	0.325	0.513	0.838	6.89
S1	15±2	0.288	0.325	0.350	0.963	0.263	1.226	4.58
S2	12±1	0.650	0.425	0.650	1.725	0.125	1.850	3.66
W1	295±8	0.300	0.388	0.425	1.113	0.125	1.238	4.41
W2	16±1	0.340	0.373	0.538	1.251	0.100	1.351	4.04
W3	238±10	0.250	0.375	0.413	1.038	0.325	1.363	5.61

3.2. Analysis of the Surface Chemistry of Activated Carbon

In an effort to find a correlation between the performance of a carbon and its surface characteristics, the detailed analysis of carbons was carried out with emphasis on the features important for the sorption process such as surface chemistry and structural parameters. The results of surface pH measurements are included in Table 1. The analysis of the data within series (N, S, or W) shows a direct (but not linear) relationship between the H_2S removal capacity of the carbon and its surface pH. The samples associated with higher pH values within a series demonstrated higher removal capacities. This suggests that basic and mildly acidic surfaces promote the H_2S adsorption capacities while more acidic surfaces (below pH equal to 4.0) suppress the capacity. Although following the same pattern, this effect is less vivid in W carbons. Here, a decrease in pH value from 4.41 (W1) to 4.04 (W2) is accompanied by about 20 times drop in the capacity (295 to 16 mg/g).

To check the extent of oxidation of the surface of carbon after the modification process (oxidation with nitric acid and ammonium persulfate) Boehm titration was performed [18]. The use of basic reagents in this method enables us to identify the number of surface acidic functional groups. In the order of their acidic strengths, these are carboxyls, lactones, and phenols (the latter is the least acidic surface group). The obtained results are presented in Table 1. Comparison of the unmodified carbons (N, S, W1, W2, W3) shows that the S and W series of samples are more chemically heterogeneous than N. The S carbon has a low content of acidic functional groups whereas all W carbons have high amounts of these groups. This pattern is expected since wood based W carbons are produced by chemical activation (using phosphoric acid) at

relatively low temperature (~ 600 °C) which favors the formation of a high content of acidic surface groups during activation [56]. N and S carbons are activated anaerobically (with H_2O and CO_2) at much higher temperature (~ 900 °C) which suppresses the formation of acidic surface groups and promotes the surface basic groups [56]. The lower content of acidic surface functional groups on these carbons is a result of exposure to the oxygen in air at lower temperature during cooling or storage. In the case of N carbon only lactonic groups represent strong acids since no carboxylic groups were detected on this carbon. Later investigations revealed trace amount of carbonate in N carbon, which may be attributed to the constituents of its precursor, the bituminous coal. The samples also differ in the amount of basic species. The N sample has the highest content of the basic groups whereas S and W3 have intermediate amounts. The W1 and W2 showed the least amount of basic surface groups.

Oxidation with nitric acid significantly increases the number of acidic groups, decreases the number of basic groups for both N1 and S1 carbons, and creates carboxylic acids in the case of N1 material. The decrease in the number of basic species compared to the initial samples is likely due to the protonation of the basic sites and the conversion of insoluble components of inorganic matter such as carbonates into soluble nitrates. The latter are removed during washing after oxidation. Oxidation with ammonium persulfate is more effective than with nitric acid for both N2 and S2. The S2 sample shows a significant increase in the number of carboxylic and phenolic groups along with a 75% decrease in the number of basic species. From the summation of all groups we may conclude that oxidation has generally enhanced the number of surface oxygen groups and that this effect is more noticeable in the case of oxidation with ammonium persulfate.

Comparison of the total number of acidic groups of each carbon with the H_2S removal capacity of that carbon shows that within a series (N, S, or W), the capacity is inversely related to the number of acidic groups. So that, N, S, W1 and W3 which have demonstrated largest capacities all have the smallest number of acidic groups whereas N2, S2, and W2 with the highest number of acidic groups have all rendered the smallest capacities within their series. A similar pattern is observed in all of the acidic groups especially in the number of carboxylic acids that are the strongest among surface acidic groups. It can be concluded that a low surface pH suppresses the process of H_2S removal on a carbon. On the other hand comparison of the number of basic group of a carbon and its capacity suggests that, within each series, the capacity is generally related to the number of basic groups.

Unlike in the N and S series where variation in acidity and basicity are considerable across the series, such effect is not so distinct in W series. Here the change is limited to 30 % variation in the number of total and each acidic group. Similar variation existed in pH analysis. This suggests that although W series generally follows the same patterns observed in N and S series with respect to the relationship between the H_2S removal capacity and surface chemistry of carbon, other factors may play a stronger role in its performance.

Detailed information about the distributions of acidic groups having pK_a between 3 and 10 can be obtained from the analysis of the potentiometric titration data (Figure 9). The method of analysis, assumptions, and numerical approach used (SAIEUS) are described in Section 2.2. The distributions of acidity constants for species on the surface of carbons are shown in Figure 9.

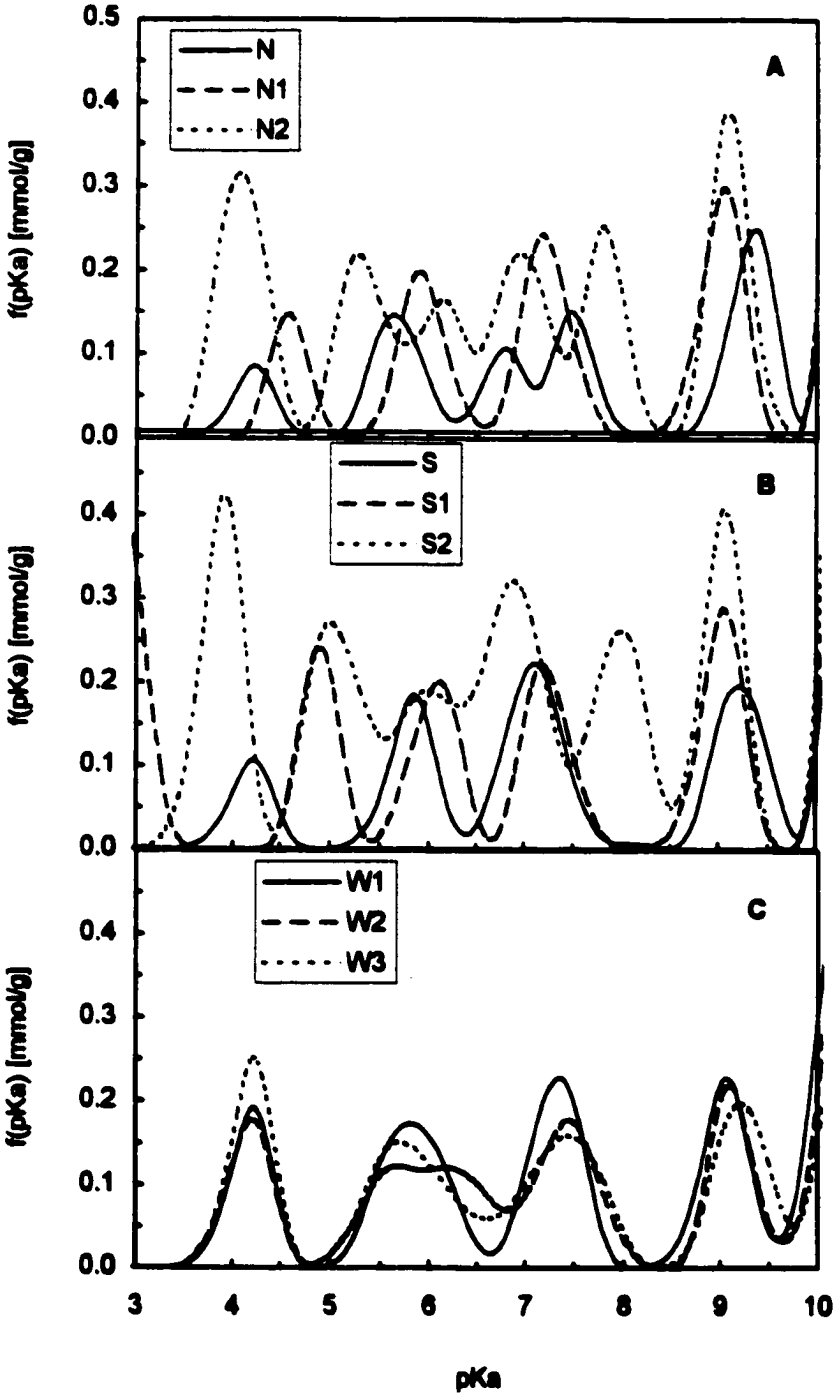

Figure 9. Acidity constant distributions for N (A), S (B), and W (C) series of carbons.

As proposed in the literature, the species having pK_a smaller than 8 are assigned to strong carboxylic acids and those with pK_a greater than 8 to phenols and quinones [57]. The results obtained for initial carbons indicate the existence of a larger number of strong acids in the case of S, W1, W2, and W3 compared to N, which is in agreement with the results of Boehm titration. However, the surface groups seem to be more heterogeneous in the case of the N sample where more peaks are revealed (at pK_a about 4.2, 5.6, 6.8, and 7.5).

After oxidation with nitric acid a slightly larger number of groups is detected for N1 carbon with disappearance of the peak at pK_a of about 6.8 present for the initial material (Figure 9A). This peak is likely related to the presence of inorganic matter, which was removed from the carbon during acid treatment. The changes in the acidity after oxidation are more pronounced in the S series, as shown from the Boehm titration results. The S1 sample shows a significant increase in the population of groups with pK_a smaller than 5.5 (Figure 9B), along with the creation of new strongly acidic species, beyond the limits of our experimental window. After oxidation with ammonium persulfate, even though peaks at similar positions are revealed for both carbons, the number of groups is larger in the case of S2 material. Those results indicate similarity in the quality of groups created using the same oxidant [15, 57].

A close look at the distribution of acidic groups in W series (Figure 9C) indicates that remarkable similarity in the acidity of the surface of carbons exists. The pK_as of the species are almost the same (4.2, 5.8, 7.3, 9.1) which is due to having the same precursor and activation method. Unfortunately, due to the limitation of this kind of titration, the presence of acids stronger than pK_a equal to 3 and their amount can not be precisely

evaluated. If some strong phosphoric acid species are built into a carbon matrix, or their washing was incomplete, they contribute to the low pH value of the carbon surface. Indeed, in spite of similarities in pK_a distributions, the observed differences in the pH values (Table 1) indicate the presence of certain acidic or basic species on the structure of our carbons which can not be detected using classical acid/base titration methods. The measured pH values suggest that the concentration of strong acids may differ by orders of magnitude between the W2 and W1 samples. It is also possible that the presence of sodium phosphates (average content for Westvaco carbons is 0.3%) significantly enhances the buffer capacities of the W1 and W3 carbons. Sodium hydroxide is used very often to neutralize the acidic surface of carbon obtained by phosphoric acid activation. An indication that this step was used for the W3 and W1 carbons were their basic leachates from the initial washing in a Soxhlet apparatus, while the pH of W2 leachate was around 2.

The results obtained from acid/base titration are in general agreement with the pH values collected in Table 1. They represent the average acidity of the carbon surface indicating that all carbons in W series are more acidic than S which is itself more acidic than N. The pK_a distributions for W carbons and S are similar in the position of the peaks. They all show four peaks around pK_a equal to 4.2, 5.8, 7.3, and 9.1. The last three peaks in W1 and S are almost identical in position and magnitude. The peak around 4.2, which is due to strong carboxylic acids, is slightly larger in W. Owing to such a feature, the surface of W1 is more than two orders of magnitude more acidic than S. Similar comparison between S and N carbon reveals why the surface of S is more acidic than N due to a slightly larger peak around 4.2. The N2 and S2 have both shown a similar pH of

3.6 owing to a profound peak around 4. Both carbons have shown smallest capacities in their series. This indicates that surface acidity, which is an important factor in the H_2S removal process, is basically determined by the number of strong carboxylic acids with pK_a around 4. Only small differences in pH and total number of acidic groups exist between W1 and oxidized carbons N1 and S1. The latter have shown peaks with less acidic strength (higher pK_a). On the other hand, much smaller capacities were observed for them in comparison with W1. This reconfirms the initial perception that other factors besides surface chemistry play a role in the performance of these carbons.

The differences in the surface chemistry are mainly caused by the presence of oxygen-containing functional groups. The presence of oxygen groups on the surface of carbons was also detected by means of temperature programmed desorption (TPD) [56]. The curves obtained for the total emissions, CO, CO_2, and H_2O are presented in Figures 10, 11, and 12. Table 2 shows the amounts of volatile products emitted during TPD experiments in two temperature ranges (120-500 and 500-1000 °C). The most acidic groups (carboxyls, lactones) are desorbed as CO_2 in the temperature range 200 to 650 °C, while less acidic (phenols, carbonyls) and basic groups (pyrones) are desorbed mainly as CO or CO + CO_2 at the temperature range between 500 – 1000 °C [56, 58]. Water is the result of the decomposition of two carboxylic groups at low temperatures (T< 350 °C) or from the decomposition of hydroquinones and phenols at T> 600 °C [56, 58].

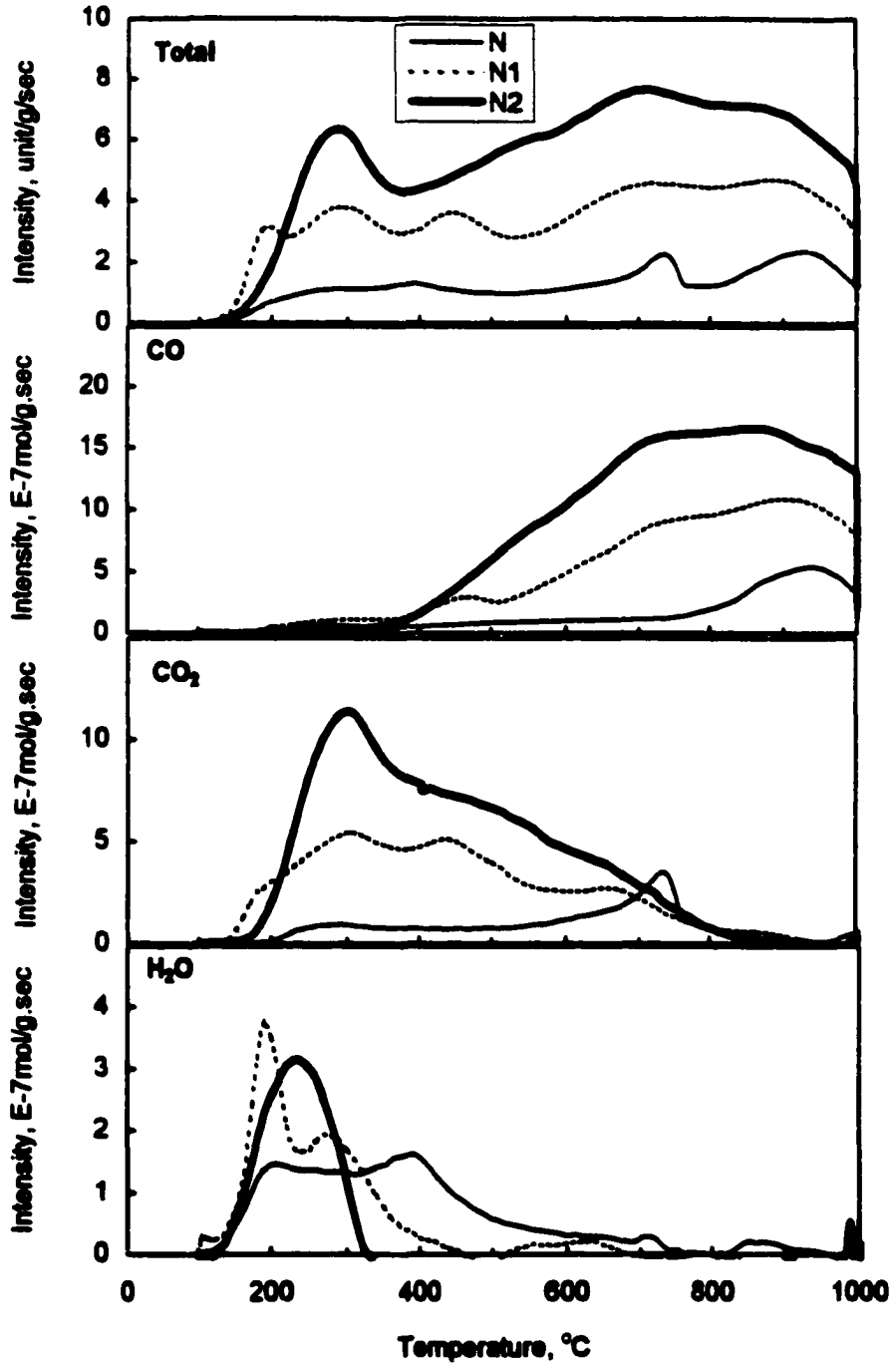

Figure 10. Thermodesorption spectra for N series.

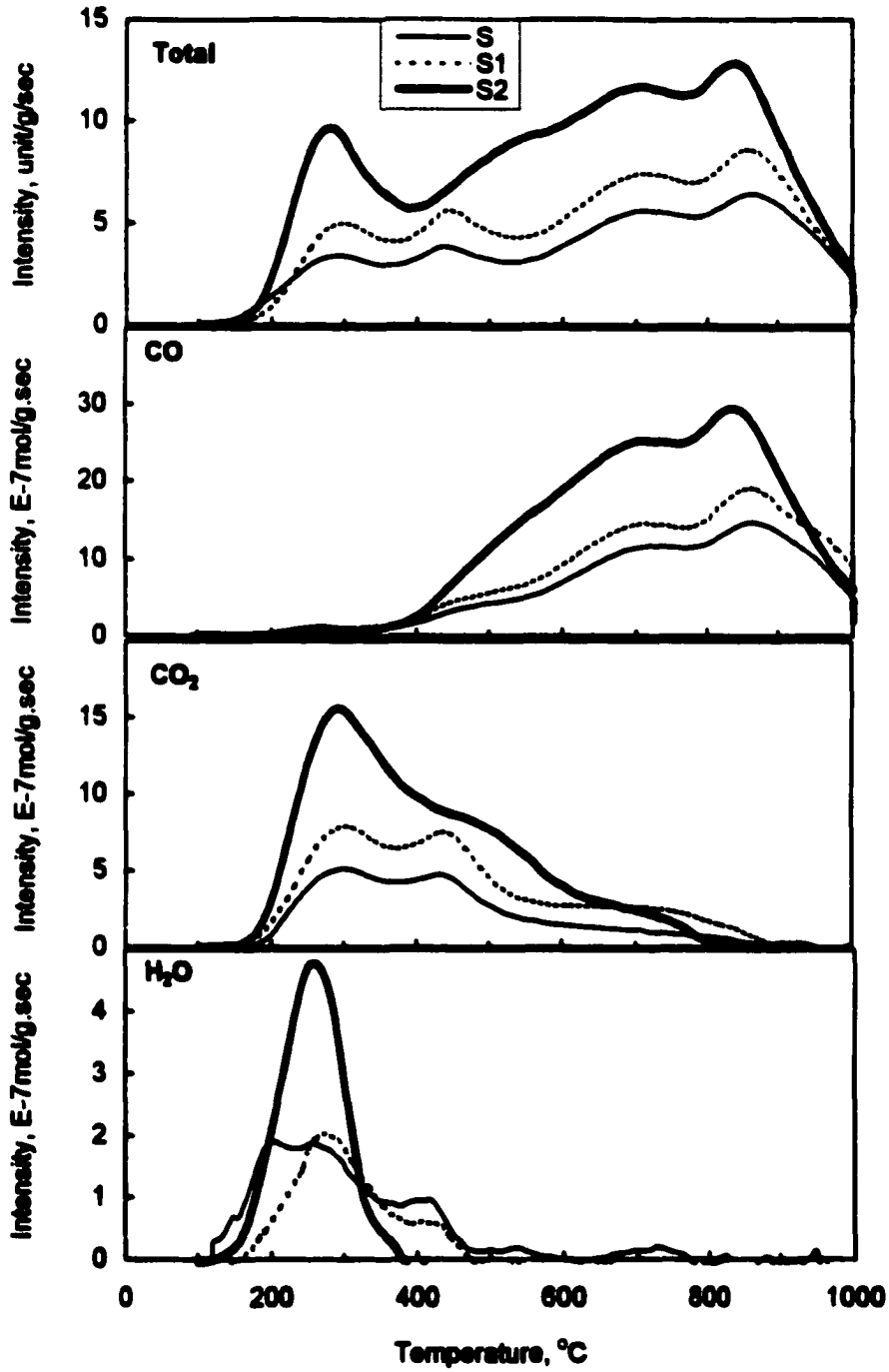

Figure 11. Thermodesorption spectra for S series.

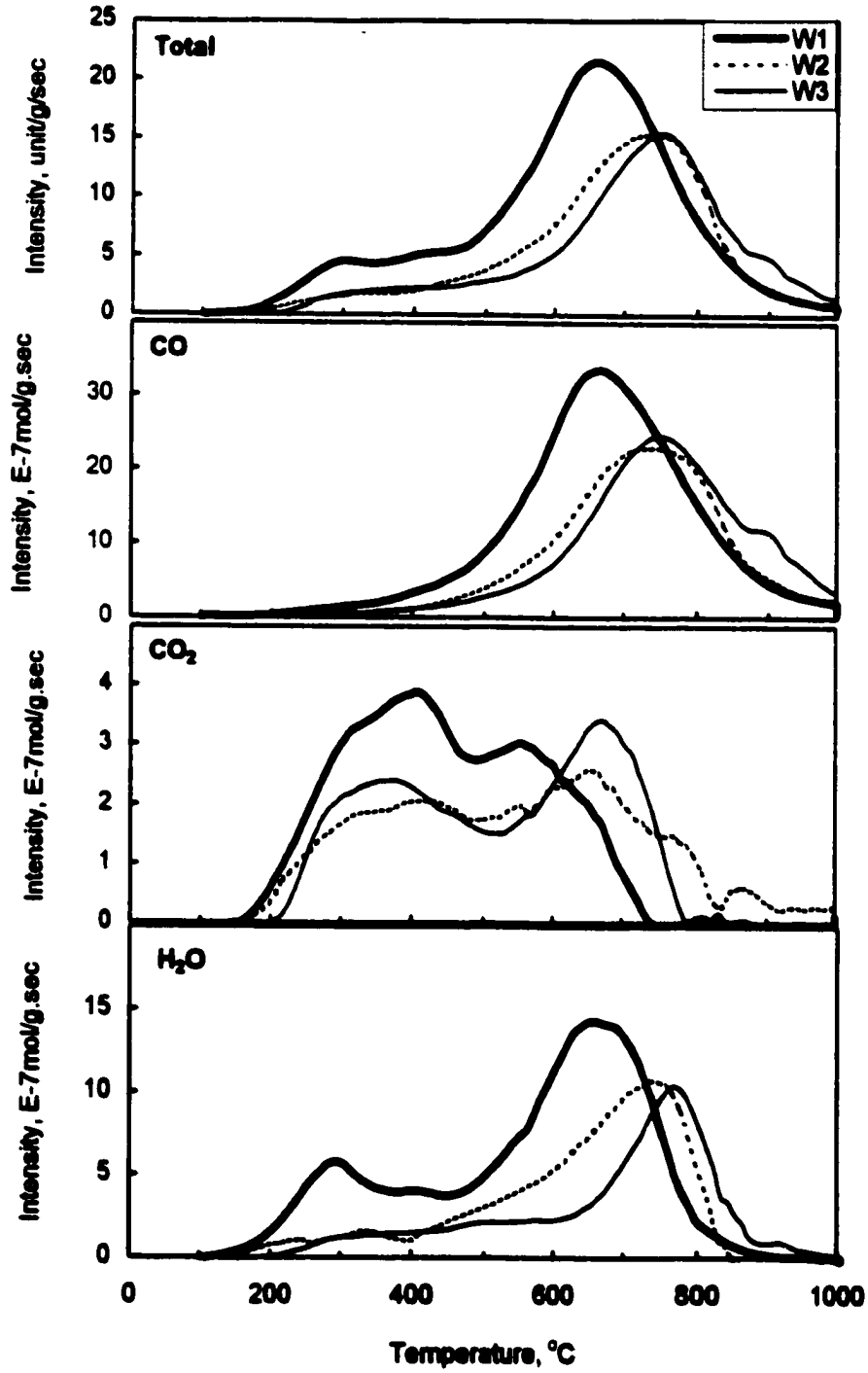

Figure 12. Thermodesorption spectra for W series.

Table 2. Amount of Gases Thermodesorbed in Different Temperature Ranges [mmol/g]

Sample	Temperature Range						Total
	120-500 °C			500-1000 °C			
	CO	CO_2	H_2O	CO	CO_2	H_2O	
N	0.03	0.06	0.14	0.55	0.22	0.05	1.05
N1	0.10	0.45	0.16	1.68	0.4	0.01	2.80
N2	0.06	0.73	0.17	2.79	0.54	0.00	5.56
S	0.08	0.35	0.14	2.08	0.31	0.02	2.98
S1	0.09	0.54	0.10	2.58	0.53	0.01	3.85
S2	0.11	0.99	0.27	4.22	0.49	0.00	6.08
W1	0.27	0.31	0.45	3.14	0.28	1.22	5.67
W2	0.08	0.18	0.15	2.34	0.37	0.84	3.93
W3	0.09	0.19	0.13	2.48	0.29	0.73	3.91

As expected, the total amounts of CO and CO_2 desorbed from oxidized carbons significantly increased as a result of oxidation [56]. Both N2 and S2 carbons show distinctive peaks in CO_2 and H_2O spectra indicating the presence of considerable amount of carboxylic acids. Their surface pHs and capacities for H_2S removal were the lowest in their series. Analysis of the data in Table 2 for N and S series shows an inverse correlation between the H_2S removal capacity of carbon and amount of either lower range CO_2 or higher range CO in each series. It is noteworthy that S2 carbon has released the maximum amount of the two gases in the mentioned ranges in both series. This carbon has shown the lowest capacity among the six carbons in the N and S series. This is an indication that similarities exist in the behavior of the carbons in the two series, despite their different origins. The TPD data confirm the results of titrations and clearly show that oxidation with ammonium persulfate creates more oxygen groups on the carbon surface than does oxidation with nitric acid. The peak at 730 °C representing CO_2 on the TPD curve for the N sample is related to the presence of carbonate impurities. The titration results showed that these species disappear after oxidation (Figure 9A).

Comparison of the results obtained for W series with N and S series in Table 2 shows that the total amount of gases desorbed from W2 and W3 are similar to S1 whereas the amounts for W1, N2, and S2 are similar to each other. However, the presence of a major peak in CO_2 spectra for oxidized N and S series in the low temperature range differentiates them from W series. It is clearly seen from Figure 12 that the total amounts of volatile species desorbed from W2 and W3 are approximately the same whereas the amount desorbed in the case of W1 is significantly higher. Moreover, the maximum of the largest peak for the latter sample is shifted toward lower temperature (670 °C)

compared to the other two samples (750 °C). This may be related to small differences in the carbonization temperatures during the manufacturing process or the presence of water containing inorganic impurities. The feature of the carbon surface that may contribute to the observed differences is the presence of phosphates, which are known for improving thermal stability [60, 61].

It is noteworthy that in the case of Westvaco carbons we observe a significant amount of desorbed water. This amount is much higher than those for N and S series. Comparison of the spectra for the three series shows that in N and S series the desorbed water is always accompanied by CO_2 whereas desorption of most of the water in W series is accompanied by CO.

Analysis of the total amount of CO and CO_2 (Table 2) shows that W1 has more oxygen groups on the surface than W2 and W3. The chemical inventory represented by TPD spectra is much broader (more groups detected) than those provided by titration methods (Table 1, Figure 9) due to the fact that titration methods detect only acids and bases having certain pK_a values which are capable of interacting with the titrant [18, 57]. In the TPD method all decomposed groups contribute to the emission, regardless of their chemical character. Moreover, differences in the curves, their ranges and maxima positions, provide information on the distributions of oxygen groups [56, 58].

3.3. Water Adsorption

The results reported by other researchers indicate that in most cases the presence of moisture enhances the adsorption and oxidation of hydrogen sulfide [11, 12]. When the H_2S breakthrough tests were done at dry condition the capacity was remarkably low

(Table 3). According to the mechanism proposed by Hedden et al., dissociative adsorption of hydrogen sulfide in aqueous environment has a significant impact on its oxidation [27]. It is well known that the "clean" surface of activated carbon is hydrophobic with very low affinity to water adsorption [5]. The presence of heteroatoms, especially oxygen, significantly changes the situation. Heteroatoms are arranged in the form of active chemical groups analogous to organic species, which, due to their polarity and possibility to attract water via hydrogen bonding, become primary adsorption centers [62]. Thus, the affinity of activated carbon to retain water depends on the number of oxygenated groups present on the surface [54, 55, 62], which act as primary adsorption centers. Further adsorption of water on the already adsorbed water molecules leads to the condensation in small pores even at relatively low humidity. To investigate the affinity of our carbons to retain moisture, water adsorption isotherms were measured at relative pressure smaller than 0.3 at 20 °C. (Figure 13). The adsorption capacity at $p/p_o = 0.3$ is reported in Table 3. The water sorption results show that the sorption capacity of S carbon is higher than N. This result is expected since the S carbon has more oxygenated groups and more developed microporosity [55]. After oxidation with nitric acid, water uptake significantly increases for the N1 carbon, while for the S1 only a small enhancement is observed. This difference follows the effect of oxidation described above. After oxidation with ammonium presulfate the amounts adsorbed for N2 and S2 considerably increase (Table 3), especially for the latter sample. Relatively small differences are observed in the sorption capacities in the W series.

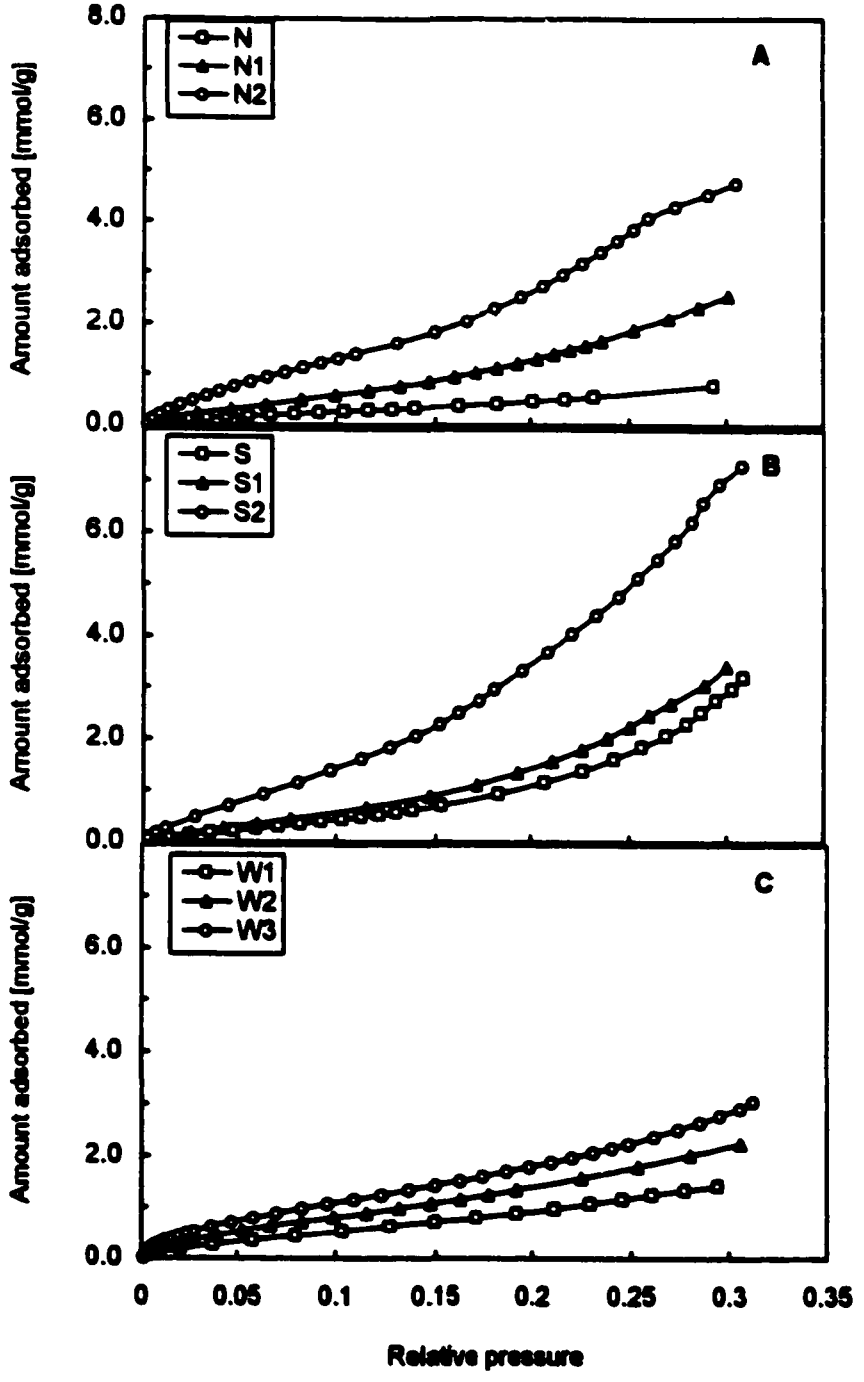

Figure13. Water adsorption isotherms at 20 °C for N (A), S (B), and W (C) series.

Table 3. Water Sorption*, Dry H_2S Capacities and Breakthrough Capacities

Sample	H_2O uptake	Dry H_2S Capacity	H_2S Breakthrough Capacity
	mmol/g	mg/g	mg/g
N	0.78	4.6	96
N1	2.56	8.3	48
N2	4.78	9.5	28
S	3.2	4.8	112
S1	3.41	6.8	15
S2	7.31	8.7	12
W1	1.43	2.5	295
W2	2.24	4.5	16
W3	3.06	6.5	238

* At 30 % relative humidity and 20 °C.

Comparison of the water uptake results with the measured H_2S capacities of carbons (Table 3) shows that an inverse relationship exists between the H_2S capacity of a carbon and its water affinity. At the first glance this correlation might seem contradictory with the fact that H_2S capacity in the absence of humidity is always very low (Table 3). It is noteworthy that, a direct relationship, as expected, exists between total (All) amount of surface oxygen groups and the affinity for water sorption (Tables 1 and 3). Analysis of the data shows that a correlation with more acidic groups (carboxylic and lactonic) can better explain the sudden rises in water sorption especially for N1, N2, and S2 carbons. It is reasonable to assume that oxygen in the more acidic sites is more potent in forming hydrogen bonds and hence enhances the water sorption. For example, N1, S1, W2, and W3, all showed similar content of carboxylic acids and their water sorption capacities are close. N2 and S2, which have revealed a large content of carboxylic acids, have shown high affinities towards water. It may be concluded that while some amount of water is required for the effective removal of H_2S, too high affinity toward water is an indication of surface acidity that will impede the removal process [15].

3.4. Outline of the Reactions in the Adsorbed Water Film

In this section, we outline a preliminary feature for the pathways of H_2S adsorption/oxidation on the surface of activated carbon, based on our investigation of the surface chemistry of the carbons and the existing literature. We found that the presence of humidity and the formation of the water film are essential conditions for the process [27]. This indicates that chemical reactions taking place in aqueous environment play the major role in the immobilization of H_2S in comparison with physical adsorption. It was

also found that to have an effective removal the surface pH of carbon should not be too acidic. This suggests that the initial step for the oxidation of H_2S is its dissociation and the formation of hydrosulfide ion. These findings are in agreement with the work of other researchers. Klein and Henning [26] emphasized that the formation of a water film on the surface of the carbon at low temperatures is an essential condition for the proceeding of the reaction. They reaffirmed the mechanism initially proposed by Hedden et al. [27] for oxidation of H_2S in the water film on the surface of activated carbon:

$$O_2 \rightarrow O + O \qquad (3.1)$$

$$H_2S \rightarrow HS^- + H^+ \qquad (3.2)$$

$$HS^- + O \rightarrow S + OH^- \qquad (3.3)$$

Oxygen radicals are formed by the homolytic bond dissociation of molecular oxygen on the surface of activated carbon. The produced sulfur is deposited in the pores resulting in the gradual fouling of the catalyst (activated carbon). The formation of sulfuric acid as a side reaction in the presence of humidity is also indicated [26]:

$$H_2S + 2\,O_2 \rightarrow H_2SO_4 \qquad (3.4)$$

The formation of sulfuric acid marks a major increase in the acidity and will suppress the process of dissociation and immobilization of hydrogen sulfide.

3.5. Structural Parameters of Activated Carbons

If H_2S is to be effectively removed from the air stream, its oxidation products will deposit in the pores, causing their gradual blockage. In an effort to regenerate the carbons, they were washed in a Soxhlet apparatus. Monitoring the changes in the porous structure in different stages of this study (i.e. initial, exhausted and washed carbons) is expected to provide information about the nature and amount of the oxidation products. Data describing the porous structure is obtained from sorption of nitrogen at its boiling point (−196 °C) [63].

Before the experiments the samples were dried to remove any residual H_2S and weakly adsorbed species such as water. The samples were then outgassed at 120 °C and 10^{-5} torr. Although the mass balance of the sulfur compounds might be affected by this preparation procedure it is expected that the bulk of them will remain intact [20].

Nitrogen adsorption isotherms for the initial, exhausted, and Soxhlet washed samples are shown in Figures 14 to 16. The results obtained for initial N and S series are typical of microporous carbons. They show that the pore structures of all carbons in N and S series are similar and oxidation with nitric acid or ammonium persulfate does not impose significant changes on the porosity. The isotherms for the initial W series indicate that considerable volume of mesopores exist in these carbons. For all series of samples a significant decrease in nitrogen uptake upon exhaustion (adsorption of H_2S) is noticed. The isotherms for all exhausted carbons fall bellow the initial carbons in an amount proportional to the delivered capacity. An exception is the isotherm for NE, which has undergone a major shift downward, much more than its capacity. The decrease in sorption capacity in the case of NE is more significant than for SE. This indicates that the

oxidation products block the micropores to a greater extent in the case of the former carbon. Considering that N and S have similar H_2S removal capacities (Table 1) and nitrogen sorption capacities (Figures 14 and 15), the observed difference may be attributed to the type of the oxidation products deposited on each carbon.

For all washed samples, an increase in the sorption uptake is noticed compared to their exhausted counterparts. However, the amounts adsorbed are lower than for the initial materials. It is interesting to note that in general, washing is more effective in the case of the S series (Figure 15) than for N series (Figure 14) or W series (Figure 16), suggesting a higher yield of water soluble sulfur species in this carbon. Washing in Soxhlet has been most effective for S1S and S2S so that much of the oxidation products are removed from their pores and their isotherms approach their initial counterparts. In fact the isotherm for S2S is even above S2. This indicates that some residues, which had remained in S2 from the carbon preparation process, were later washed with oxidation products in S2S. NS and SS show moderate recovery in their pores upon washing. Small recoveries of the pores are observed for all carbons in W series. In the cases of N1S and N2S, the amount of deposited products increased during washing so that their isotherms either overlap or are below those of the exhausted samples. This suggests that some chemical transformations have taken place in their deposited products during washing resulting in further blocking of the pores. It is possible that sulfur has undergone in-washing oxidation to sulfuric acid. The latter, due to its larger molecule, can be strongly adsorbed in small pores and can further block their entrances. This suggests that washing has not been sufficient [20].

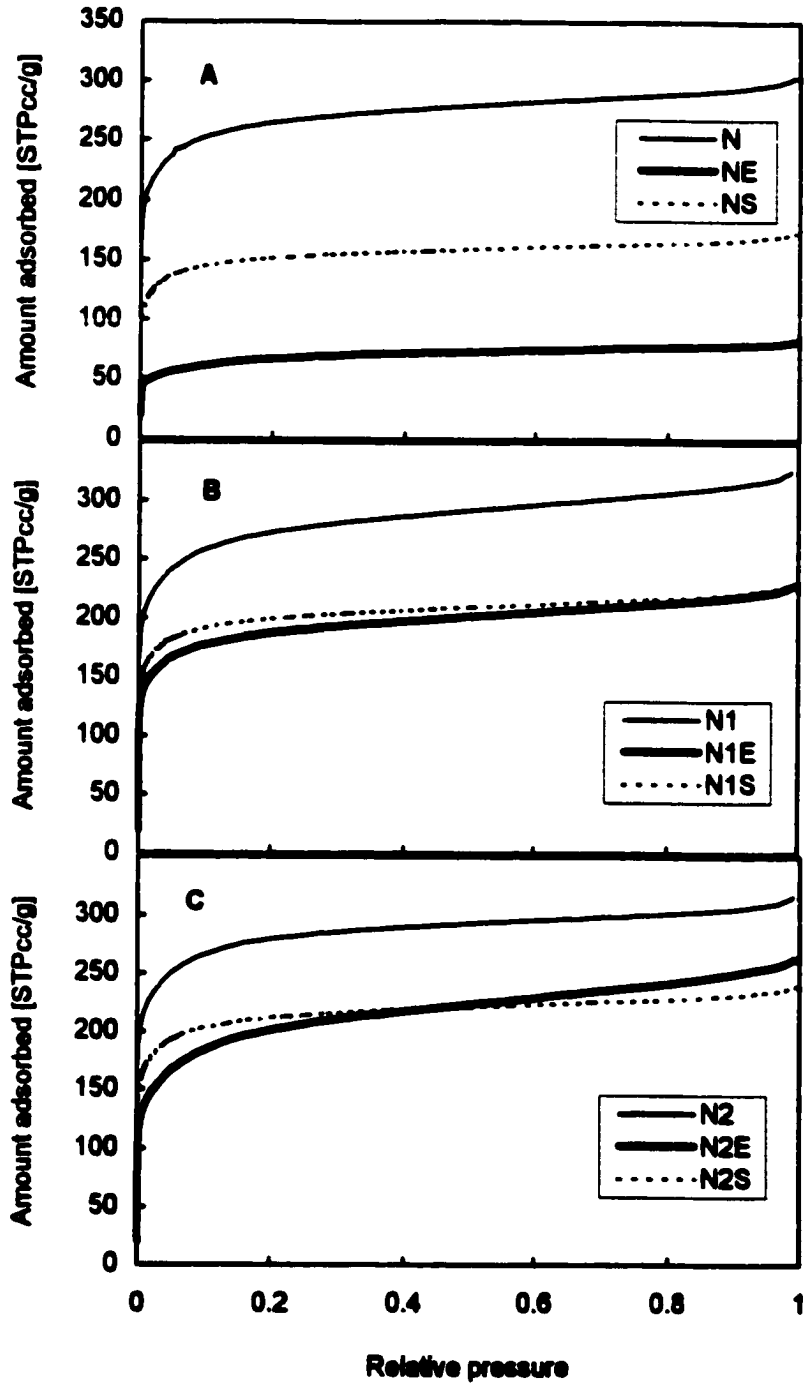

Figure 14. Nitrogen adsorption isotherms for N (A), N1 (B) and N2 (C) series.

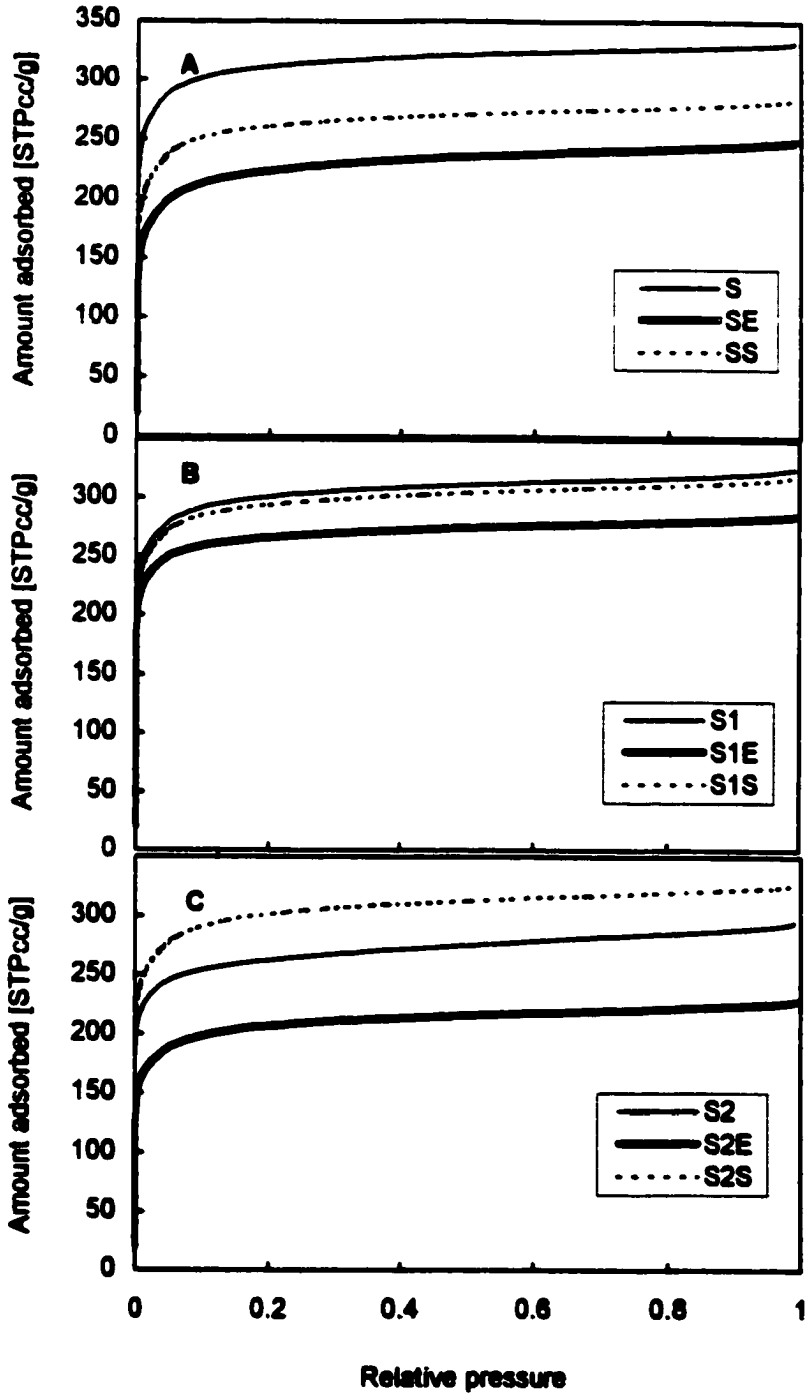

Figure 15. Nitrogen adsorption isotherms for S (A), S1 (B) and S2 (C) series.

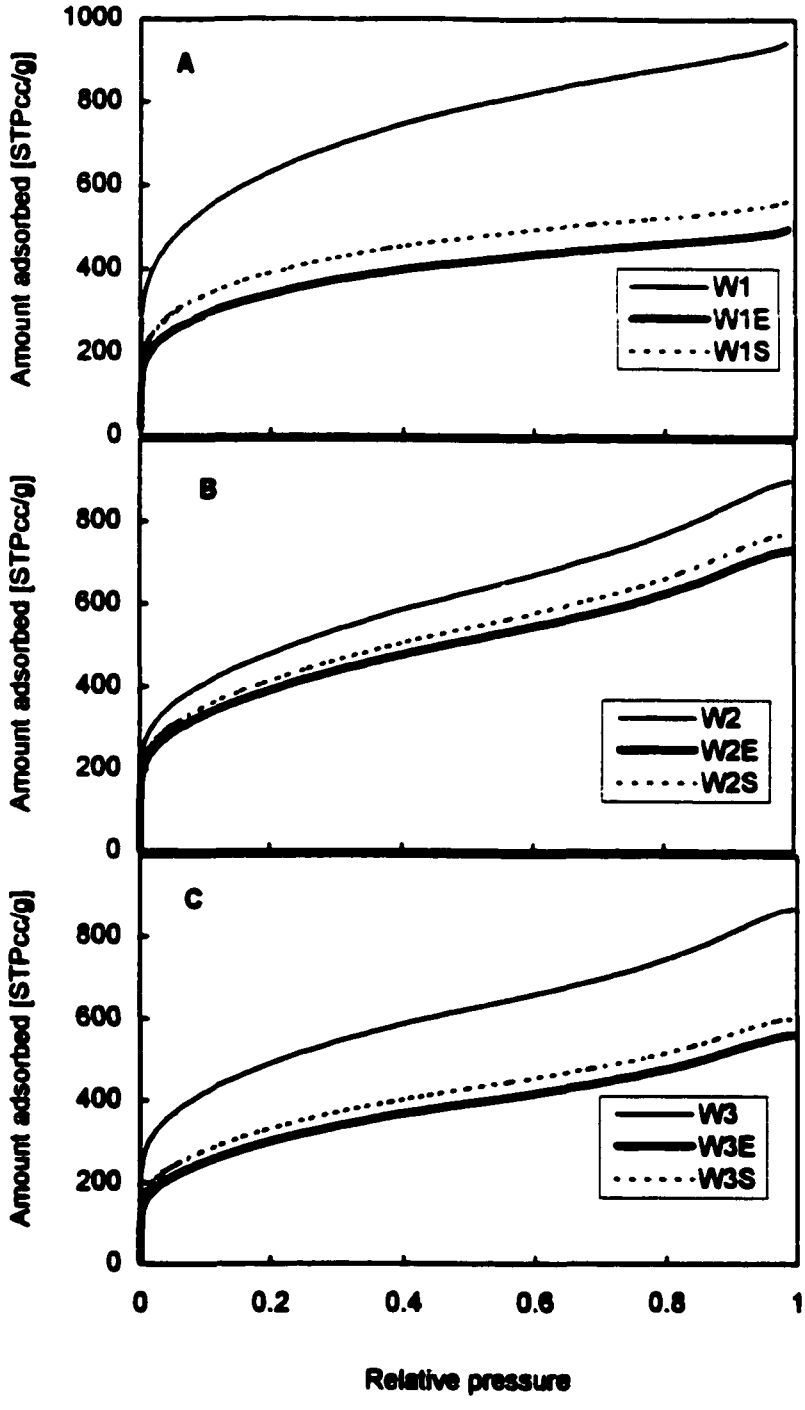

Figure 16. Nitrogen adsorption isotherms for W1 (A), W2 (B) and W3 (C) series.

The structural parameters are calculated from its nitrogen adsorption isotherm, using density functional theory (DFT) [53, 64]. The calculated pore size distributions (PSD) are shown in Figures 17 to 19. The volume of subgroups of micropores: less than 5 Å ($V_{\leq 5Å}$), less than 10 Å ($V_{\leq 10Å}$), less than 20 Å ($V_{\leq 20Å}$); volume of mesopores (V_{meso}); total pore volume (V_{total}); and the specific surface area (S_{N2}) are collected in Table 4. The initial carbons differ in surface areas and pore volumes. As mentioned earlier, the N and S carbons represent microporous carbons with high volumes of pores smaller than 10 Å. The porous structure of the S material is more developed than the N. Most of the pores in N and S are smaller than 30 Å and 20 Å, respectively (Figures 17 and 18). Comparison of the data in Table 4 indicates that in the N series, oxidation does not affect the pore structure, while for the S series a small decrease in the surface area and micropore volume is noted along with a slight increase in the volume of mesopores. It is interesting that while oxidation of S carbon with nitric acid decreased the volume of pores smaller than 10 Å (a peak centered at around 7 Å), oxidation with ammonium persulfate left these pores almost intact with a significant decrease in the volume of pores represented by peak at about 15 Å (17). As discussed earlier, this decrease may be a result of residue remained in carbon due to the incomplete washing after oxidation process. A proof of this is that the 15 Å peak is almost fully recovered (in comparison with S) in S2S, upon additional washing in Soxhlet.

A major characteristic of W series is their high total pore volume. While total pore volume for N and S series is around 0.40 cm^3/g for W series it is around 1.20 cm^3/g (Table 4). Even if the effect of density differences among the carbons is taken into account, the total pore volume for W series per cubic centimeter of carbon is still two

times more than N and S series. But unlike N and S series, the bulk of pore volume in W series is attributed to the mesopores, which are less active in adsorption processes. The volume of pores smaller than 10 Å in W series is less than N and S series. As expected from the isotherms, W2 and W3 carbons have very similar PSDs whereas the volume in pores of W1 is much higher and the contribution of small micropores is significant. Moreover, the distribution of W1 is narrower and almost all pores are smaller than 100Å [19].

Comparison of the results of H_2S removal capacity (Table 1) and the structural parameters (Table 4) shows that although some proportionality exists between the pore volume and the observed capacity, a correlation can not be found. Several researchers have reported that H_2S adsorption/oxidation at high temperature is primarily governed by porous structure of adsorbent especially pores under 10 Å [22, 33]. Our results, however, indicate that at ambient temperature, although some elements of porous structure contribute to the H_2S removal process, the performance of a carbon overall cannot be governed by its structural parameters. This is another indication of the role of surface chemistry in the reactions that take place in the water film.

Application of carbons as H_2S adsorbents significantly decreased the surface areas and pore volumes. The decrease in these parameters for each carbon is in agreement with its H_2S removal capacity. An exception is the NE carbon, which is discussed later. Since similar structural parameters are observed for N and S series, comparison of their performance may highlight the effect of their surface chemistry on the process. In the case of NE carbon, the volume in very small pores significantly decreased owing to the deposition of H_2S adsorption/oxidation products (Figure 17A). Washing with water in

Soxhlet (NS) resulted in the partial reopening of those pores for nitrogen molecules due to the removal of some of the oxidation products. On the other hand, in SE -which has similar capacity to NE- considerable volume of micropores is still accessible for nitrogen and washing does not significantly change its distribution shape (Figure 18A). In N1E, N2E, S1E, and S2E, which have shown smaller capacities, considerable volume of micropores, are still intact. This suggests small amount of oxidation products is present on the surface. As discussed earlier, the cases of N1S and N2S are interesting in that their sorption capacities have decreased after washing indicating that their oxidation products have undergone some spatial/chemical transformations during washing. A detailed analysis of distributions for N1S and N2S (Figures 17B and 17C) shows that products in pores under 10 Å are reduced while those in pores above 10 Å have actually increased. The size of sulfide ion is about 2 Å whereas the size of a molecule of sulfuric acid is about 5 Å [65]. It is reasonable to assume that further oxidation of deposited sulfur in N1E and N2E during washing can in fact reduce the sorption capacities of N1S and N2S. The distributions for SS, S1S and S2S show small recovery in pore volume after washing. This small increase can be owing to the fact that these carbons are resistant to washing. The presence of small micropores causes difficulty of desorption and limits the access of water to the deposited products. Usually more energetic processes like steam washing or heating at high temperature are needed for effective regeneration of these carbons [66].

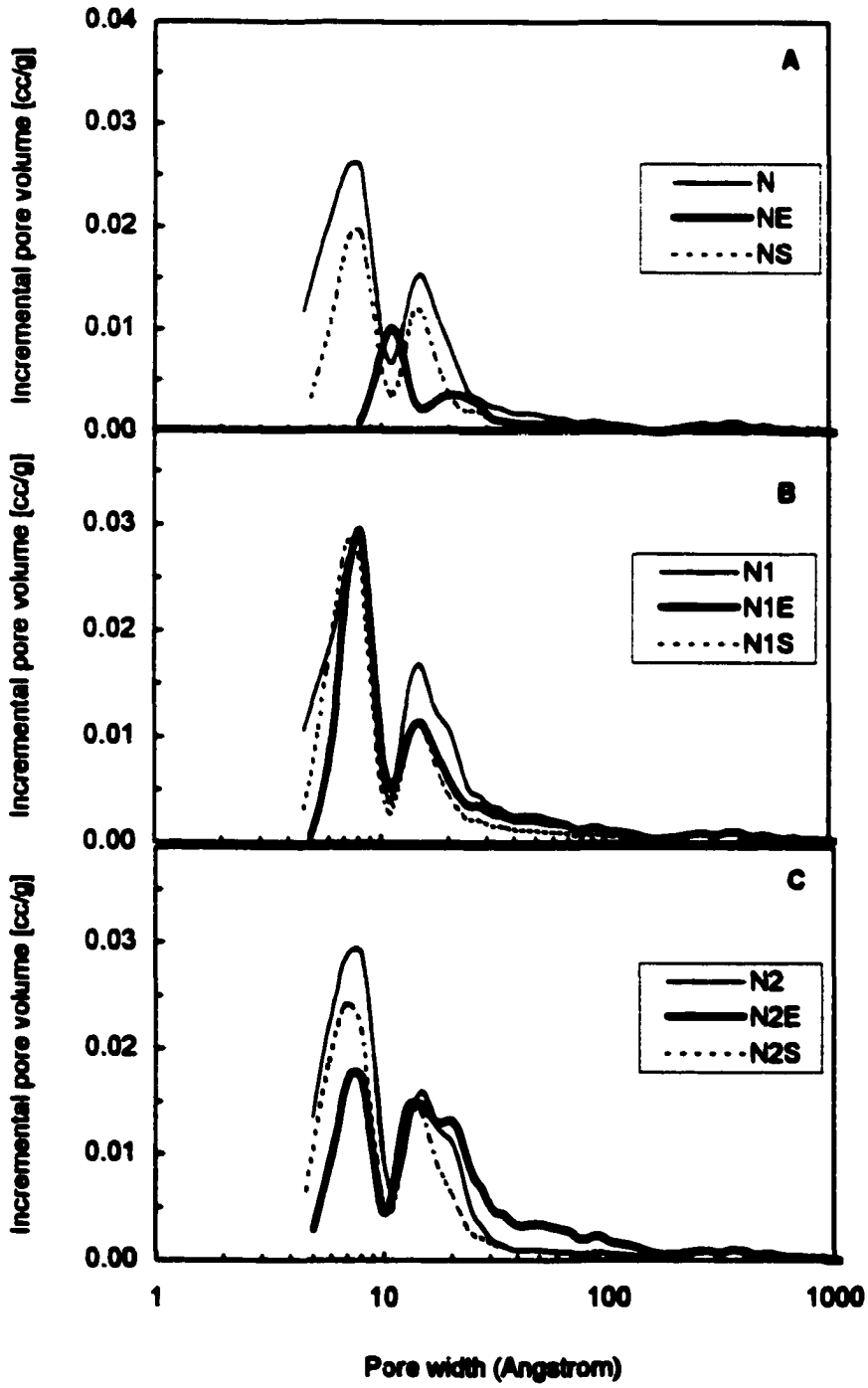

Figure 17. Pore size distributions for N (A), N1 (B), and N2 (C) series.

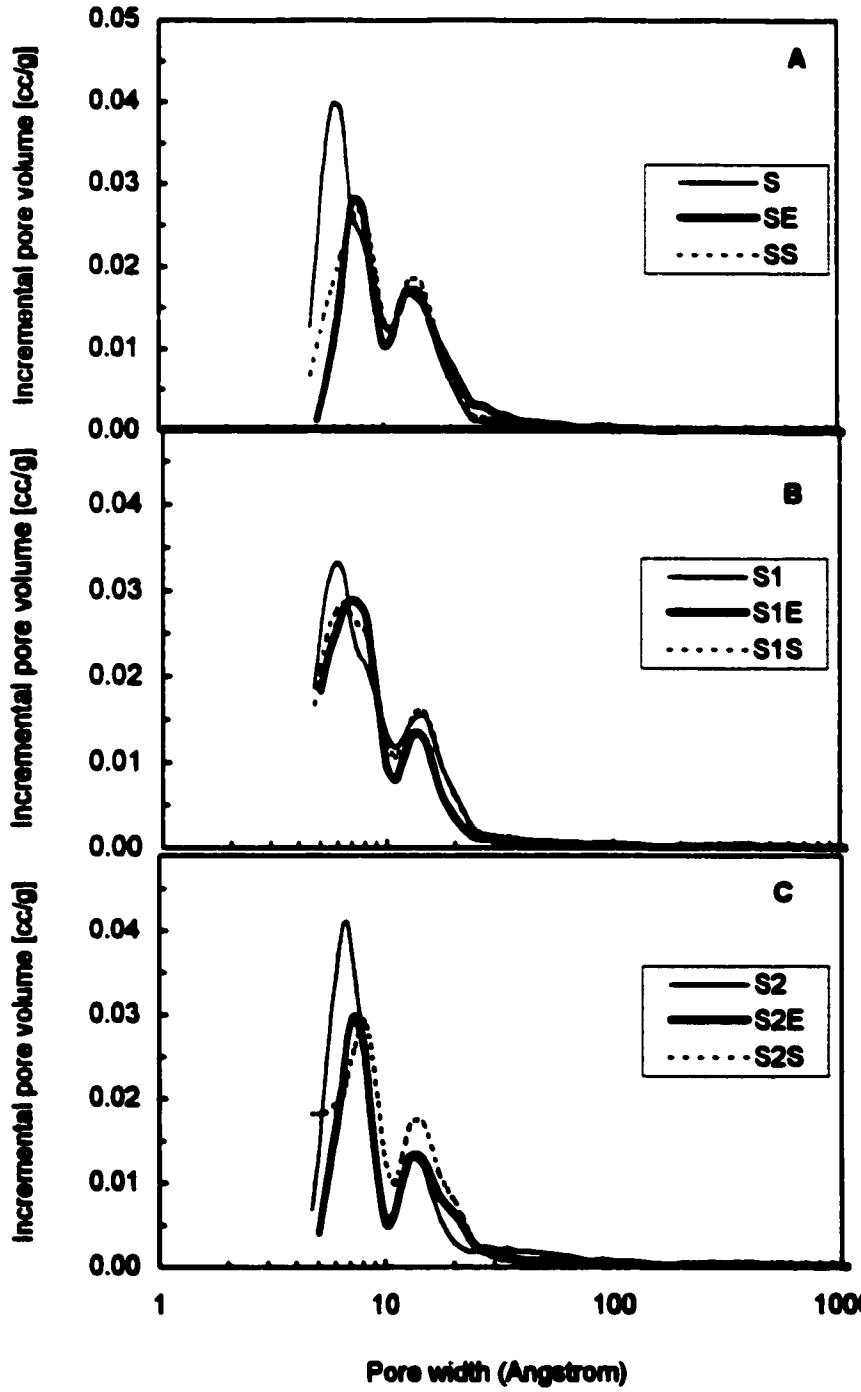

Figure 18. Pore size distributions for S (A), S1 (B), and S2 (C) series.

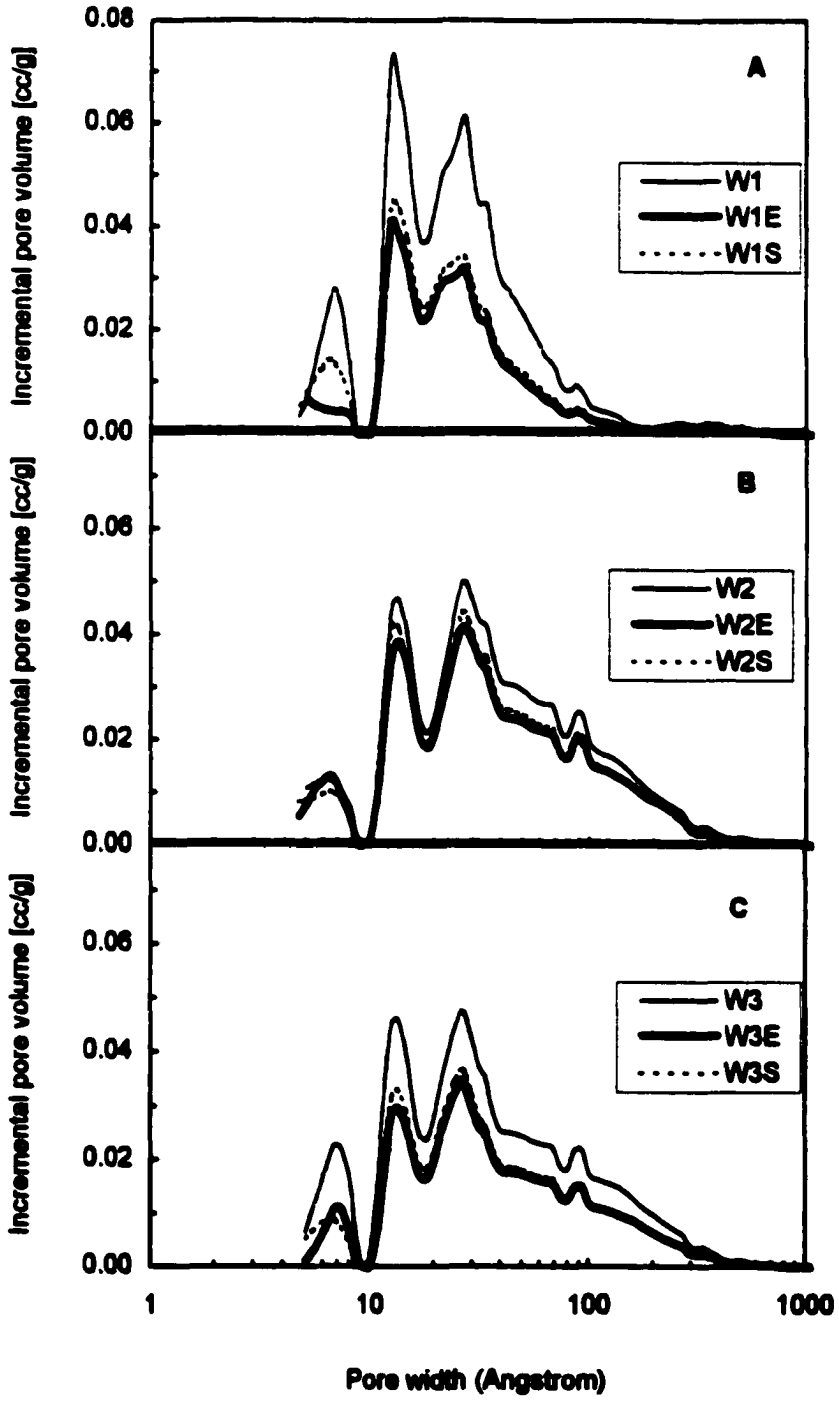

Figure 19. Pore size distributions for W1 (A), W2 (B), and W3 (C) series.

Table 4. Structural Parameters Calculated from Sorption of Nitrogen

Sample	Micropores			Mesopores		Surface
	$V_{\leq 5Å}$ cm^3/g	$V_{\leq 10Å}$ cm^3/g	$V_{\leq 20Å}$ cm^3/g	V_{meso} cm^3/g	V_{total} cm^3/g	S_{N2} m^2/g
N	0.026	0.209	0.310	0.057	0.370	787
NE	0.000	0.016	0.060	0.030	0.092	118
NS	0.003	0.121	0.186	0.029	0.218	436
N1	0.023	0.206	0.312	0.077	0.391	782
N1E	0.001	0.149	0.225	0.064	0.293	524
N1S	0.010	0.178	0.244	0.039	0.286	618
N2	0.014	0.217	0.325	0.050	0.377	799
N2E	0.003	0.106	0.221	0.109	0.332	508
N2S	0.017	0.172	0.260	0.040	0.305	654
S	0.035	0.279	0.393	0.019	0.412	1030
SE	0.001	0.158	0.277	0.038	0.316	616
SS	0.017	0.203	0.327	0.028	0.356	771
S1	0.044	0.259	0.366	0.028	0.395	972
S1E	0.018	0.224	0.306	0.021	0.328	787
S1S	0.038	0.247	0.353	0.031	0.388	919
S2	0.020	0.248	0.322	0.040	0.363	876
S2E	0.004	0.168	0.256	0.032	0.290	612
S2S	0.036	0.231	0.347	0.033	0.382	869
W1	0.021	0.127	0.561	0.651	1.213	1400
W1E	0.007	0.033	0.285	0.329	0.615	650
W1S	0.004	0.078	0.359	0.368	0.732	860
W2	0.026	0.078	0.359	0.849	1.211	1025
W2E	0.004	0.075	0.308	0.690	1.003	880
W2S	0.015	0.066	0.313	0.719	1.034	890
W3	0.004	0.121	0.410	0.768	1.182	1110
W3E	0.009	0.047	0.231	0.535	0.767	630
W3S	0.008	0.049	0.255	0.560	0.817	700

Analysis of the data collected in Table 4 also provides information about the type of sulfur species present on the surface of the carbon. H_2S adsorption on the N carbon causes 80% decrease in the pore volume. The observed decrease in pore volume for other carbons in N and S series is only about 20 %. Similar changes occur in the surface areas. While there is a correlation between the value of H_2S breakthrough capacity and the decrease in the total volume of pores for other carbons in N and S series, such a trend does not exist for NE carbon. The value of the measured capacity is too low to be responsible for the deposition of such a big amount of sulfur species capable of blocking the micropores to the observed extent. It is likely that in the case of NE the oxidation products clog the access to micropores. Hence, these pores, although not effectively occupied, can not be penetrated by nitrogen molecules [20].

Considerable volume of pores in W series is occupied by H_2S oxidation products (Figure 19 and Table 4). The changes in the pore volume are related to the expected sulfur deposit evaluated from the breakthrough capacity data. The decrease in the total pore volume is about 50% for W1E, 40% for W3E, and 15% for W2E [19]. It is interesting to note that the breakthrough capacities in W series are not directly proportional to the decrease in the pore volume; changes in the PSDs are much more pronounced for the W1E compared to the W3E carbon. This is probably related to the more homogeneous pore structure of the former material. Changes in the volumes of small pores ($V \leq 10Å$) suggest that over 70% of the initial pore volume is inaccessible after exhaustion in W1E. This value is 60% for W3E and only 3% for W2E. These are in agreement with the measured H_2S capacities for W series. Washing in Soxhlet was not able to significantly recover the initial pore volume probably owing to a significant

residue of insoluble elemental sulfur. However, it was the most efficient in the case of W1S carbon. For the other two samples, W2S and W3S, only a small increase in the structural parameters is observed. Washing does not remove sulfur from small pores ($V \leq 10$Å) in the case of the W2 and W3, while for W1S more than 50% regeneration of the pore volume is observed. In fact a lower volume of these pores is found for W2S (Table 4). Analysis of the distributions for pores smaller than 10 Å for W2S and W3S (Figure 19) shows that the volume of deposited products in W2S and W3S has slightly increased during washing process. As discussed earlier, this might be an indication that further oxidation of the surface products in small micropores has taken place during washing.

3.6. Analysis of the Oxidation Products

The type and behavior of the oxidation products of H_2S on the carbon surface are important for outlining a mechanism for the process to provide maximum efficiency in the removal of H_2S and the regeneration processes. The sulfur species and oxygen groups were analyzed using thermo-gravimetric method [19, 20]. The weight loss (TG), its derivative with respect to temperature (DTG), and the temperature difference (DTA) curves obtained for samples from the experiments performed in nitrogen are collected in Figures 20 to 28. Each Figure is composed of three parts: A, B, and C. Part A shows the TG results providing information on the changes in the weight of sample with respect to temperature. Part B shows the DTG, which provides information on the position and the extent of the peaks, associated with major weight losses. These peaks reflect the decomposition of species taking place during the thermal treatment. Part C shows the

temperature difference between the sample and a blank in the course of experiment. It provides information on the type of chemical and physical reactions occurring at different temperatures. An exothermic reaction marks a peak in the curve whereas an endothermic reaction is shown as a valley. Valuable information can be derived from the comparison of the three parts. Although tests were carried out starting from room temperature, the curves are plotted from 120 °C to eliminate the interference by the adsorbed water so that the weight at 120 °C is considered as 100 %. The weight losses for our carbons in these temperature ranges are reported in Table 5. Also included in Table 5 is the ash content which is measured as the residue of spontaneous ignition of the carbons heated to 1000 °C in a TA instrument. The ash content is a measure of the presence of inorganic constituents that may play a role in the process.

It is noteworthy that N series and W series contain considerable inorganic constituents whereas much less ash content was found in S series. Figures 20 and 23 show that the initial N and S samples do not have any distinguished peaks on DTG curves indicating a low content of surface oxides [15, 19]. The total weight loss for these carbons is around 5 %. Oxidation with nitric acid and ammonium persulfate resulted in the creation of more surface oxygen groups. The total weight losses for N1 and N2 increased to around 10 % whereas for S1 and S2 was around 17 %. The decomposition of strong acids from carbon's surface such as carboxyls occurs at the temperature range between 200 °C and 650 °C [20, 56] whereas the decomposition of phenols and basic pyrones takes place between 500 °C and 1000 °C. The low temperature peaks for all oxidized samples have similar intensities but in the higher temperature range the weight loss for S1 and S2 is slightly bigger which indicates higher content of surface oxygen

groups for these carbons compared to their counterparts in the N series. The TA results are in agreement with the findings of Boehm titration and TPD on the surface oxygen groups (Tables 1 and 2).

The W series are characterized by a major weight loss (about 18%), owing to a broad peak centered around 700 °C (500 °C to 800 °C) (Table 5 and Figures 26 to 28). These carbons are wood based and are chemically activated at temperatures around 600 °C, hence, nothing can be said with certainty about the type of the groups decomposing above their manufacturing temperature. The high ash content of all carbons in W series may be attributed to the presence of unwashed P_2O_5.

All of the DTG curves for exhausted carbons reveal a well defined peak around 250 °C. A second outstanding peak is observed around 330 °C in the samples which have rendered considerable capacity (N, N1, S, W1, and W3).

As indicated above, the decomposition of strong acids from carbon's surface such as carboxyls occurs at the temperature range between 200 °C and 650 °C [56] and might impose some interference with sulfur peaks. The decomposition of phenols and basic pyrones takes place between 500 °C and 1000 °C, minimizing the interference with sulfur products.

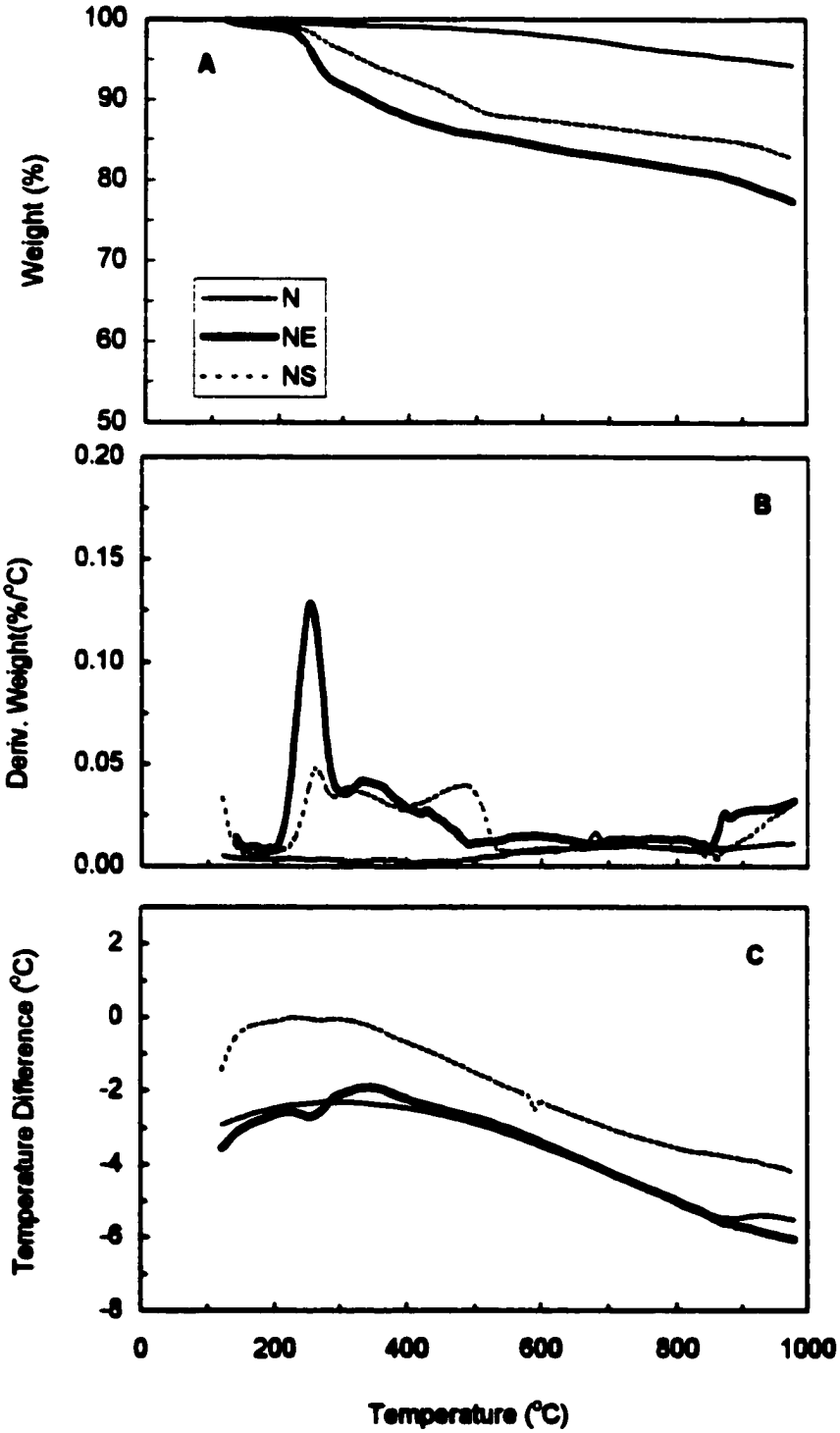

Figure 20. Thermal analysis results for N series. TG (A), DTG (B) and DTA (C).

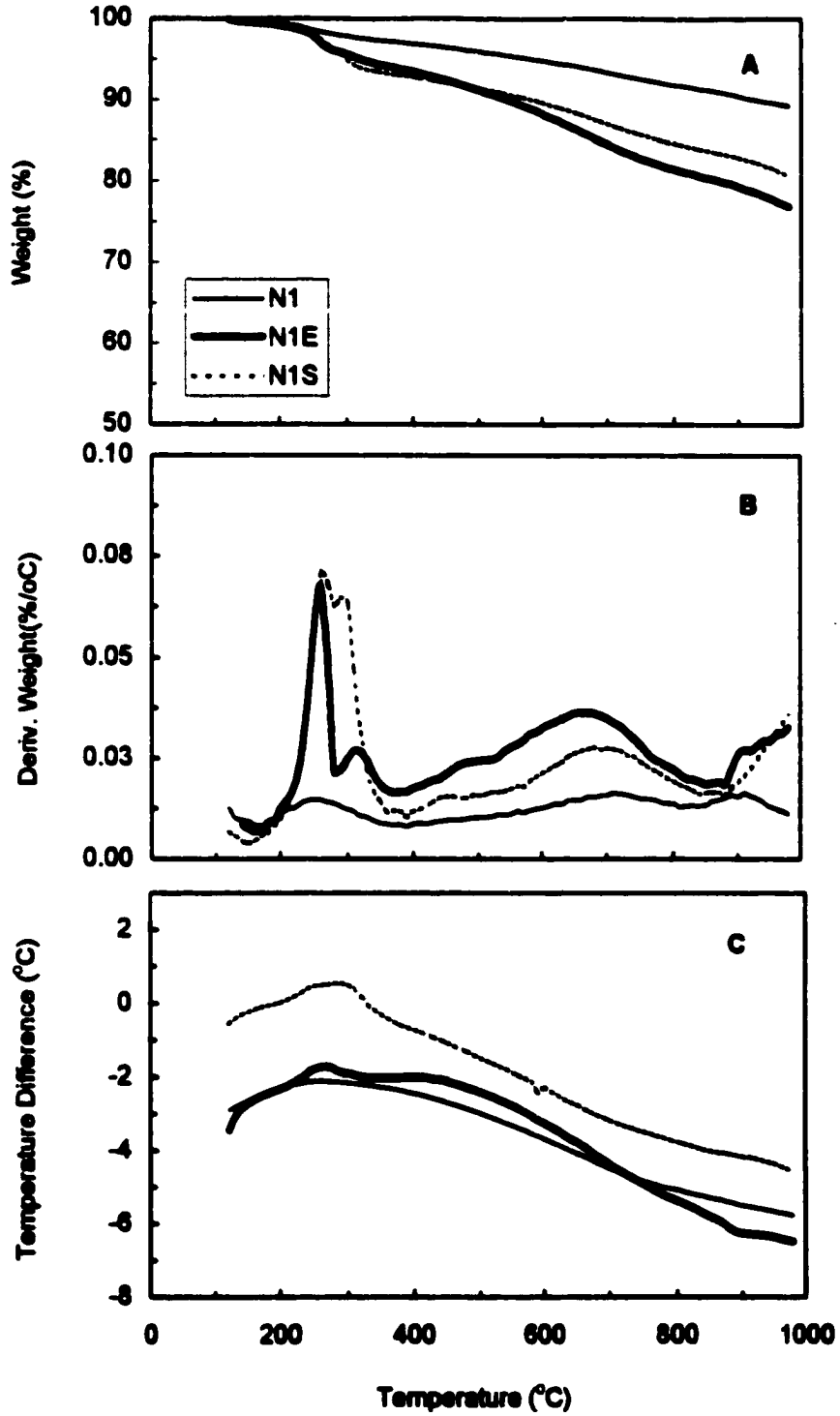

Figure 21. Thermal analysis results for N1 series. TG (A), DTG (B) and DTA (C).

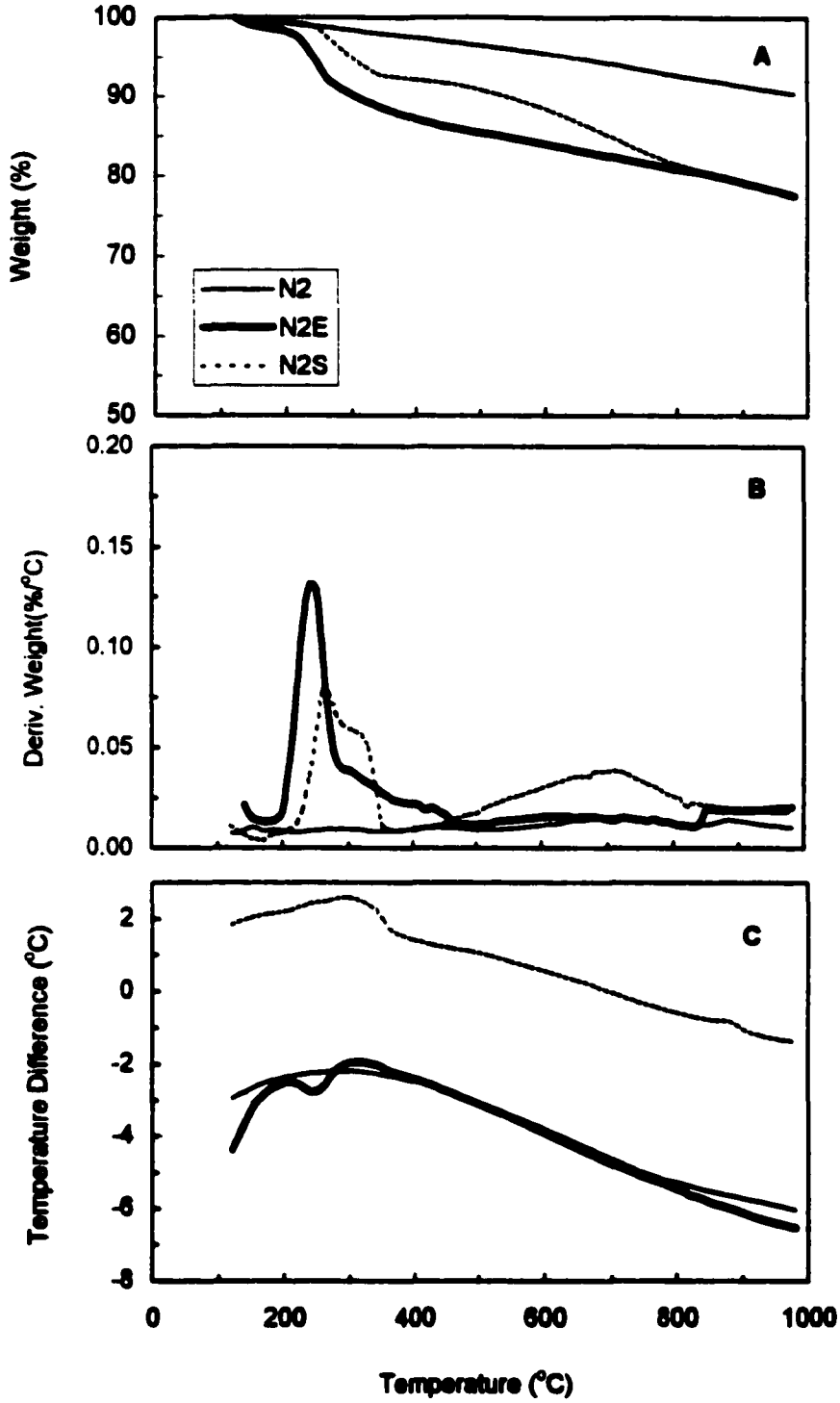

Figure 22. Thermal analysis results for N2 series. TG (A), DTG (B) and DTA (C).

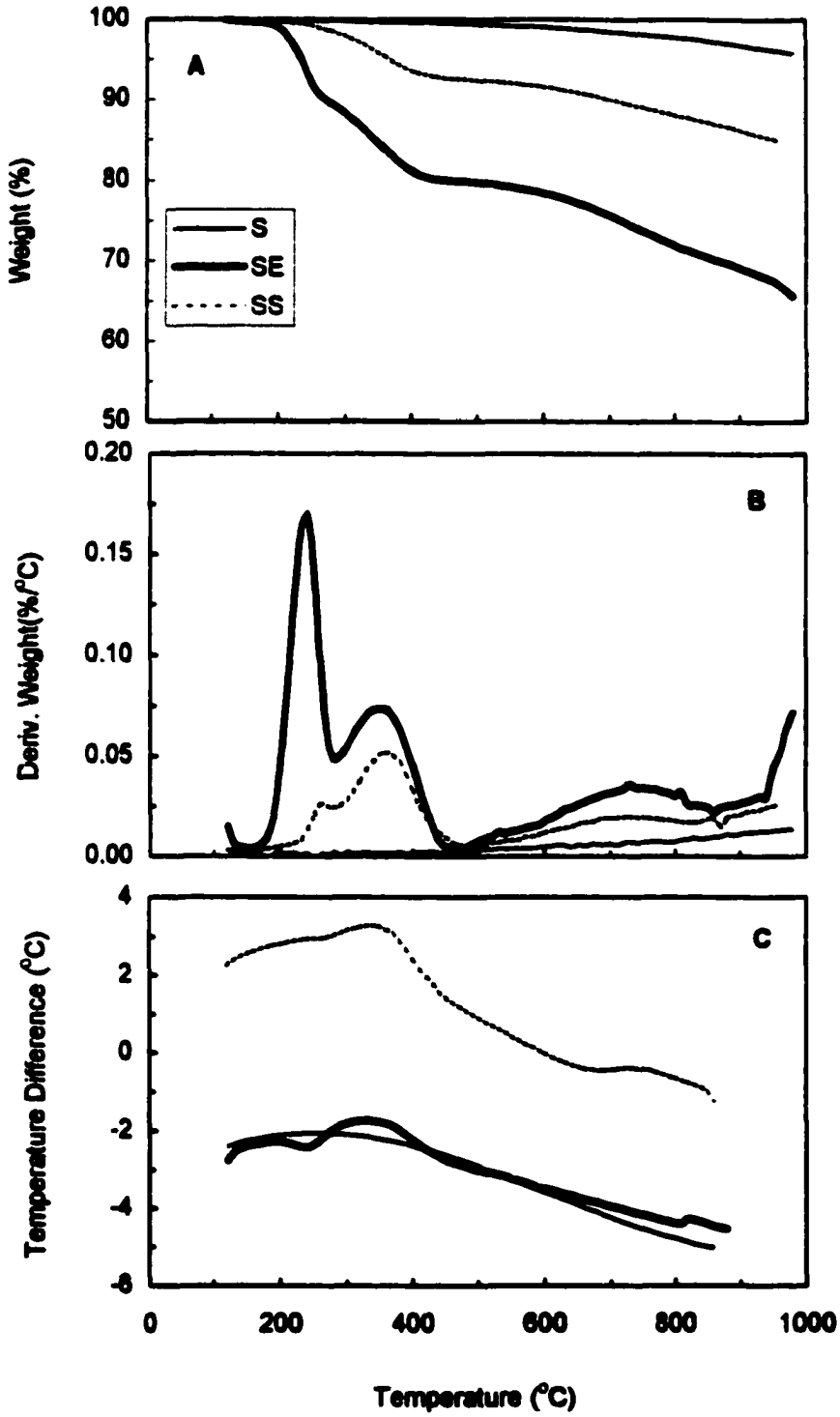

Figure 23. Thermal analysis results for S series. TG (A), DTG (B) and DTA (C).

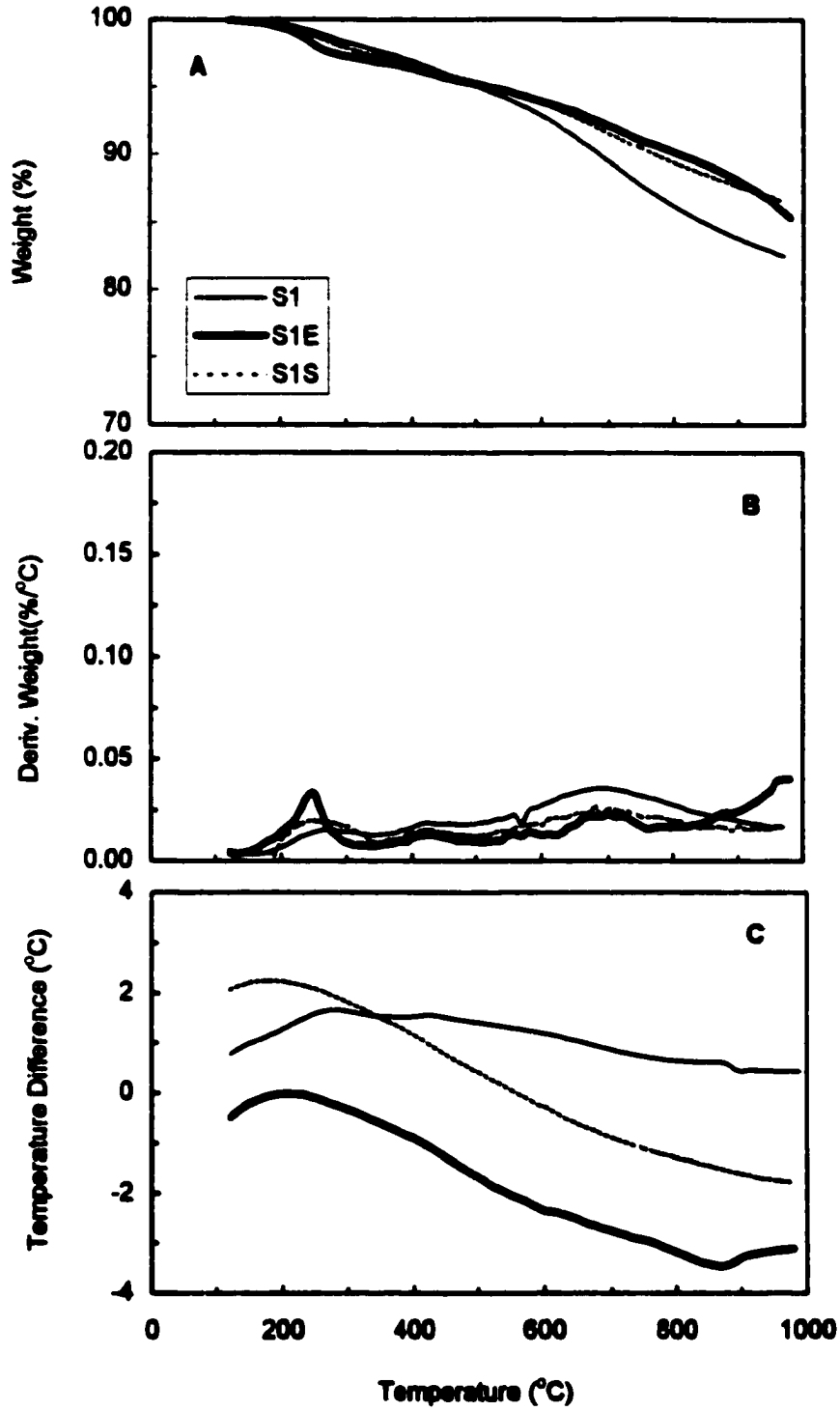

Figure 24. Thermal analysis results for S1 series. TG (A), DTG (B) and DTA (C).

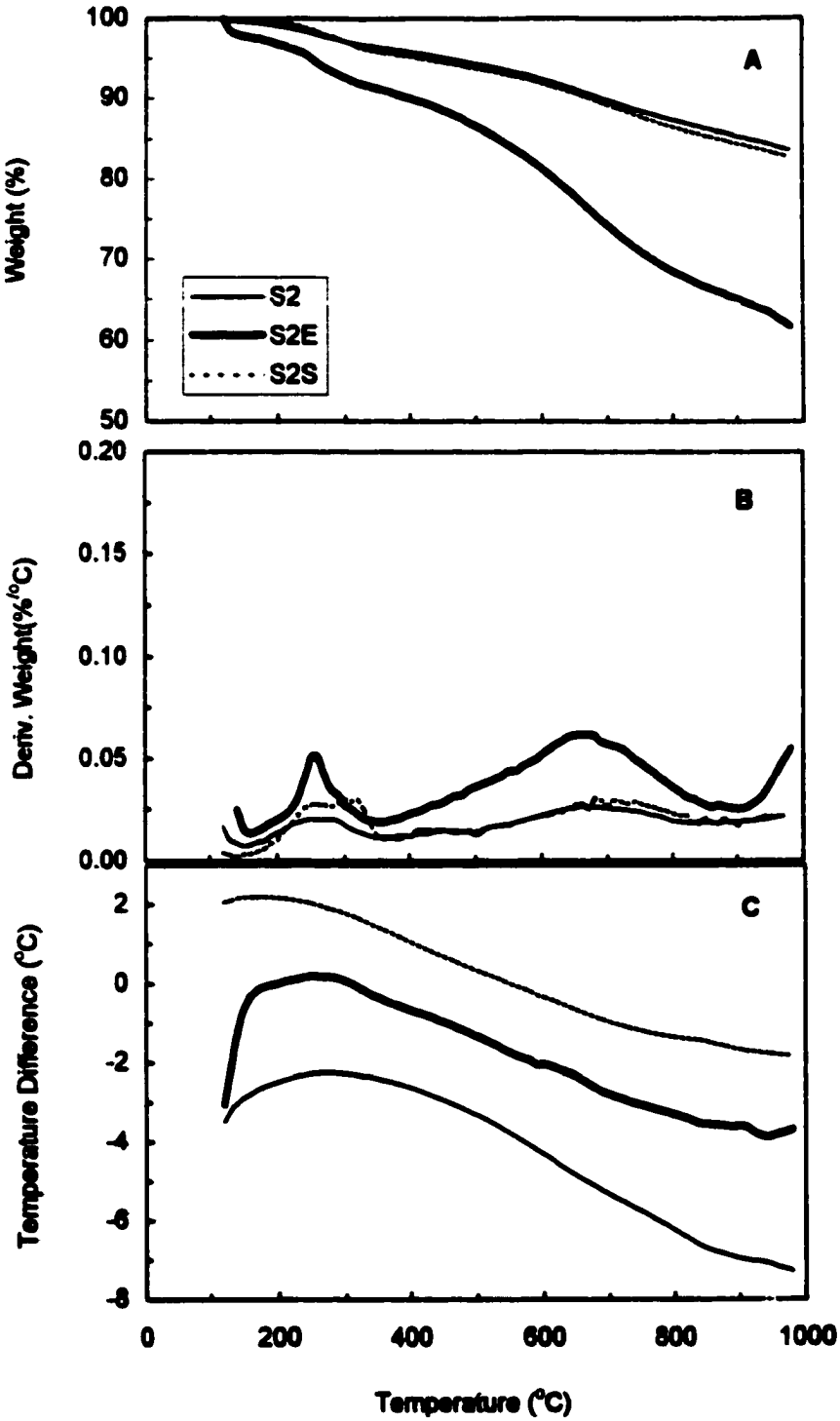

Figure 25. Thermal analysis results for S2 series. TG (A), DTG (B) and DTA (C).

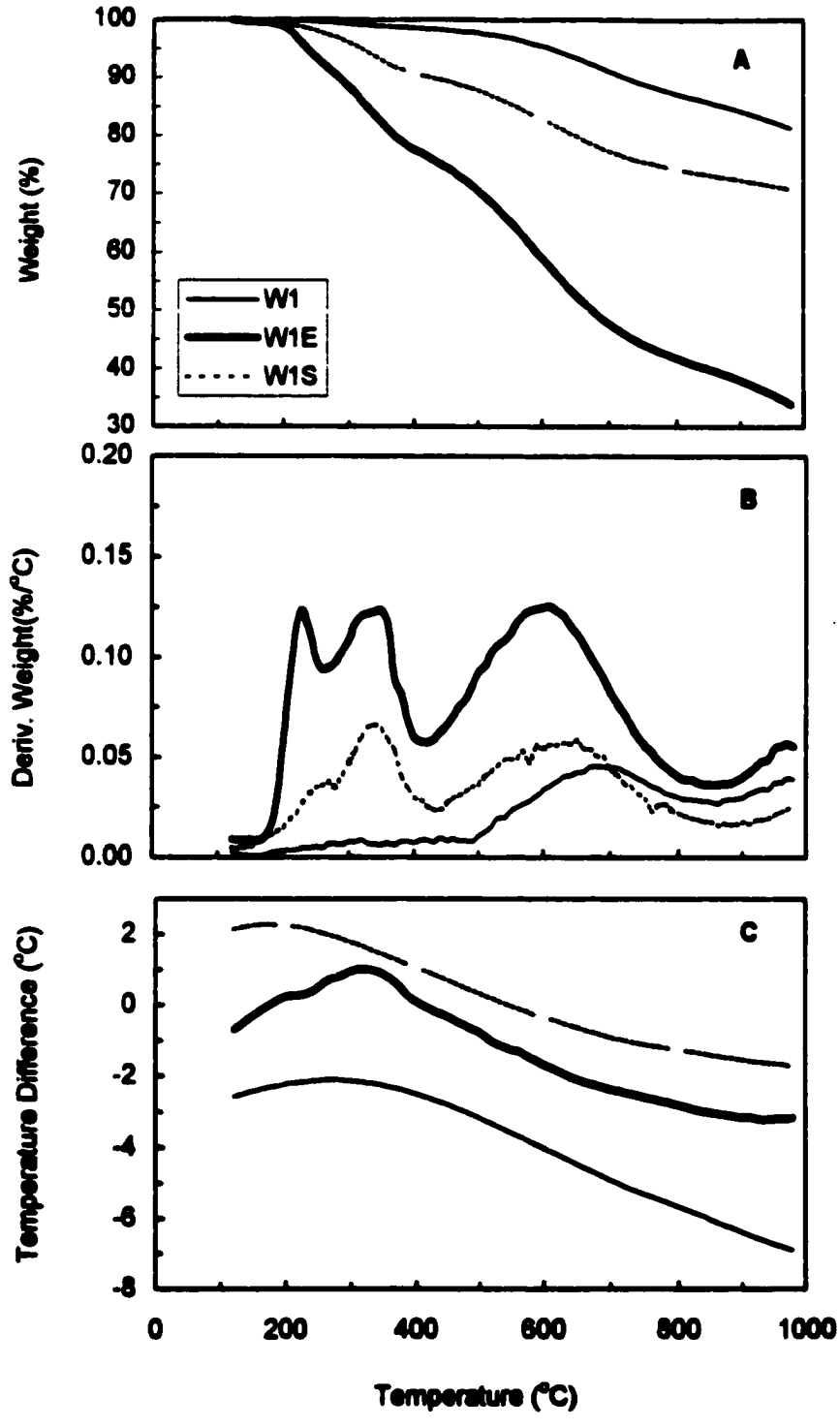

Figure 26. Thermal analysis results for W1 series. TG (A), DTG (B) and DTA (C).

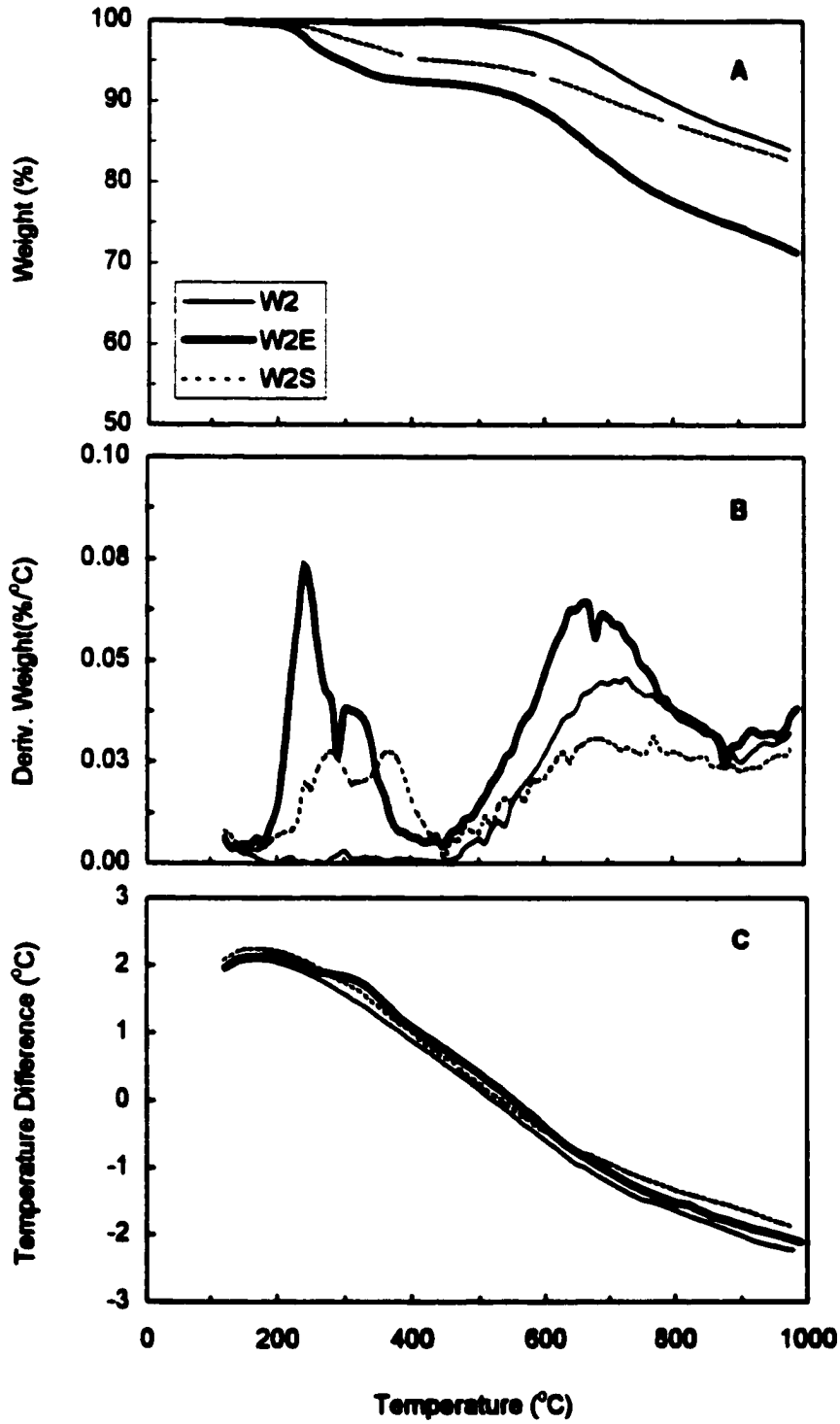

Figure 27. Thermal analysis results for W2 series. TG (A), DTG (B) and DTA (C).

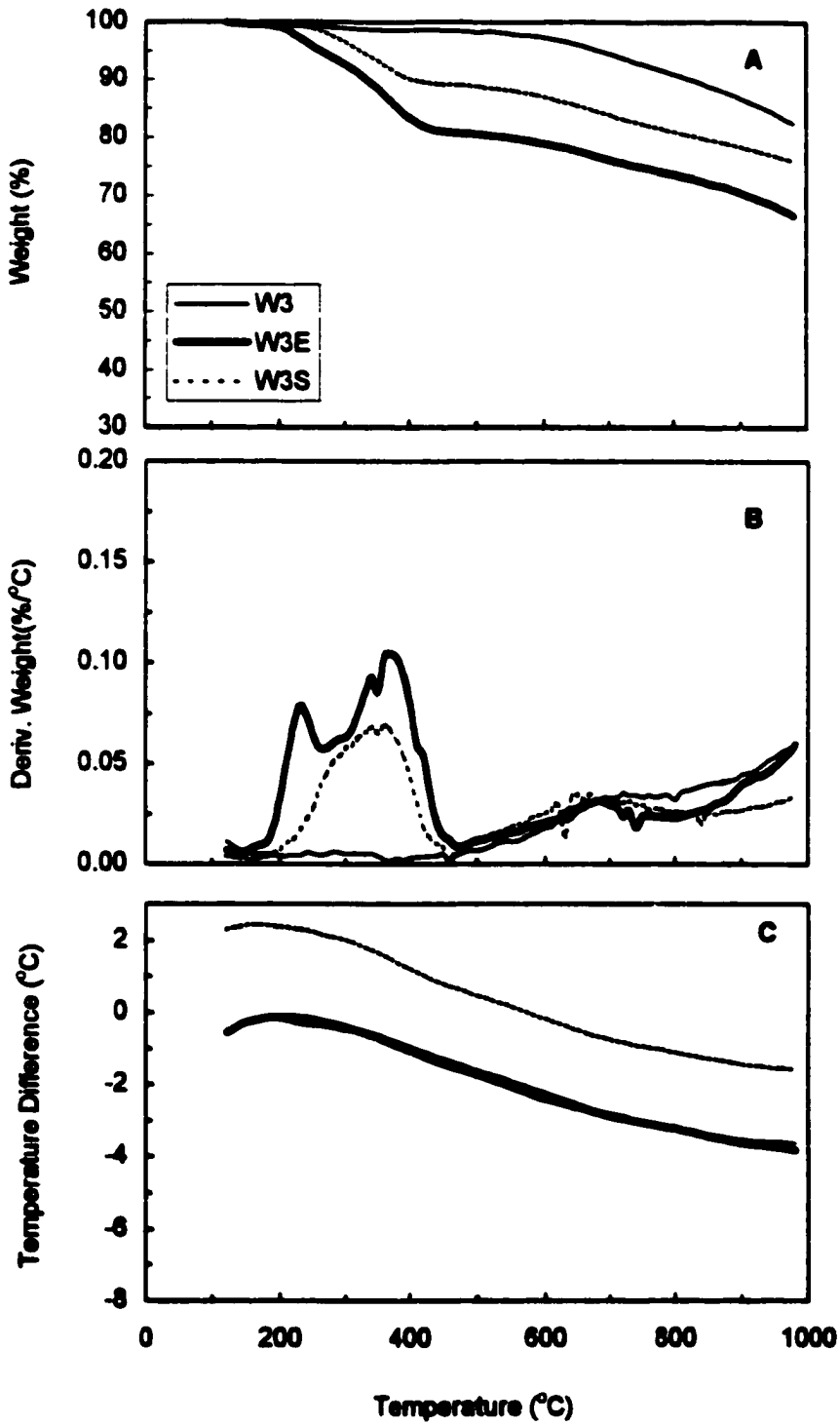

Figure 28. Thermal analysis results for W3 series. TG (A), DTG (B) and DTA (C).

Table 5. Thermal Analysis Weight Loss in Different Temperature Ranges

Sample	Temperature Ranges			Ash Content	Surface pH
	120-500 °C [%]	500-800 °C [%]	120-1000 °C [%]	[%]	
N	1.4	2.6	5.7	3.4	7.7
NE	14.4	4.0	22.5	2.8	2.0
NS	11.2	3.2	17.2	-	4.2
N1	4.1	4.1	10.7	3.0	4.5
N1E	8.8	9.7	23.1	3.5	2.1
N1S	8.6	6.8	19.3	-	4.1
N2	3.6	3.8	9.6	1.7	3.6
N2E	14.5	4.6	22.4	1.4	2.1
N2S	9.2	9.4	22.2	-	3.0
S	0.6	1.6	4.2	1.1	6.9
SE	20.2	7.8	34.4	1.1	2.0
SS	4.3	1.2	8.3	-	5.8
S1	5.0	8.7	17.9	1.1	4.6
S1E	4.8	5.1	14.7	1.1	2.8
S1S	4.7	5.9	13.7	-	4.7
S2	5.6	7.0	16.3	1.2	3.7
S2E	13.3	18.1	38.2	0.5	2.5
S2S	6.2	7.3	17.1	-	5.0
W1	2.2	10.5	18.7	3.1	4.4
W1E	29.5	28.7	66.1	1.7	1.8
W1S	12.3	13.6	29.3	-	2.6
W2	0.5	9.8	16.0	3.8	4.0
W2E	8.3	14.1	28.2	3.0	3.0
W2S	5.4	7.3	17.3	-	4.1
W3	1.7	7.3	17.6	5.2	5.6
W3E	19.4	7.0	33.4	2.1	2.0
W3S	11.2	7.9	24.1	-	2.9

To verify the position of peaks attributed to sulfur compounds, a sample of W-1 carbon was mixed with elemental sulfur and heated at 140 °C until no visual trace of the sulfur was found at the exterior of the carbon. The sulfur, then, was assumed to have been adsorbed in the pores of carbon. Another sample was prepared by impregnating W1 with dilute sulfuric acid. The obtained thermal analysis (TA) curves for these samples are presented in Figure 29. For the sample containing elemental sulfur a well-defined broad peak representing evaporation of sulfur with maximum at 330 °C was noticed. When the carbon was impregnated with sulfuric acid the broad peak with a maximum at 250 °C was revealed. It is worth noting that sulfuric acid, as an oxidant, changed the chemistry of W1 increasing the content of surface oxygen groups represented by the peak centered at 700 °C.

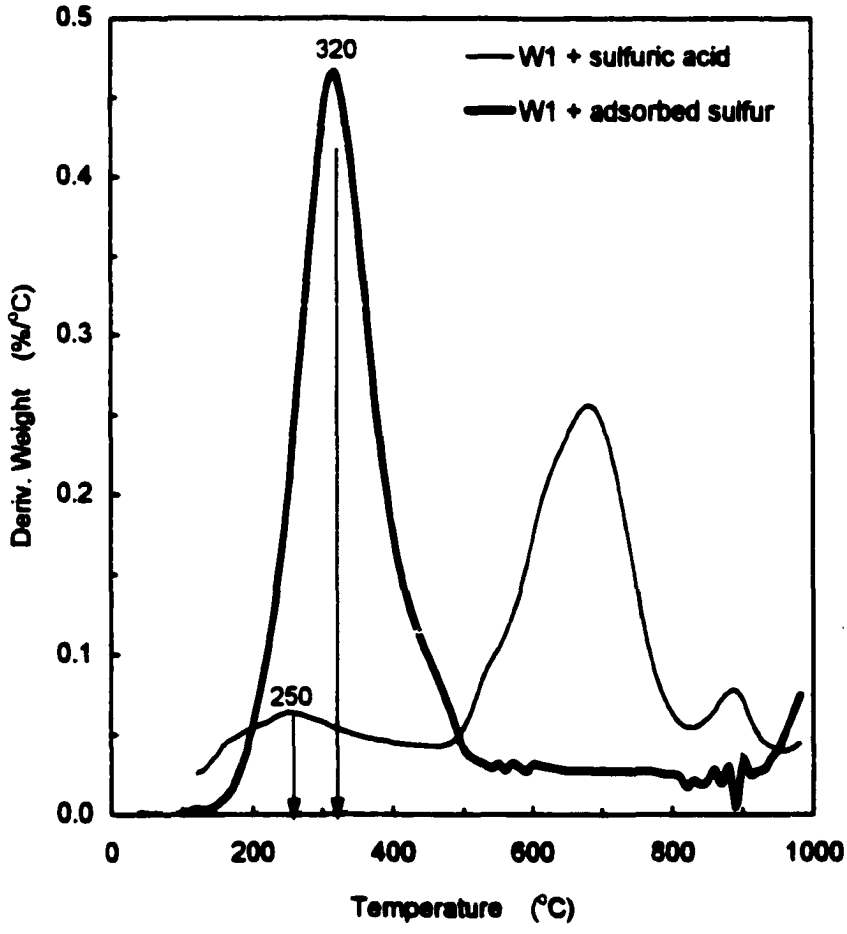

Figure 29. DTG curves for W1 carbon with sulfuric acid or sulfur.

Peaks at the positions similar to those observed in our experiments were also reported in the literature. Rodriguez-Mirasol et al. [66] in their study of adsorption of SO_2 found the peak at 280 °C associated with strongly adsorbed sulfur dioxide, whereas Chang reported the peaks at 280 °C and 490 °C had evolved from various forms of sulfur built into the carbon matrix [67]. Based on these findings and the results of our experiments with the model materials, we assign the first peak at about 250 °C to the presence of oxidized sulfur compounds including sulfuric acid. We assume that H_2SO_4, when present on the carbon surface, upon excessive heating in an inert atmosphere, reacts with carbon material and is reduced to SO_2. The temperature of the peak is in the range of the model material. The presence of sulfuric acid at high temperature in the course of TA experiment alters the chemical inventory of the carbon matrix by introducing new oxygen groups. The second peak (at 330 °C) is assigned to "elemental sulfur" as a result of our finding in sulfur impregnated experiment. Elemental sulfur, however, boils at 444 °C [65] due to its stable long polysulfide chain or S_8 rings. In evaporation of sulfur the long chains are broken down as the energetic sulfur atoms break loose [68]. Steijns and Mars proposed that sulfur in micropores of the size 4-10 Å is present as long-chain biradicals [22]. It is conceivable that sulfur radicals can desorb at lower temperature than sulfur chains due to their structure. Based on these, we assign the second peak at 330 °C to sulfur as *sulfur radicals*.

After H_2S sorption the weight loss significantly increases in the exhausted samples. The W1E shows the most profound peaks on the DTG curve at all temperature ranges (Figure 26). Three well-defined peaks with maxima around 230 °C, 440 °C, and 600 °C are revealed. This sample loses about 50 % of its weight in TA experiment due to

the evolution of sulfur and oxygen products of adsorption process alone (when the weight loss due to W1 is subtracted). That includes products evolved as a result of their interaction with carbon during TA experiment. It is clearly seen that even the third peak, now shifted to around 600 °C, has undergone a major extension. This is an indication that products of the first and second peak do interact with carbon surface probably in introducing more oxygen groups. The comparison of the temperature difference (DTA) curve for W1E with W1 reveals an exothermic effect before the sulfur dioxide desorption, an endothermic effect concurrent with sulfur dioxide desorption and an exothermic effect concurrent with sulfur radicals evolution. The first two effects are attributed to the formation and desorption of sulfur dioxide whereas the last effect indicates that the sulfur evolution is concurrent with some bond forming activities. This can be the formation of sulfur-sulfur bonds or sulfur-carbon bonds. According to Chang, considerable sulfur could be fixed on the surface of a coconut based and a pitch based activated carbon by heating at 475 °C in an inert atmosphere. The resulting sulfur-carbon complex was then stable up to 700 °C in TA measurement [67]. We may conclude that not only surface oxygen groups but also surface sulfur groups may be introduced to the carbon when exhausted carbons are heated.

Considerable recovery of weight loss is observed in the TA curves for W1S. The net weight loss (when the carry over weight loss from W1 is subtracted) is only about 10 % which marks a major improvement compared to 50 % for W1E. Although all three peaks in DTG are reduced, the major reduction is observed for the sulfur oxide peaks. Sulfur oxides being highly soluble can be removed more than the insoluble elemental sulfur. Unlike for W1E, the DTA curve for W1S is featureless, much alike the curve for

W1. This is expected since even though deposited products are not completely removed, their activities are reduced. These results are in agreement with the sorption analysis where an increase in the pore volume after washing was noticed for W1S sample owing to the removal of some of the sulfur oxides and colloidal sulfur.

The W3E sample has shown slightly less capacity for H_2S removal than W1E but its weight loss in TA is much smaller (Table 5). An explanation for this behavior can be found in the extent of the sulfur oxide peak, which is much narrower than that of W1E (Figure 28). As indicated above, this carbon is more basic than W1 (Table 1) and its volume of micropores is smaller (Table 4). It is likely that this carbon has higher selectivity (ability of a carbon to favor the formation of a species against the other products of oxidation of H_2S) toward sulfur in comparison with W1E. As a result, the washing has been less successful in retrieving the deposited products despite the larger pores in this carbon. The DTG curve for W2E reveals a well-pronounced peak for sulfur oxides and a smaller one for elemental sulfur (Figure 27). This means that despite its less capacity this carbon has more selectivity towards sulfur oxides. Washing has been more effective for this carbon in the W series owing to more solubility of the deposited products and larger pores (Table 4). In our interpretation of the data we are aware of the presence of carbon dioxide released as a result of interaction of H_2SO_4 and carbon, especially when the yield of sulfuric acid was high. We assume that the amount of CO_2 is much smaller than the amount of sulfur species present on the carbon surface, especially when sorption of hydrogen sulfide was significant.

The highest TA weight loss in N and S series, found for SE, is in agreement with its high H_2S removal capacity (Table 5). The most profound peaks for sulfur oxides also

appear on the DTG curve for the SE sample. The intensity of the peak at around 250 °C is slightly lower for NE and significantly lower for the oxidized samples (Figures 20 to 25). Similar trend is observed for the second peak of exhausted samples located around 330 °C. This peak is assigned to the sulfur radicals. For SE a well defined peak is revealed in the temperature range 250 °C to 450 °C. In the case of NE several species are removed in this temperature range resulting in a broad peak extended to 500 °C. The DTG curves for oxidized samples differ from their initial counterparts. While on the curve for N1E a peak similar to that for SE is present, its intensity is lower. The DTG curve for N2E is interesting in that this carbon, despite its low capacity for H_2S removal, has shown a high selectivity for sulfur oxides. S1E and S2E show even more selectivity for sulfur oxides so that their DTG curves are featureless in the second peak region suggesting that very small amount of sulfur radicals have formed during hydrogen sulfide adsorption.

A general trend observed for all exhausted carbons is that more acidic environment favors the formation of sulfur oxides and sulfuric acid despite rendering small H_2S removal capacities. On the other hand, basic environment favors the formation of elemental sulfur (sulfur radicals) rendering high capacities.

As mentioned above, N has a trace amount of unwashable carbonate from its precursor. This imposes a basic environment in its micropores. The results of nitrogen adsorption and thermal analyses for NE suggest that, unlike in other carbons, considerable amount of sulfur eight-member rings or polymers have formed on this carbon causing the blockage of micropores. This is in partial agreement with the radical pathway mechanism proposed by Hedding and Rao [27] for the oxidation of H_2S in which the oxygen radicals (i.e. superoxide anion) are the active oxidants [69, 70]. It is

proposed by Hoigne and Bader [71, 72] that while common promoters for the formation of potent superoxide anion from less active hydroxyl radical include aryl group and carboxylic acids, bicarbonates and carbonates are the major inhibitors of such a transformation. Both aryl groups and carboxylic acids are abundant on the surface of oxidized carbons promoting the formation of highly potent superoxide ion which is capable of oxidizing sulfur to its higher states such as SO_3. On the contrary, caustic impregnated carbons are characterized by a huge content of carbonate and bicarbonate, which form as a result of reaction between the caustic and atmospheric carbon dioxide [6]. These compounds act as scavengers of hydroxyl radical and compete with sulfur. Hence, the oxidation will hardly exceed the lower states such as elemental sulfur.

Sulfur radicals may be considered as active forms of sulfur with a low energy of activation for oxidation [22]. Although the number of sulfur atoms in the radicals are variable it is reasonable to assume that in comparison to sulfur rings, they are smaller compounds and they desorb at a lower temperature. In fact while the elemental sulfur (ring) boils at 444 °C, the peak assigned to the desorption of sulfur radicals is located at around 330 °C. Another noteworthy behavior of sulfur radicals is their interaction with surface groups resulting in an array of intermediates and new radicals [73]. Unlike unreactive, insoluble and bulky sulfur rings, these compounds are capable of interactions with carbon surface during washing process causing its oxidation along with creation of more water soluble sulfur oxides. The DTG curves representing the SS carbons (Figure 23) and the data collected in Table 5 indicate a significant regeneration of the carbon surface. On the other hand, bulk of the sulfur content remains deposited on NS (Figure 20). It is notable that in the case of NS a new peak is observed after washing around 490

°C. This is likely the result of the desorption of sulfur polymers, created from radicals during washing and strongly adsorbed on the carbon surface. If formed, the sulfur rings are resistant to oxidation and cannot be easily removed by washing. It follows that they are likely to constitute permanent deposits on the carbon surface, diminishing its capacity for regeneration. In the case of N1S and N2S, the sulfur radical peak is shifted toward lower temperature where sulfur oxides desorb. The intensity of this peak has significantly increased. This feature suggests that the sulfur radicals have actually been oxidized to sulfur oxides during washing. Similar trend is observed in S2S in smaller scale. S1E is the only carbon on which only sulfur oxides have formed during adsorption process. They are effectively removed by washing (SS).

3.7. Analysis of the Products of Oxidation of H_2S

The analysis of carbon surface chemistry and the effects of oxidation of hydrogen sulfide and subsequent Soxhlet washing on the carbon surface were also investigated using Fourier Transform Infrared Spectroscopy (FTIR). It was found that the method was more successful for wood based carbons, which contain a broader variety of surface groups and lower degree of carbonization. Two of them, W1 and W3, have superior H_2S capacities. Having smaller density of surface groups and H_2S oxidation products, the other carbons tend to reveal lower intensity peaks, which can not be easily distinguished from background. The spectra for initial W carbons are shown in Figures 30A to 32A. According to the approach proposed by Zawadzki [74] we link the bands at 1720 cm^{-1}, 1600 cm^{-1} and 1300 cm^{-1} to vibrations of C=O, C--O, and C-O bonds, respectively. They indicate the presence of various oxygen groups such as carboxyls, lactones or phenols

[19]. Since Westvaco carbons are prepared at a relatively low temperature, even the presence of oxygen groups such as aliphatic aldehydes and ketones, can not be ruled out. Carbon structure contributes to the bands at 1600 cm^{-1} and 1300 cm^{-1} [67]. The peaks observed between 1000 cm^{-1} and 700 cm^{-1} may represent either P-C bonds owing to the presence of organic phosphorus (residue from activation process) or PO_4^{3-} species [75]. Although all three carbons show similar features of surface chemistry, the bands differ in their intensities and the order of decreasing intensity is the same as the decrease in the hydrogen sulfide breakthrough capacity (i.e., W1 has the most profound peaks and W2 has the least).

New peaks are observed on the spectra upon sorption of H_2S. To exclude the interference form the initial carbon materials, the spectra of initial carbons was subtracted from both exhausted and Soxhlet washed [19, 76]. The obtained spectra are shown in Figures 30B to 32B. Inorganic oxidized sulfur species are expected to absorb energy in the range between 400-1200 cm^{-1}. Washing modifies the spectra of all exhausted samples. The most significantly decreased bands in intensity are at 580 cm^{-1}, 700 cm^{-1}, 850 cm^{-1}, 950 cm^{-1}, 1050 cm^{-1}, and 1150 cm^{-1}. They represent SO_4^{2-} (580 cm^{-1}, 1150 cm^{-1}) and HSO_4^- (850 cm^{-1}, 1050 cm^{-1}). At 580 cm^{-1} and 1150 cm^{-1} there is also a possibility of vibrations from SO_3^{2-}. The decrease in the intensity of the band around 950 cm^{-1} may be related to the removal of some water-soluble phosphates, not completely washed out prior to the breakthrough experiments. It is worth noting that the intensities of the bands for exhausted carbons are in agreement with the expected content of oxidized sulfur species; the highest intensities are noticed for W1E, the lowest for W2E.

The spectra for N and S series show less intense peaks (Figures 33 to 38). The subtracted spectra for NE and SE carbons (33B and 36B), which have demonstrated notable H_2S capacities, show small band increases around 580 cm^{-1}, 1050 cm^{-1}, and 1150 cm^{-1} in comparison with their washed counterparts. The TA results indicated that much of the peak associated with sulfur oxides in SE was removed during washing in Soxhlet. Interesting observation can be drawn from the subtracted spectra for N1E and N1S (Figures 34B). The TA results indicated that this carbon had oxidized its sulfur radical deposits to additional sulfur oxides during Soxhlet washing. The FTIR results for N1S show a new peak at 680 cm^{-1}, associated with sulfur oxides. The spectra for N2E and N2S (Figure 35) show a similar trend but with less intensity.

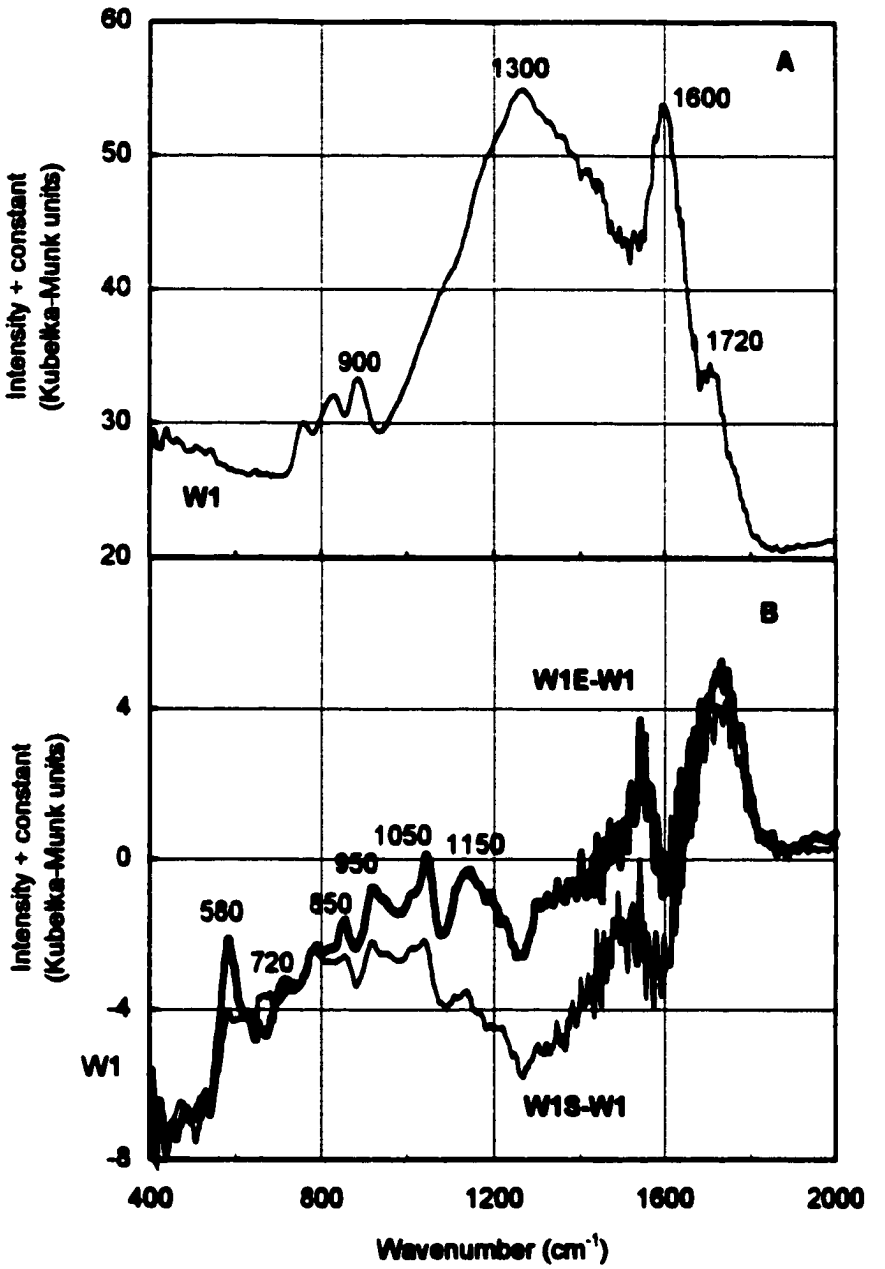

Figure 30. FTIR spectra for W1 (A) and the exhausted and washed carbons after the subtraction of the initial material (B).

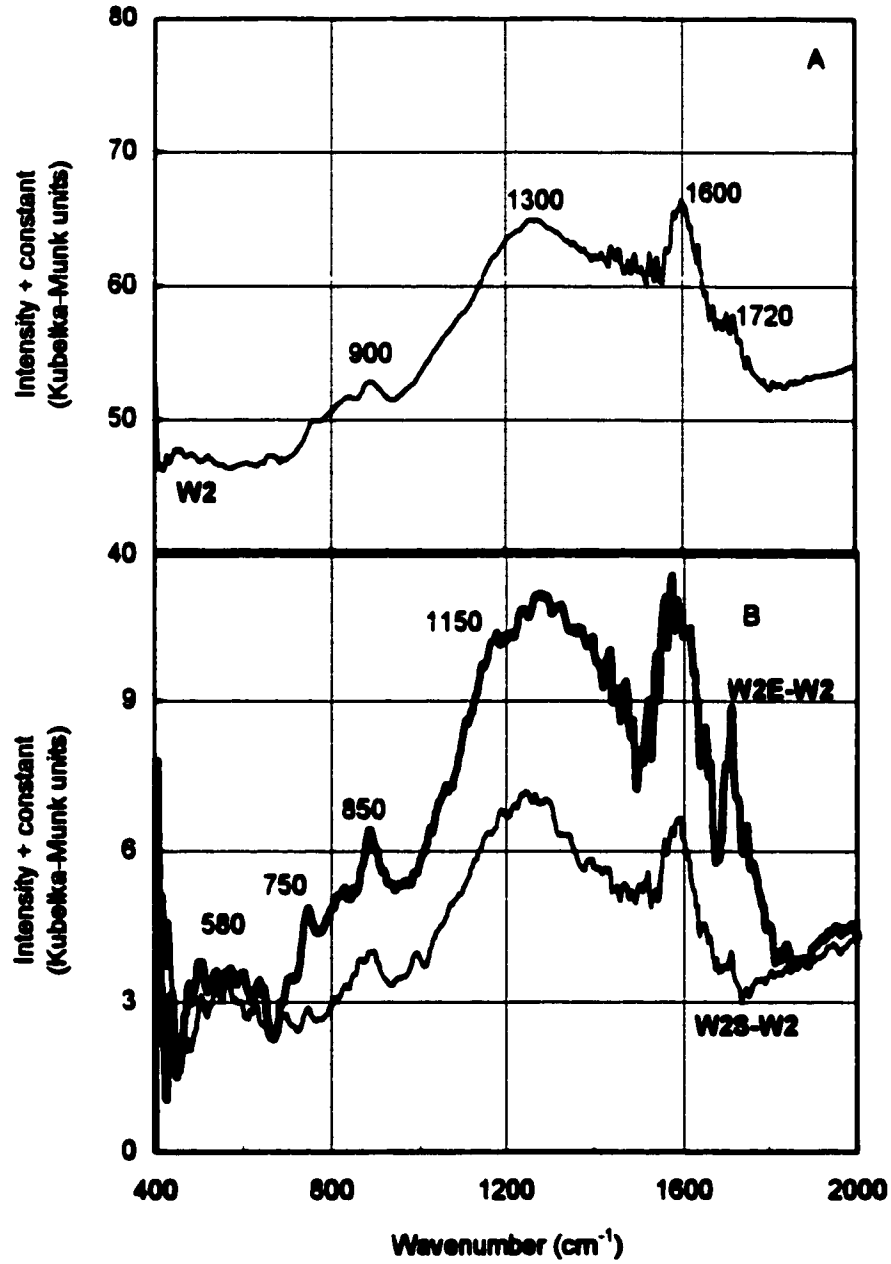

Figure 31. FTIR spectra for W2 (A) and the exhausted and washed carbons after the subtraction of the initial material (B).

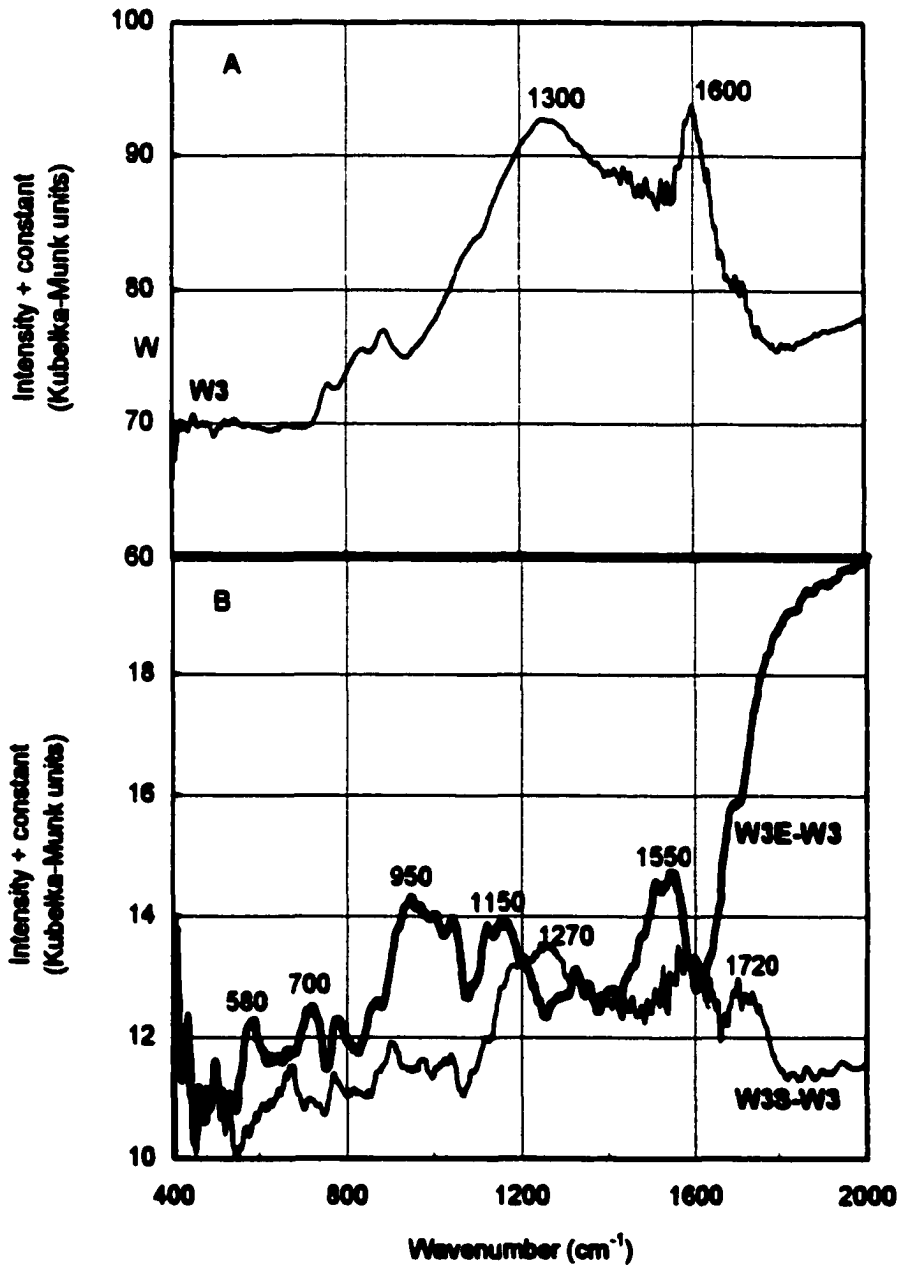

Figure 32. FTIR spectra for W3 (A) and the exhausted and washed carbons after the subtraction of the initial material (B).

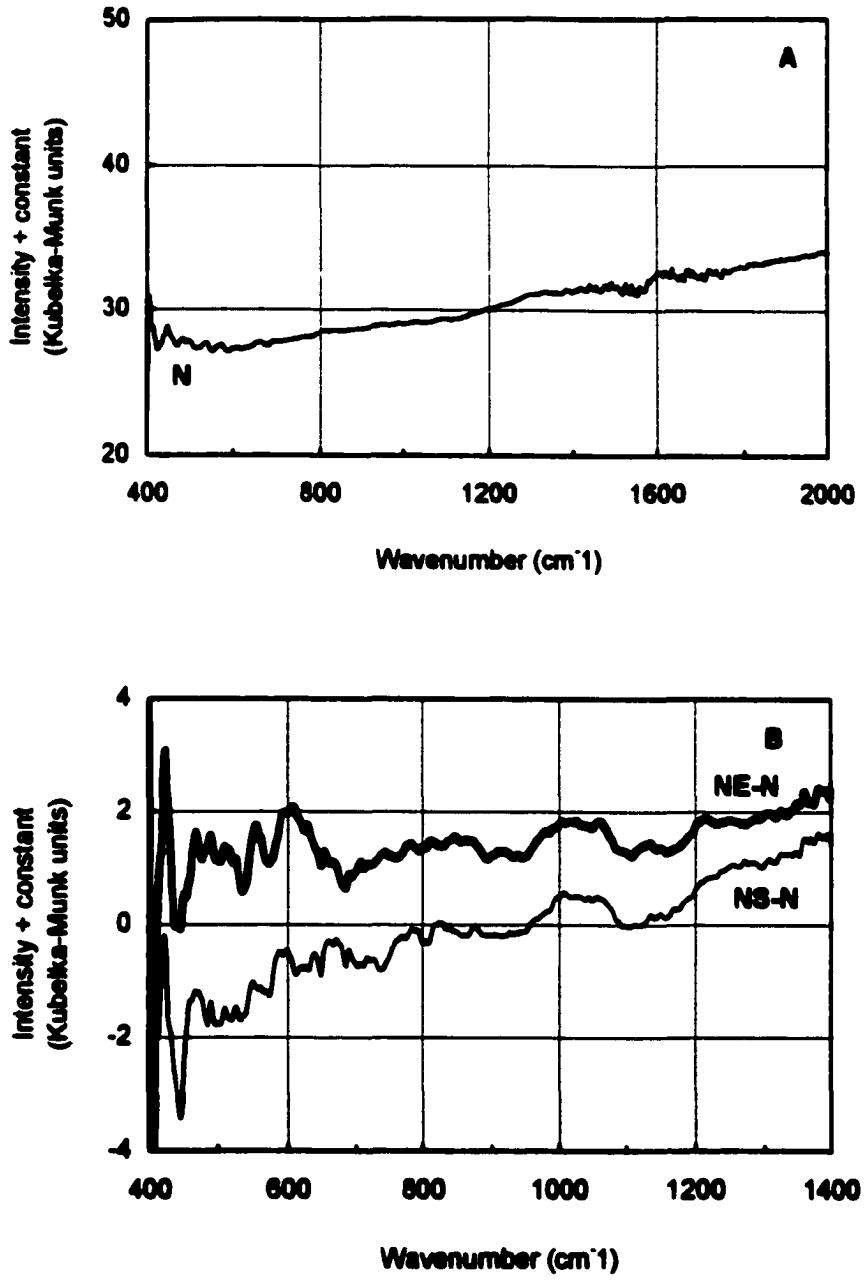

Figure 33. FTIR spectra for N (A) and the exhausted and washed carbons after the subtraction of the initial material (B).

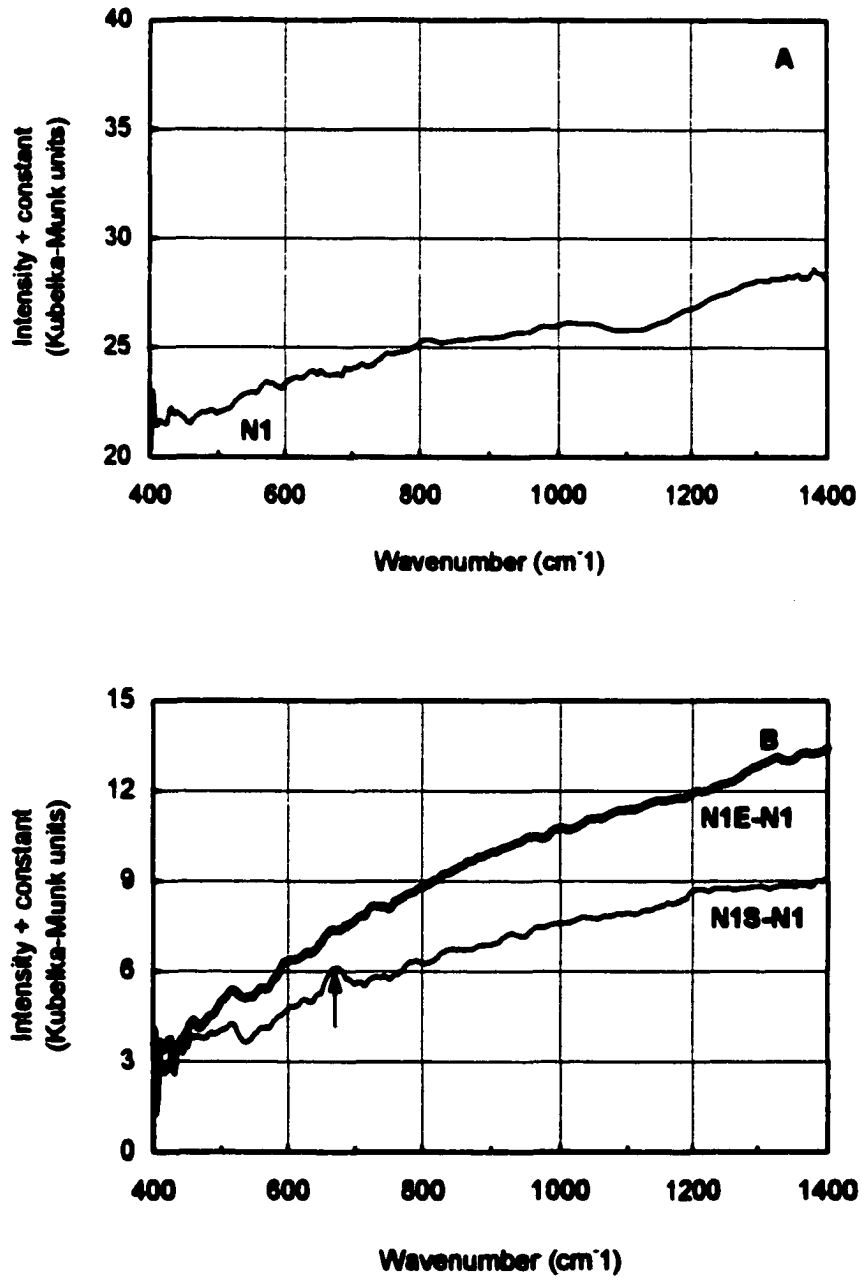

Figure 34. FTIR spectra for N1 (A) and the exhausted and washed carbons after the subtraction of the initial material (B).

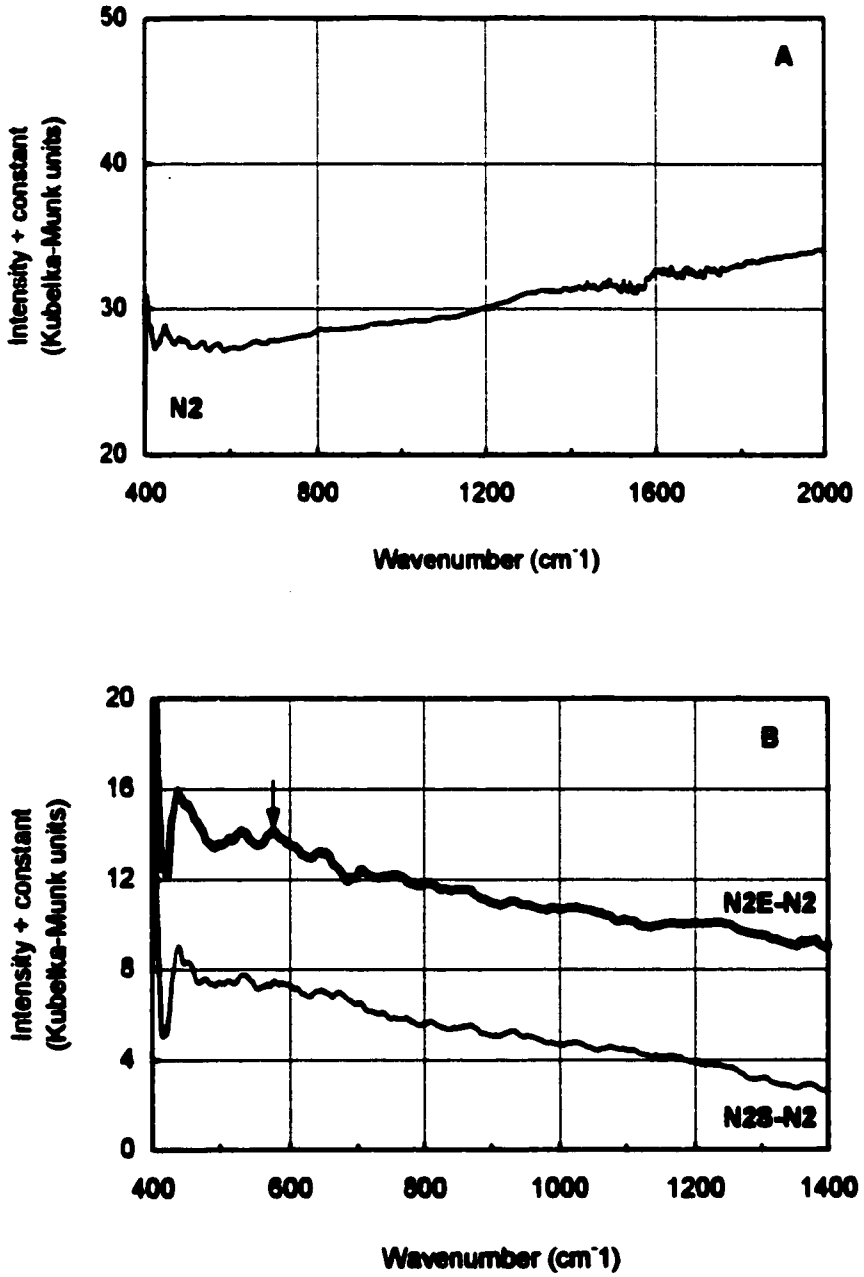

Figure 35. FTIR spectra for N2 (A) and the exhausted and washed carbons after the subtraction of the initial material (B).

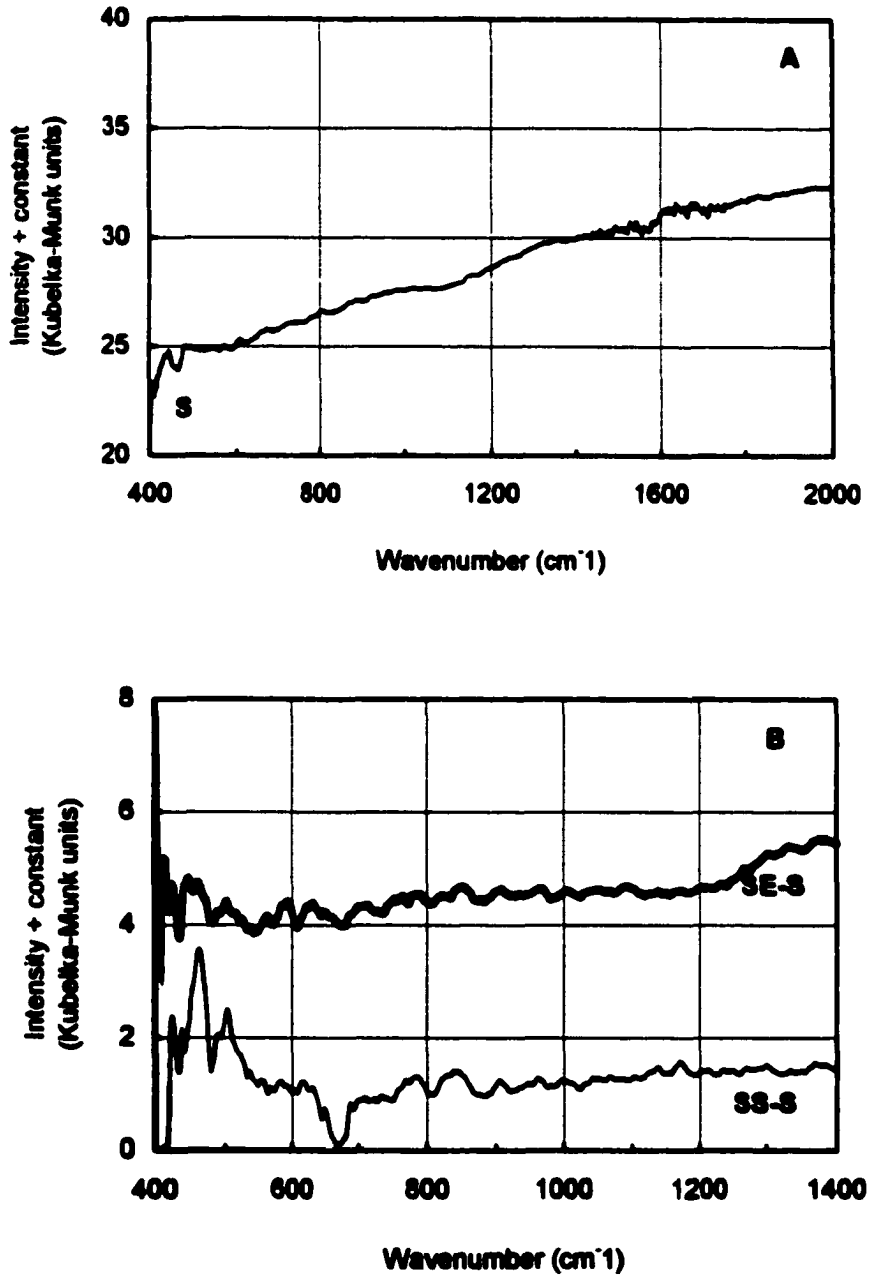

Figure 36. FTIR spectra for S (A) and the exhausted and washed carbons after the subtraction of the initial material (B).

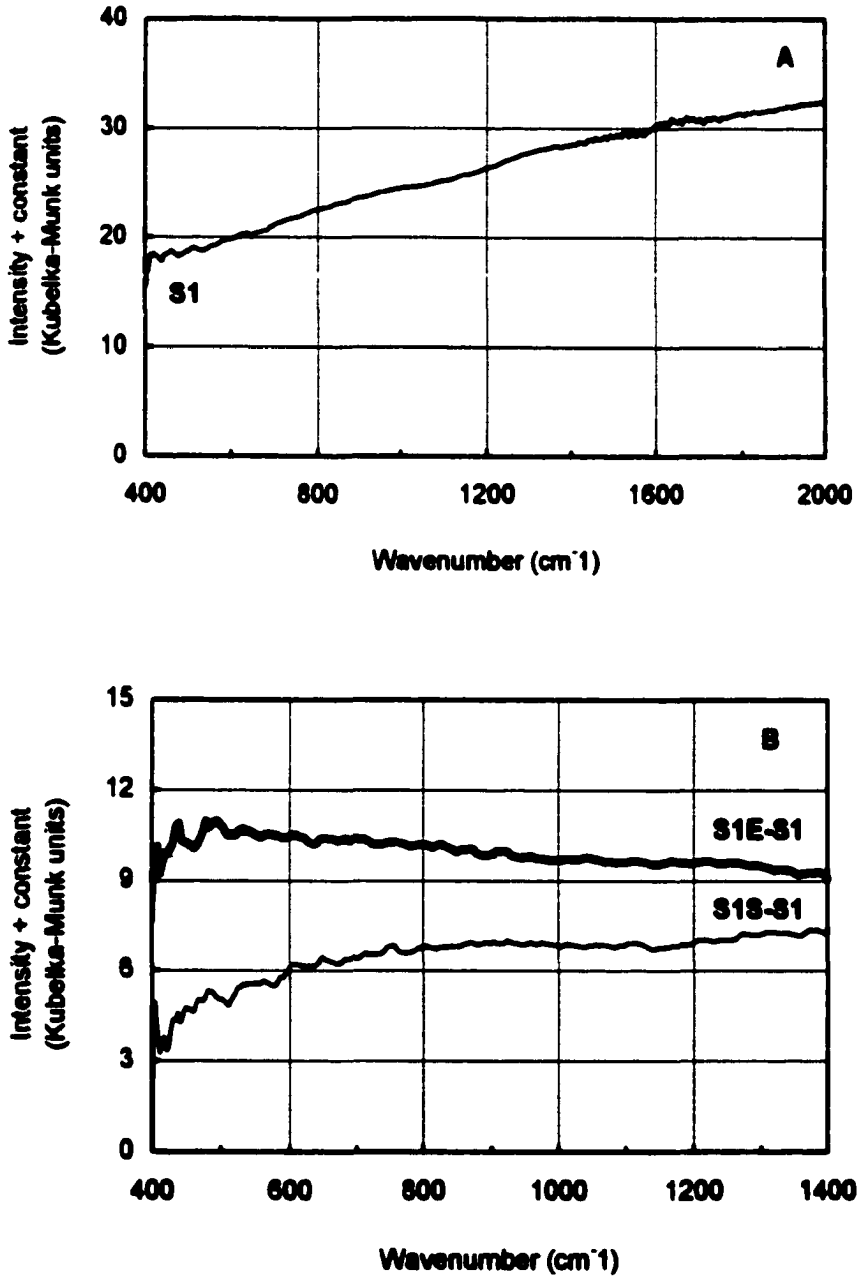

Figure 37. FTIR spectra for S1 (A) and the exhausted and washed carbons after the subtraction of the initial material (B).

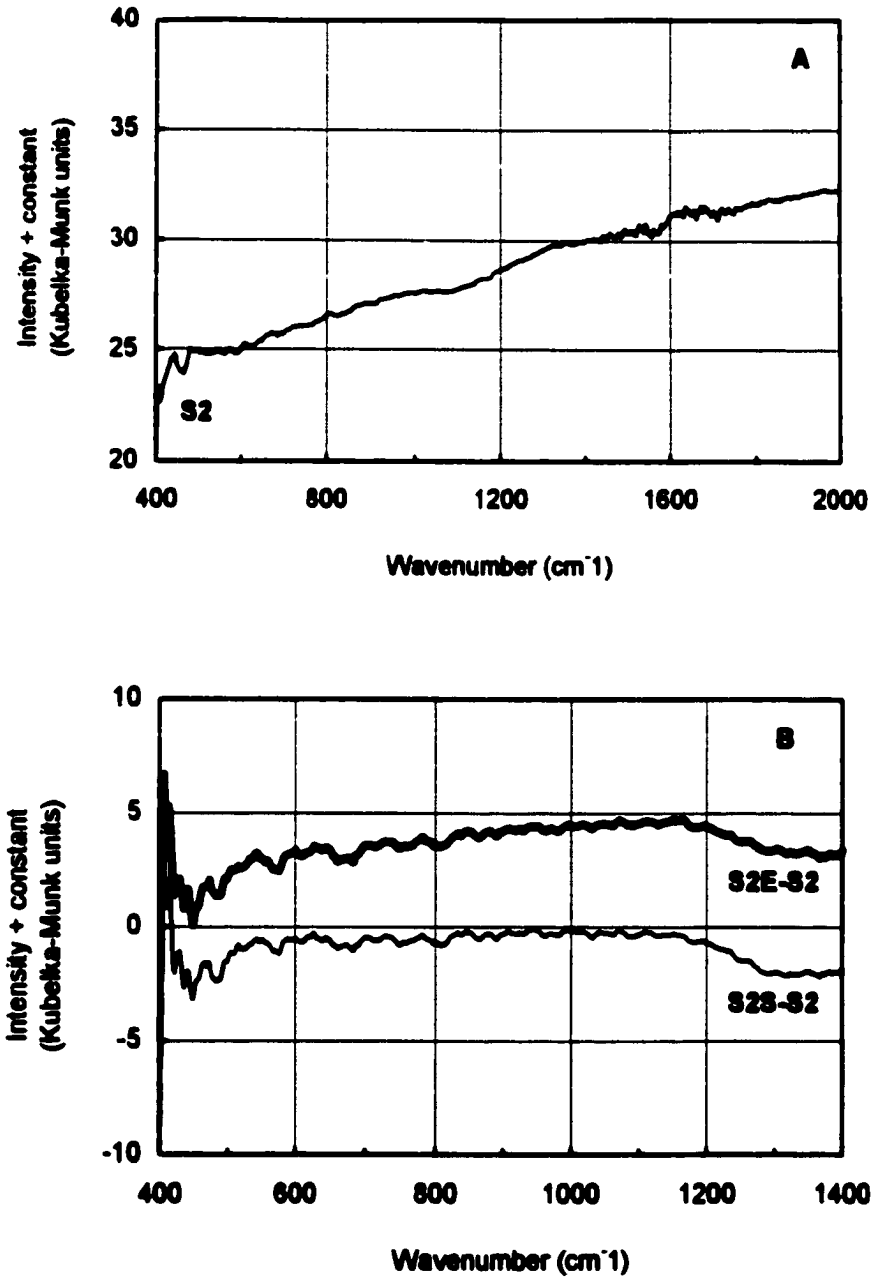

Figure 38. FTIR spectra for S2 (A) and the exhausted and washed carbons after the subtraction of the initial material (B).

3.8. Surface Parameters that Determine the H_2S Adsorption Capacity of Carbon

Analyses of surface chemistry and pore structure of carbon were discussed in previous sections. To identify the surface parameters crucial for the enhancement of the hydrogen sulfide adsorption capacity, the dependence of the measured capacity on the surface features described above was analyzed. No direct relationship between the performance of carbons as H_2S adsorbents and the parameters of pore structure was found, however, higher micropore volume along with smaller pores result in enhanced capacity (Figures 17 to 19, and Table 4). For an effective removal of H_2S, the total pore volume of carbon should be high enough to accommodate for significant amount of sulfur as the reaction product. Hence, comparison of the performances of carbons should be based not only on their breakthrough capacity but also on their total pore volume. For the purpose of comparison, the breakthrough capacity was normalized by dividing it by the total pore volume of each carbon (Table 4). As indicated above and in the literature [19, 20], immobilization of hydrogen sulfide within pore structure is a result of its dissociation in the pre-adsorbed water film to HS^- ion and adsorption of the latter followed by its oxidation. The extent of dissociation should depend on the local pH in the pore system, which is governed by surface chemistry. The comparison of characteristics of surface chemistry should be based on the surface distribution (density) of these features obtained by dividing the number of groups by the total surface area of each carbon (Table 4). Then, the dependence of normalized breakthrough capacity on five quantities affecting dissociation of hydrogen sulfide in the pore structure is analyzed. These are: pH of carbon surface, surface density of acidic groups, weight losses between 120 °C and 500 °C (associated with the destruction of strong acids such as carboxyls and

lactones [47]), the density of surface oxygen calculated from the TPD results (Table 2), and water adsorption capacity at 30 % relative humidity (Figure 39). A good linear correlation was not found in any of the cases. Analysis of the plots presented in Figure 39 suggests that there is a certain threshold value in each of those parameters beyond which significant changes in the capacity occur. An estimate of the threshold values may be a surface pH of more than 4.5, 1.2 $\mu eq/m^2$ of acidic groups, around 3.5 $\mu mol/m^2$ of adsorbed water, 2 $\mu mol/m^2$ of surface groups' oxygen, and around 3 % of weight loss between 120 °C and 500 °C. An increase in pH beyond the reported value increases the capacity, whereas an increase in the other four parameters (number of acidic groups, weight loss, surface groups oxygen, and water adsorption) significantly decreases the performance of carbons as H_2S adsorbents.

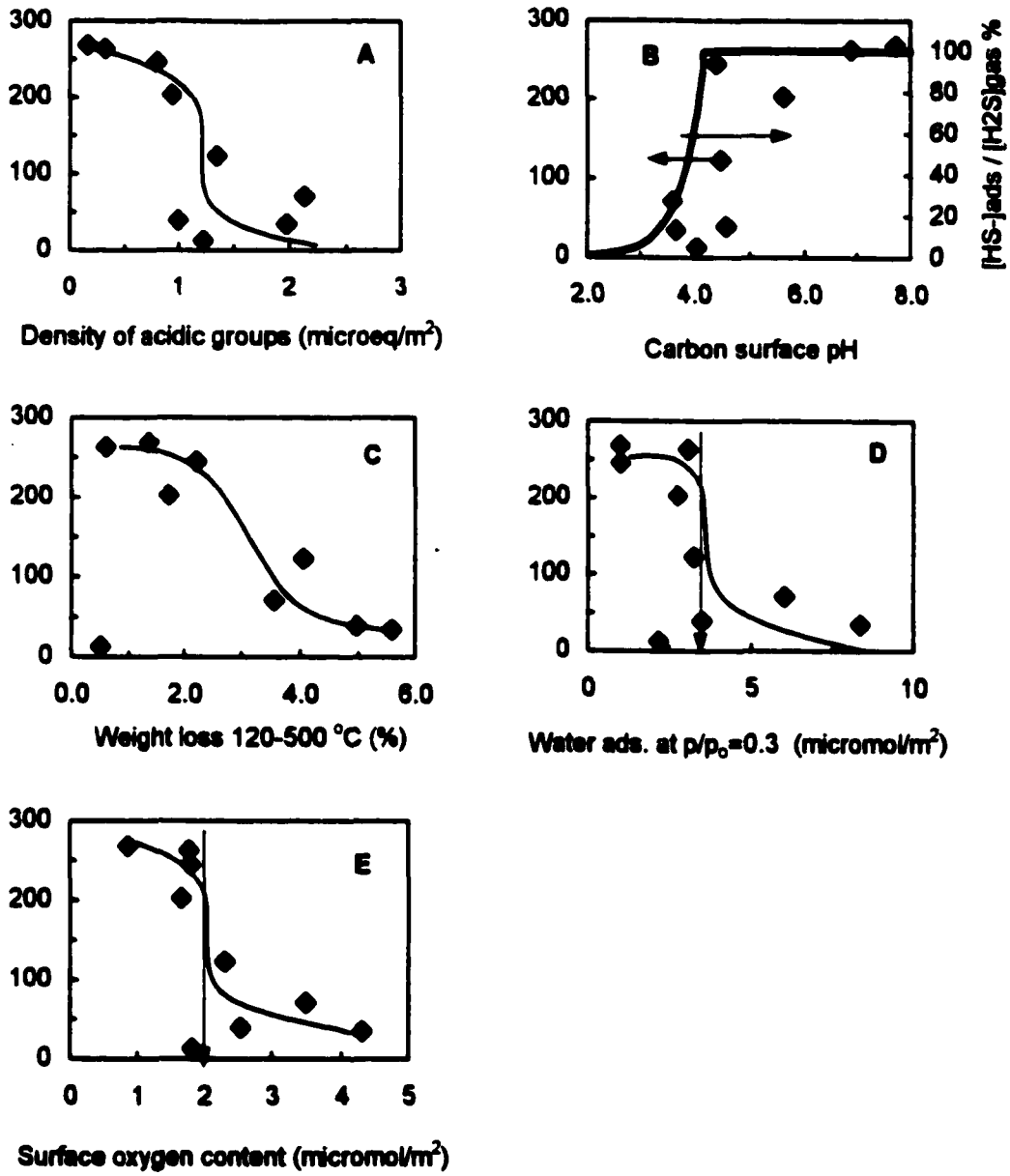

Figure 39. The dependence of normalized H_2S adsorption capacity (mg/cm^3) on several characteristics of carbons.

3.9. The Role of pH in the Mechanism of H_2S Adsorption/Oxidation on Activated Carbon

Based on the above, the following pH dependent mechanism is proposed for the adsorption/oxidation of H_2S on the surface of activated carbon. It is assumed that the process proceeds as: 1) H_2S adsorption on the carbon surface, 2) its dissolution in water film, 3) dissociation of adsorbed H_2S in in water film, and 4) surface reaction with oxygen:

$$1)\ H_2S_{gas} \xrightarrow{K_H} H_2S_{ads} \qquad (3.5)$$

$$2)\ H_2S_{ads} \xrightarrow{K_S} H_2S_{ads\text{-}liq} \qquad (3.6)$$

$$3)\ H_2S_{ads\text{-}liq} \xrightarrow{K_a} HS^-_{ads} + H^+ \qquad (3.7)$$

$$4)\ 2HS^-_{ads} + O^*_{ads} \xrightarrow{K_R} 2\,S_{ads} + H_2O \qquad (3.8)$$

where H_2S_{gas}, $H_2S_{ads\text{-}liq}$, and H_2S_{ads} are concentrations of H_2S in gas, liquid and adsorbed phases, respectively; K_H, K_S, K_a and K_R are equilibrium constants for related processes (adsorption, gas solubility, dissociation, and surface reaction constants); O^*_{ads} is

dissociatively adsorbed oxygen and S_{ads} is the concentration of surface compounds as end products of the surface oxidation reaction.

If the surface reaction (Equation 3.8) is the rate limiting step of H_2S oxidation process [43] the degree of H_2S dissociation should be high enough to start its oxidation on the surface ($HS^-_{ads} \simeq H_2S_{gas}$). Combining Equations 3.5 to 3.7 the following expression can be derived to calculate the equilibrium HS^-_{ads} concentration:

$$\log(HS^-_{ads}) = \log(K_S) + \log(K_H) + \log(K_a) + pH + \log(H_2S_{gas}) \qquad (3.9)$$

where $\log(K_a) = -7.2$ (48). Solubility of pure H_2S at 25°C in water is equal to 0.125 mol/L [65], which corresponds to $K_S = 3.1$. Adsorption constant, K_H depends on the interaction of H_2S with carbon and should be determined independently as a ratio of H_2S_{ads} to $H_2S_{ads\text{-}liq}$. For our evaluation we assumed that H_2S_{ads} is not higher than solubility of pure H_2S in water. For 3000 ppm of H_2S in gas phase it follows that $K_H = 330$. Substitution of K_S, K_H, K_a values in Equation 3.9 gives

$$\log(HS^-_{ads}) = -4.2 + pH + \log(H_2S_{gas}) \qquad (3.10)$$

This simplified expression suggests that for all carbons with average surface pH > 4.2 concentration of HS^- in the adsorbed state will be equal to H_2S in a gas phase (100% adsorption + dissociation), which is required for effective H_2S removal. The dependence of the ratio of concentration of HS^- in the adsorbed state to the concentration of H_2S in a gas phase (HS^-_{ads}/H_2S_{gas}) on the pH of carbon suspension in water (with dissolved H_2S)

calculated using Equation 3.6 is plotted in Figure 39B. The estimated value of pH is lower than the first dissociation constant (pK_a) of H_2S. As can be seen, a pH value only high enough for mild dissociation of H_2S is sufficient for its effective removal [15, 19]. In such a situation physically adsorbed H_2S, upon dissociation in the water film to hydrogen sulfide ion (HS^-), becomes vulnerable to attack by oxygen and can be oxidized to elemental S and sulfur oxides [25]. A too low pH results in physical adsorption of H_2S while a too high value leads to high concentrations of hydrosulfide ions and their oxidation to polymeric sulfur [19]. As it is seen from Figure 39B both calculated and experimental results show the same trend expressed by a sharp increase of adsorption capacity in the range of pH between 4 and 5. Although calculated above threshold pH is equal 4.2 the threshold estimated from the data presented in Figure 39B seems to be higher than 4.5. The discrepancy with the calculated value of pH is due to the fact that pH > 4.2 was obtained from simplified expression without the exact value of the adsorption constant, K_H. The calculation presented above suggests that although the threshold exists, it can not be taken as an absolute value. N1 and S1 carbons have pH > 4.2 but are not able to effectively remove hydrogen sulfide. On the other hand, less than half a pH unit difference between W1 and W2 - near the threshold- marks more than 15 times difference in their capacity. It is reasonable to assume that when the number of basic groups increases the capacity should increase (Table 1), due to enhancement in the hydrogen sulfide dissociation. However, a presentable correlation was not found for basic groups.

When the density of acidic groups exceeds 1.2 $\mu eq/ m^2$ (Figure 39A) the surface becomes too acidic to promote the dissociation of hydrogen sulfide and only its physical adsorption can occur (not high at room temperature). With such a high density of acidic

groups, sorption of water is enhanced even at a low relative pressure [55]. Although tests carried out under dry conditions have generally demonstrated negligible capacities (Table 3) [14] it is seen from our experiments that water uptake, higher than the threshold value does not increase the breakthrough capacities of unimpregnated carbons (Figure 39D). In the case of carbons used in this study the affinity for water adsorption should not be greater than 3.5 $\mu mol/m^2$ to reach the maximum capacity. It is likely that high affinity toward water is a measure of high surface acidity which inevitably thwarts the dissociation of H_2S and inhibit the removal process. Like a high water affinity, a high content of surface oxygen is indicative of the surface acidity and will impede the H_2S dissociation process. For carbon to perform effectively, the content of surface oxygen should not exceed 2 $\mu mol/m^2$.

Another parameter related to carbon acidity analyzed in this study is the weight loss from TA experiments associated with strong acids (Figures 39C). As in the cases presented above, despite the dispersion of the results, threshold values can be noticed.

3.10. Regeneration of Carbon

The analysis of sulfur species, which are formed in each step of the process, is fundamental for understanding the H_2S adsorption mechanism and its characteristics in each carbon. Using this information, efforts can be made to develop carbons which in addition to providing efficient removal capacities, can be regenerated more effectively due to the nature of their surface products.

The sulfur contents along with the speciation of sulfur compounds at various steps of carbon treatment are collected in Table 6. The results are calculated as the amount of

sulfur species per gram of *exhausted* carbon to facilitate the comparison of various methods. In this way, mass balancing of the results is attainable for checking the accuracy of our methods and analyses. This table also reports the pH values of the carbon surface. The sulfur data are calculated from H_2S adsorption (H_2S-S), DTG curves using separation of SO_2 and elemental sulfur peaks (SO_x-S) and (S^o-S) and from ion chromatography (SO_4-S) [19, 20]. Total sulfur content is reported from the results obtained in a commercial laboratory. The low pH of exhausted carbons (around 2) is always associated with the end of effective adsorption and the exhaustion of carbon. This is likely the result of the presence of sulfuric acid. The total sulfur content for all samples is in good agreement with the sulfur content calculated from H_2S adsorption. Although there are some discrepancies in the TA results, which are likely due to chemical transformations during TA analysis, washing process, presence of intermediate sulfur species, and error in separation of the peaks, the TA findings are comparable to the results of other analyses. Contrary to elemental sulfur, sulfur oxides are highly soluble in water and have been effectively removed in most cases.

Table 6. Analysis of Sulfur Species on the Initial, Exhausted and Washed Carbons

Sample	Adsorption	TA of Carbon		Leachate Ion Chrom.	Lab Analysis	Surface
	H_2S-S mg/g	SO_x-S mg/g	S^0-S mg/g	SO_4-S mg/g	Total S mg/g	pH
N	-	-	-	-	<5	7.7
NE	85	35	53	22	85	2.0
NS	-	18	50	-	69	4.2
N1	-	-	-	-	<5	4.5
N1E	39	10	11	12	35	2.1
N1S	-	16	0	-	18	4.1
N2	-	-	-	-	<5	3.6
N2E	22	24	6	6	23	2.1
N2S	-	15	0	-	30	3.0
S	-	-	-	-	<5	6.9
SE	97	42	69	22	90	2.0
SS	-	9	34	-	55	5.8
S1	-	-	-	-	<5	4.6
S1E	15	6	0	1	11	2.8
S1S	-	2	0	-	6	4.7
S2	-	-	-	-	<5	3.7
S2E	12	9	0	1	7	2.5
S2S	-	2	0	-	5	5.0
W1	-	-	-	-	<5	4.4
W1E	206	43	134	17	138	1.8
W1S	-	14	65	-	130	2.6
W2	-	-	-	-	<5	4.0
W2E	16	2	7	3	16	3.0
W2S	-	2	8	-	13	4.1
W3	-	-	-	-	<5	5.6
W3E	179	24	107	12	180	2.0
W3S	-	8	66	-	152	2.9

As expected, the bulk of the deposited sulfur species in NE (85 mg/g) has remained intact during washing (NS: 69 mg/g). Some of the soluble sulfur oxides are washed away as sulfuric acid and the effect is evident in an increase in the pH value. The amount of elemental sulfur in this carbon has remained virtually unchanged. These results indicate that the recovery of this carbon by simple methods, such as low temperature washing, is unfeasible. In the case of SE, despite its high initial sulfur content (90 mg/g), the washing has removed considerable amount of elemental sulfur and a significant part of sulfur oxides. This is demonstrated in an increase in the surface pH to 5.8, highest among all of the washed samples. The results for S1E and S2E are similar in that they have oxidized the entire sulfur to sulfur oxides. Consequently, although their capacities are very small, they have removed much of the deposited products upon washing in Soxhlet. On the other hand, W2E despite similar capacity and surface pH (in W2), has dominantly produced elemental sulfur as its end-product. Consequently, washing has not been effective for this carbon. Difference in the performance of carbons can be related to their different pore structure. The results of W1E and W3E, despite their much higher capacities follow the same pattern in formation of elemental sulfur. But the analysis of the results related to W1E, W1S, and W3S revealed two inconsistencies. The capacity of sulfur in W1E as calculated from adsorption results (H_2S-S) is equal to 206 mg per gram of carbon, which should have deposited in the pores and should be reflected in the lab analysis for total sulfur content. The latter, however, revealed only 138 mg sulfur per gram of carbon, which marks a major discrepancy in the amounts of total sulfur. Repeating the measurement in another laboratory verified the initial finding. This means that a large amount of influent sulfur is unaccounted for in the analysis of total

sulfur deposits. The initial perception might be that the missing portion might have escaped the adsorbent in gaseous form possibly as sulfur dioxide. But repetition of the breakthrough test did not show any evidence of SO_2 in the off gas during the experiment (using permanganate solution as reagent). In that case, they might have evolved from the carbon in the oven drying, after the experiment, for removal of weakly adsorbed adsorbates such as water. Considering the fact that W series of carbons are chemically activated in a temperature resulting in a low degree of carbonization, contrary to carbons activated at high temperatures, a high content of hydrogen containing groups are likely to remain in W carbons. These hydrogen-containing groups can undergo "sulfoxidation" in the presence of oxygen and sulfur compounds (especially sulfur dioxide) at ambient temperatures even without a catalyst [73]. The formation of allylic polysulfides at 0-83 °C on the treatment of olefins with SO_2 and H_2S is also reported. On further heating, the polysulfide formed in sulfur-olefin reactions decomposes to H_2S and more complex products involving more resistant S-C bond [73].

Another discrepancy arouse upon the comparison of the TA results for W1S and W3S with the reported results from the lab analysis. While TA results show a major removal of oxidation products from these carbons upon washing, the lab analysis for total sulfur content shows that the bulk of sulfur is still intact in these carbons. As indicated above, from the three profound peaks in the exhausted carbons in TA, the first two were attributed to sulfur compounds and the third to surface oxygen groups. The amount of sulfur species were then evaluated from the conversion of the weight loss associated with the first two peaks into sulfur content. This was based on the assumption that contribution of sulfur compounds to the third peak is small owing to the high activation energy for the

formation of S-C bond, which requires high temperature for the reaction. It was previously reported [67] that considerable sulfur was incorporated into carbon by heating a mixture of sulfur and carbon at 475 °C. This temperature is above the desorption of second TA peak which for W series usually ends around 400 °C. This peak was found to be associated with sulfur radicals (elemental sulfur). Unless some of the sulfur species have contributed to the third peak at lower temperature, the discrepancy in TA and lab results can not be explained. To investigate the correctness of our hypothesis a sub-sample of W1E was heated at 150 °C for 5 hours in the presence of a small current of air to remove some of the sulfur products despite their low vapor pressure. Figure 40 shows the TA results for W1E and the heated sample (W1Eheated) in addition to W results. It can be seen that while the first peak attributed to sulfur oxides has remained intact, the sulfur radicals peak is considerably diminished. But the major reduction is observed in the third peak. The extent of this peak is reduced to the level comparable with its counterpart in W carbon. It can be concluded that the third peak observed in all of the exhausted carbons is affected by the amount of the sulfur products and specifically by the extent of the second peak (sulfur radicals). It is also interesting that when the amounts of sulfur products are small (W1Eheated), their desorption supersedes the formation of carbon-sulfur complexes.

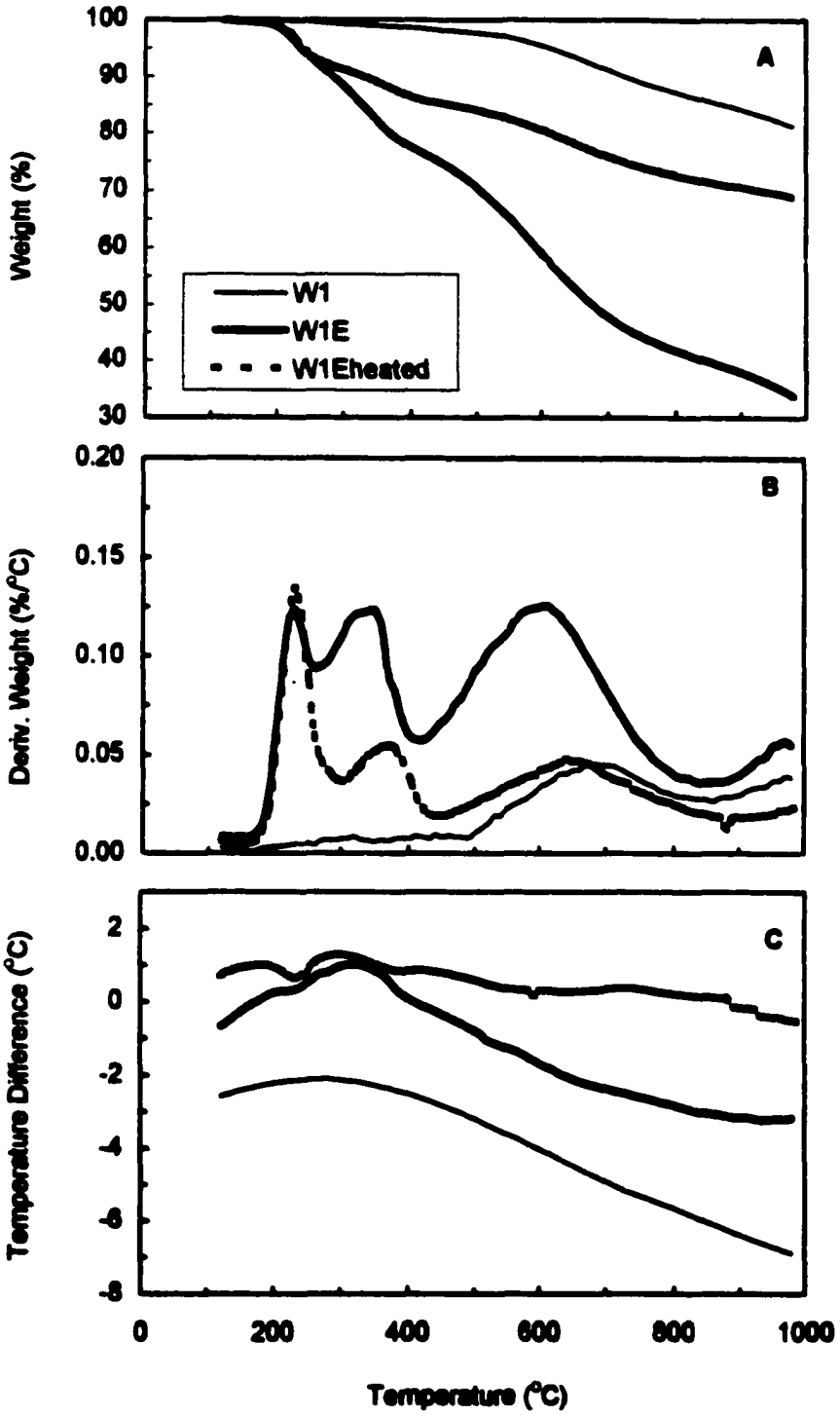

Figure 40. Thermal analysis results for W1, W1E and W1Eheated. TG (A), DTG (B) and DTA (C).

These findings are important in heat processes used for regeneration of exhausted carbons. They also explain the discrepancy observed in comparison of TA and lab results for W1S and W3S. It is evident that the part of sulfur that has contributed to the third peak and desorbs as carbon sulfur compounds, such as for instance CS_2, above 600 °C, is unaccounted for in our TA estimates. This further proves that washing has been least effective in these carbons owing to the low temperature formation of organic polysulfides. Although they decompose at higher temperatures, at the low temperature of washing in Soxhlet, organic polysulfides protect the attached sulfur, rendering the washing process ineffective.

From the standpoint of *in situ* regeneration of exhausted carbons, the results of Soxhlet washing are important. The results obtained for N1, are of particular interest since despite its intermediate H_2S removal capacity, it has been capable of oxidizing the entire produced sulfur radical during the washing process. The high oxidized sulfur residue and relatively low pH of N1S are likely due to insufficient washing. Despite this, efficiency of washing in this case was the highest (49%). The highest was also the yield of water soluble sulfur oxides. This is the result of removal of carbonate during acid oxidation. Considering its acceptable H_2S removal capacity and the ease of washing of the exhausted carbon, the N1S sample shows promising behavior from the standpoint of feasible regeneration.

To verify our initial findings on NS and N1S and to further explore the effect of washing time on the products of oxidation, a subsample of each of NE, N1E and SE was washed in the Soxhlet apparatus for 60 hours. The choice of SE was made due to its similar pore structure and H_2S removal capacity to those of NS. The TA results on these

samples are shown in Figures 41 to 43 along with the results of 24 hour washing. The effect of extensive washing on NS is seen as a decrease in intensity of the peak associated with sulfur radicals (330 °C) (Figure 41B). Although the sulfur oxide peak shows a small decrease in intensity the bulk of sulfur oxides remains intact so that a minor recovery is observed in weight loss (Figure 41A). This indicates that the deposited sulfur polymers are not only unwashable but also they practically lock up the soluble sulfur oxides inside the micropores. On the other hand, the comparison of the DTG curves for the 24 hour and 60 hour washed N1E samples (Figure 42B) shows a significant decrease in the intensity of the peaks associated with sulfur oxides and radicals. As a result, a major recovery in the weight loss (Figure 42A) is observed in the washed carbon, so that it is comparable with the results obtained for the initial N1 carbon (Table 5). The DTG results of extensive washing of SE (Figure 43B) show that despite considerable removal of the sulfur radicals, a new peak around 450 °C (similar to in NS) is revealed. This peak, as shown for NS, is associated with sulfur polymers, which are unwashable. Once again, the sulfur oxides peak has essentially remained intact reconfirming that when bulky deposits of sulfur polymers are formed they can seal the micropores preventing any contact even between soluble constituents and the washing water. Under this condition, part of the micropores is permanently removed from the matrix and regeneration of carbon with simple means is impossible.

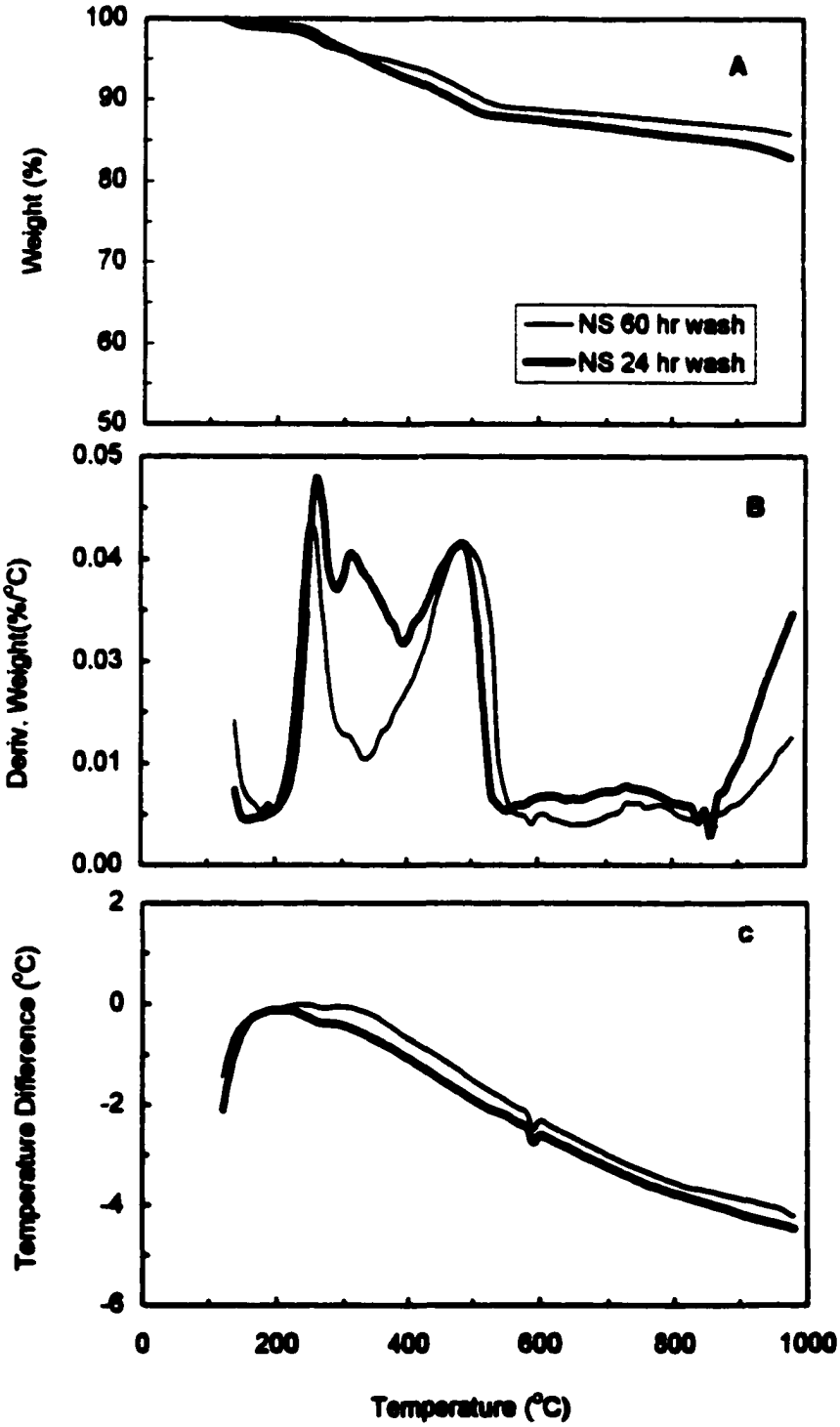

Figure 41. Thermal analysis results for NS 24 hour and 60 hour wash. TG (A), DTG (B) and DTA (C).

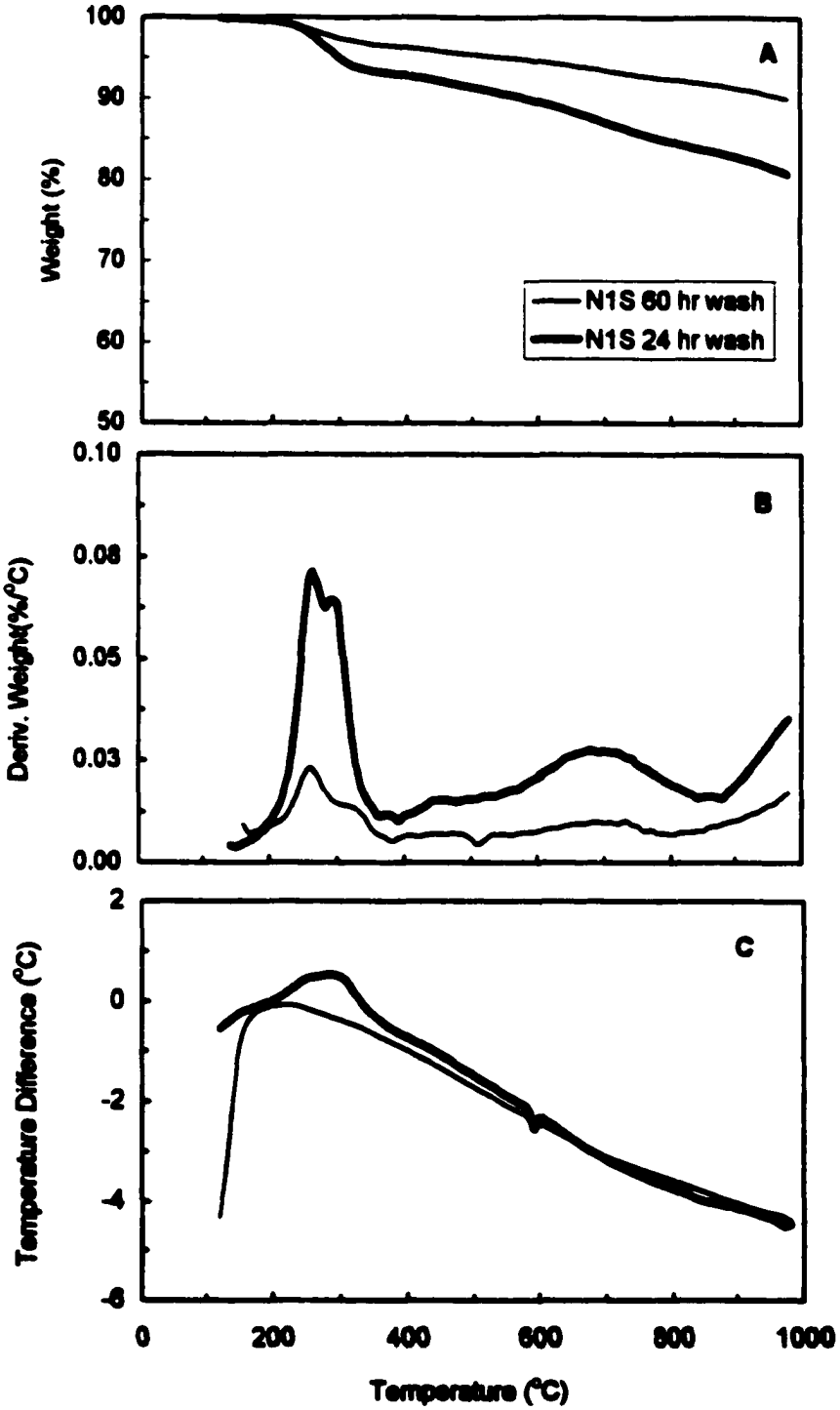

Figure 42. Thermal analysis results for N1S 24 hour and 60 hour wash. TG (A), DTG (B) and DTA (C).

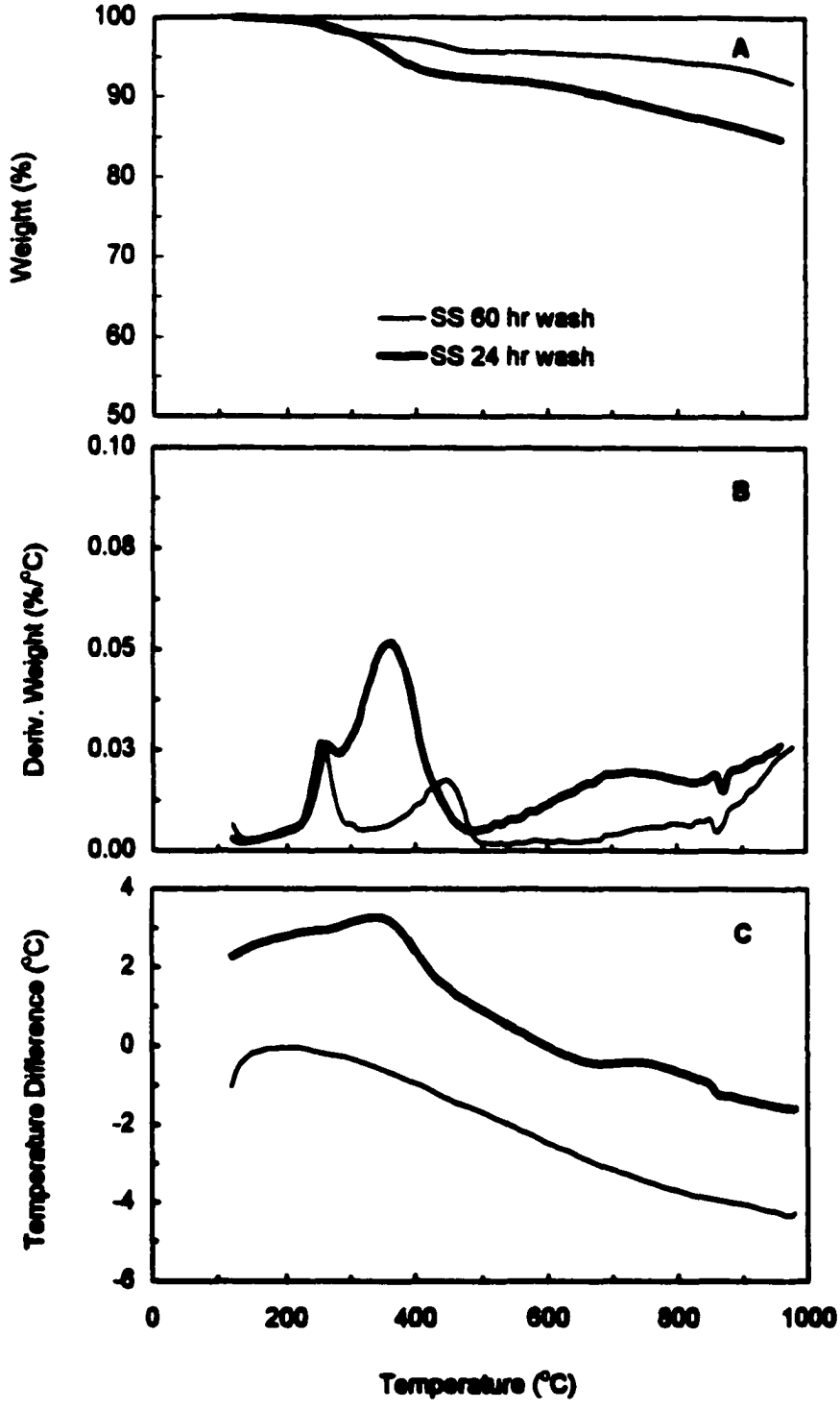

Figure 43. Thermal analysis results for SS 24 hour and 60 hour wash. TG (A), DTG (B) and DTA (C).

3.11. The Study of the Performance of Nitrogen-Containing Modified Carbon as a Support for the Proposed Mechanism

Based on the observations outlined in previous sections several conclusions can be drawn about the effect of carbon properties on the performance of carbons for H_2S adsorption/oxidation:

1. The dissociation of H_2S is the initial step for its oxidation and the fundamental precondition for the process. While moderately acidic pH is still capable of facilitating the dissociation, a too low pH will always inhibit the process.
2. The capacity of a carbon is a function of its pore structure provided that the dissociation requirement is met.
3. Introduction of surface oxygen groups will enhance the density of electron deficient sites and promote the formation of sulfur oxides rather than elemental sulfur. On the other hand the presence of aliphatic hydrogen containing groups will always promote the formation of organic polysulfides [73] which will protect sulfur from further oxidation. Similar effect is observed in caustic impregnated carbons upon the formation of sulfur complexes [10]. The final product of oxidation, in both cases, is dominantly sulfur polymer which is insoluble and cannot be easily desorbed by heating due to the formation of resistant sulfur-carbon complexes before evaporation [67, 73].
4. Presence of very small micropores (pores smaller than 10 Å) can enhance the formation of sulfur oxides owing to the availability of higher heats of adsorption which can contribute to higher energy transformations. These pores also ensure high dispersion of sulfur radicals and prevent the creation of sulfur polymers.

5. Sulfur radicals are the initial products of oxidation, which can then form sulfur polymers or be further oxidized to sulfur oxides depending on the conditions of the experiment and properties of the carbon surface.
6. Regeneration of carbon by washing is only feasible when oxidation of H_2S can proceed to soluble sulfur oxides either during H_2S adsorption or washing thereafter.

In this section, the findings on the possibility of affecting the selectivity of oxidation products will be discussed. For this purpose specific modifications were enforced on a carbon using our observations and the existing technology to provide the favorable selectivity in the products of oxidation. The modification procedure of W1 is discussed in details in Section 2.1. As discussed earlier, W1 was characterized by its high pore volume, relatively small ratio of volumes of micropores to total pores, and a very high capacity for H_2S removal. Elemental sulfur constitutes much of the oxidation products in W1E (Table 6). Washing was proved to be least effective in this sample as lab analysis reports that almost the entire sulfur deposits remain intact after washing.

Two samples of W1 were impregnated with urea and heat-treated at 450 °C and 950 °C to incorporate nitrogen in the carbon structure and decrease the size of the pores [9, 44]. This modification is targeting at the formation of water soluble sulfur oxides as the main product of the oxidation of H_2S. The surface properties, elemental analysis, porous structure and performance of W1 and its modified counterparts (W1u450 and W1u950) were then compared with a commercial carbon (Centaur®) which is produced under a patent for catalytic oxidation of gases including H_2S [9].

The results of elemental analysis presented in Table 7 show a significant increase in nitrogen content of the samples after modification with urea. As expected, the nitrogen content of W1u950 is lower than W1u450. In the case of the latter, due to the low temperature of modification, nitrogen is likely in the form of amides, free NH and NH_2, bonded NH and NH_2, or NH_4^+ species bonded to aliphatic branches. They decompose at high temperature [70]. After heat treatment at 950 °C the majority of nitrogen is incorporated into carbon matrix as a component of an aromatic ring in a pyrdine-like configuration [77]. Evidently, that nitrogen content for W1u950 is higher than for Centaur®. This is likely a result of differences in the surface area of the two carbons. When surface area is higher the accessibility of crystallite edges to incorporate nitrogen is greater as has happened in the case of W1u950. An increase in the carbon content accompanied by a decrease in hydrogen content indicates changes in the degree of carbonization (W carbon was manufactured at about 600 °C).

It is noteworthy that although the pH significantly increased for wood based carbon samples after modification with urea, it is still lower than that of Centaur® (Table 7). The surface functional groups have changed not only owing to the presence of nitrogen but also, as mentioned above, as a result of treatment at 950 °C. Such a high temperature is expected to significantly alter the degree of carbonization and to reduce the number of acidic groups, which decarboxylate above about 200 °C [56]. On the other hand, exposure of carbons after thermal treatment to air promotes oxidation as a consequence of the thermodynamically unstable edges of crystallite layers [5].

Table 7. Elemental Analysis, pH, and Surface Chemistry of Nitrogen-Containing Carbons

	Elemental Analysis [%]					Surface Chemistry [mequiv/g]			
Sample	C	H	N	Ash [%]	pH	Acidic	Basic	All	Basic/All
W1	85.1	2.3	0.2	3.15	4.41	1.100	0.260	1.360	0.20
W1u450	82.3	2.0	7.5	3.23	6.45	0.595	0.570	1.165	0.49
W1u950	91.3	0.7	2.4	1.47	6.71	0.575	0.350	0.925	0.38
Centaur®	90.6	0.7	1.1	4.34	8.30	0.400	0.425	0.825	0.51

Although nitrogen-containing groups do not fit under Boehm's categories, they can behave as acids or bases in water solution and can be titrated similarly. The results summarized in Table 7 show significant changes in acidity after thermal treatment with urea. In the case of W1u450 sample the number of acids significantly decreased. This change is accompanied by a more than two-fold increase in the number of bases. For W1u950 the content of surface acids is slightly smaller than for W1u450 but the decrease in the content of bases is more pronounced. In the case of Centaur®, the number of bases is higher than that of acids, yielding an average pH > 7. To evaluate the overall changes in the chemical character of surface we defined the degree of basicity as the ratio of the number of basic groups to all species detected on the surface. Analysis of these values indicates significant increase in the basicity for the urea treated carbon samples.

The alteration of the chemical nature of W1 carbon caused by the thermal treatment with urea is also seen in Figure 44 which collects TA curves obtained in nitrogen. The similarities in the chemistry of W1u950 and Centaur® are apparent in DTG curves (Figure 44B). At the temperature range between 200 °C to 400 °C, where carboxylic groups are expected to decompose [56], the weight loss for both W1u950 and Centaur® is negligible.

Thermal treatment, especially at 950 °C, shrunk the carbon grains by about 30% . The changes in the pore structure affect the nitrogen sorption isotherms. Surface areas, S_{N2}, micropore volumes, V_{mic}, and total pore volumes, V_t, were calculated using DFT [51, 78]. The results are summarized in Table 9. As expected, based on the shrinkage of grains, the surface area decreased 20% and 40% for W1u450 and W1u950, respectively. The same changes are noticed in the pore volumes. It is interesting to note that the

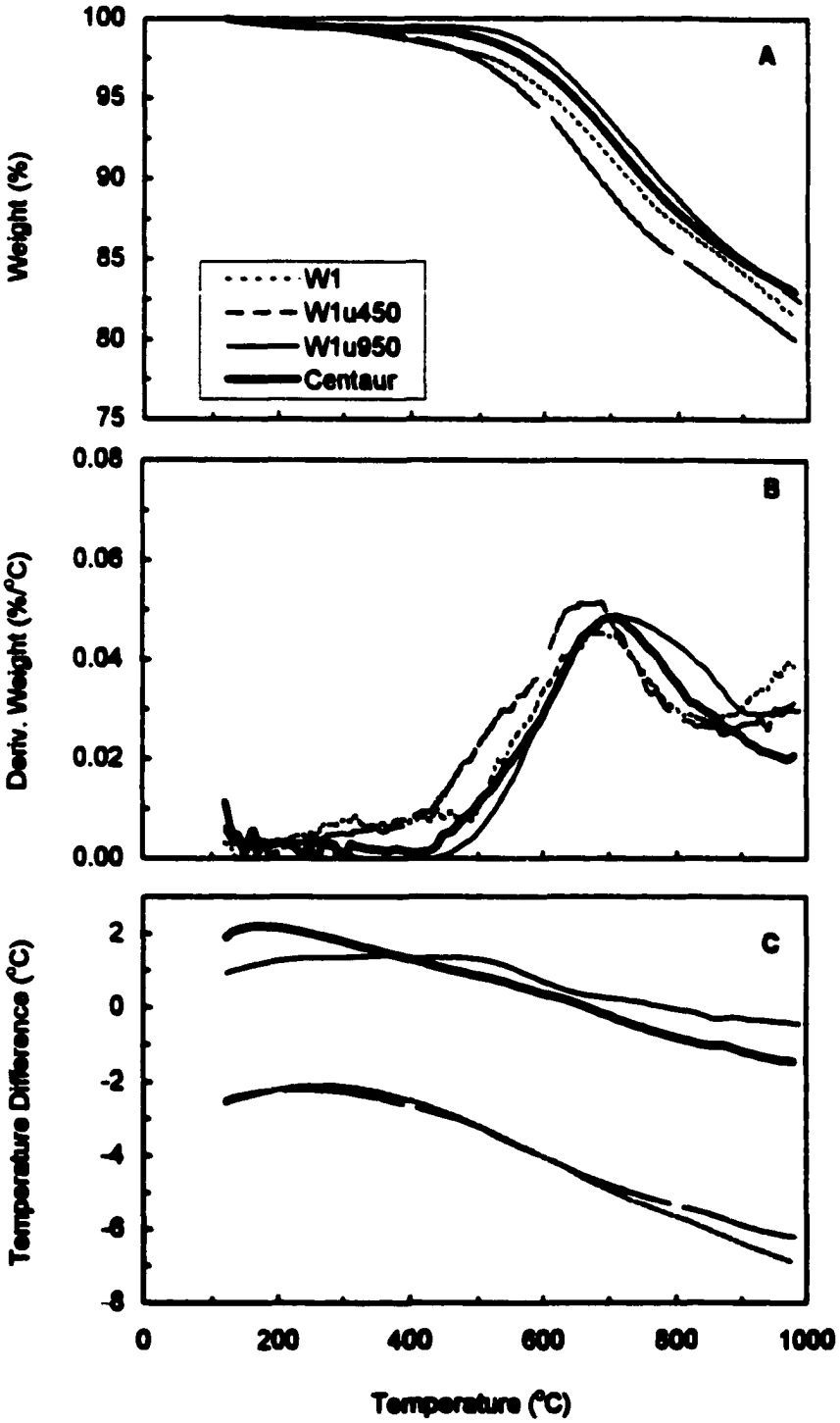

Figure 44. Thermal analysis results for W1, W1 urea treated samples and Centaur. TG (A), DTG (B) and DTA (C).

surface area and pore volume of Centaur® are much smaller than those of the modified samples, however, Centaur®'s relative microporosity (V_{mic}/V_t) is the highest.

Detailed view of the pore sizes and their contribution to total porosity can be obtained from the analysis of the PSDs presented in Figure 45. Although similarity in the surface structural features of W1u950 and Centaur® exists for very small micropores, comparison of the curves clearly distinguishes Centaur® from the other carbons owing to its relatively homogeneous pore structure and low pore volume. Small micropores, as it was indicated previously [22, 49], are active in the process of hydrogen sulfide immobilization. In the case of samples modified with urea the volume of pores is significantly smaller compared to the initial carbon.

The performance of carbons studied as H_2S adsorbents/oxidizing media is summarized in Table 8. The breakthrough capacity of carbons after modification with urea is slightly lower compared to the W1 carbon. The low pH values of urea modified carbons after exhaustion indicate the high yield of sulfuric acid which permits regeneration using water [20]. In the case of Centaur®, although the capacity is lower, its decrease in pH is greater than that of other carbons suggesting higher yield of water-soluble acid. In Table 8 we also report the normalized capacity calculated by dividing the H_2S breakthrough capacity in mg/g by the total pore volume of the adsorbent. The results indicate that the normalized capacity of all urea-modified carbons is around 30% higher than that for the unmodified W1 material.

Figure 46 collects the DTG curves for exhausted carbons. Compared to the initial samples, they differ significantly in the total weight loss. This shows that sulfur-carbon complexes, which cause much of the weight loss in W1E, do not form in the modified

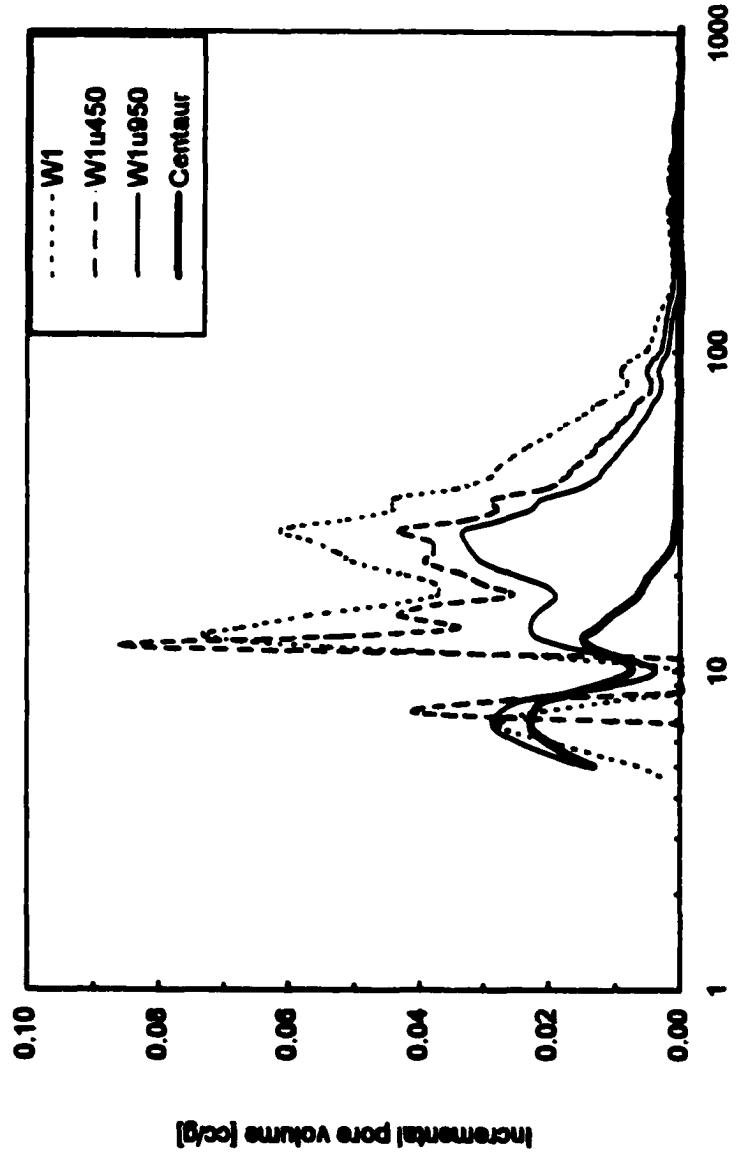

Figure 45. Pore size distributions for W1, W1 urea treated samples and Centaur.

Table 8. Structural Parameters of Nitrogen-Containing Samples, and Characteristics of the Exhausted Carbons

Sample	Structural Parameters Calculated from Sorption of Nitrogen				Characteristics of Exhausted Carbon			
	S(DFT)	V_{mic}(DFT)	V_t	V_{mic}/V_t	H_2S breakthrough capacity	Capacity per unit pore volume	pH	SO_x/S (first peak/ second peak in DTG)
	[m^2/g]	[cm^3/g]	[cm^3/g]		[mg/g]	[mg/cm^3]		
W1	1400	0.56	1.21	0.46	298	246	1.88	0.54
W1u450	1145	0.47	0.90	0.52	272	302	2.31	1.81
W1u950	1024	0.37	0.71	0.52	276	389	2.03	3.02
Centaur®	630	0.24	0.30	0.80	104	346	1.47	All SO_x

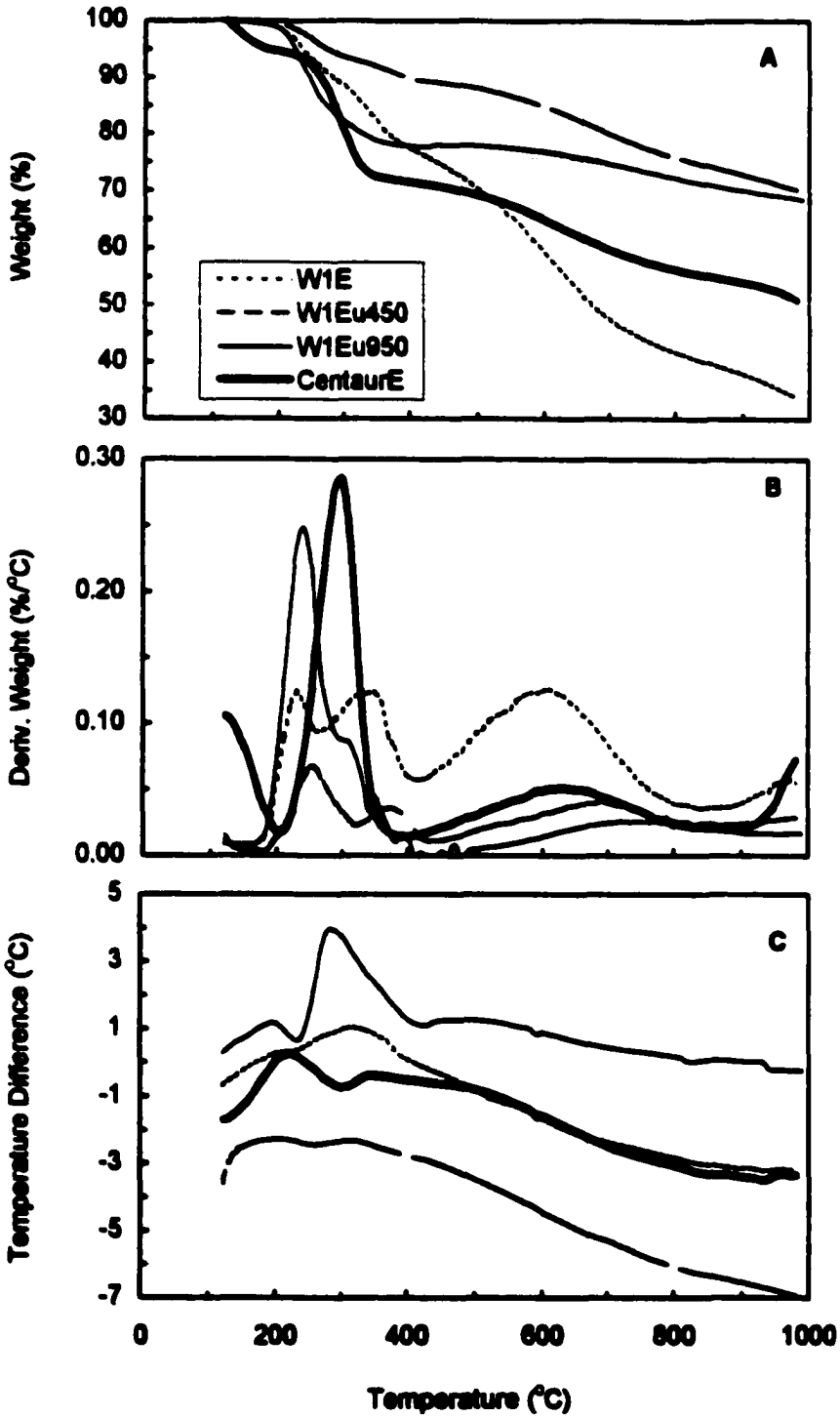

Figure 46. Thermal analysis results for Exhausted W1, W1 urea treated samples and Centaur. TG (A), DTG (B) and DTA (C).

samples. Major differences are observed in the weight losses between 200 °C and 400 °C which are associated with the products of H_2S oxidation [19, 67, 79]. As described previously, the peak around 250 °C represents sulfur oxides (water-soluble) whereas the peak at ~350 °C is related to the presence of elemental sulfur deposited in the pores of carbons [19]. To compare the performance of carbons in the process of conversion of H_2S to sulfur oxides, the weight loss represented as the first DTG peak was divided by the weight associated with the second peak. In the case of CentaurE only one large peak is formed which suggests that H_2S is converted mainly to sulfur oxides. The performance of W1Eu950 is similar to that of CentaurE, however, a shoulder at 350 °C for the former carbon suggests some percentage of deposited sulfur. But the results of DTA (Figure 46C) for this carbon show a major exothermic effect for W1Eu950 concurrent with the sulfur shoulder. This means that sulfur is not a product of adsorption process but rather the product of reduction of sulfur dioxide as a result of oxidation of carbon at high temperature during TA experiment. Nevertheless, the comparison of the peak areas (i.e., weight losses) for urea modified samples to W1 indicates much higher degree of H_2S oxidation to SO_x (Table 8). The performance of W1Eu950 is much better than W1Eu450. It is likely the result of incorporation of nitrogen in aromatic rings.

In order to understand the mechanism of the oxidation process we first should compare the behavior of carbons impregnated with caustics to carbons containing nitrogen for their effectiveness as hydrogen sulfide adsorbents. On the surface of the former materials hydrogen sulfide is converted mainly to elemental sulfur [6, 7]. Their pH is very high, higher than that of carbons modified with urea, so the average pH here is not a unique factor limiting the oxidation products and inhibiting the adsorption. Sulfur

radicals upon formation, however, will quickly polymerize in caustic polusulfides and will be protected against further oxidation. The distinctive feature of carbons modified with urea is the presence of nitrogen groups highly dispersed in small pores, contrary to KOH or NaOH being in abundance in liquid phase in pores of caustic carbons. The incorporation of nitrogen enhances the amount of adsorbed anions [77]. It was demonstrated previously that pyridine-like nitrogen in the carbon structure increases the polarity of the carbon surface and the amount of adsorbed water [80]. Moreover, the presence of nitrogen groups provides the direct contact of HS^- ions with the carbon matrix, which promotes the immediate creation of active sulfur radicals. It also results in the presence of superoxide ions [70, 77]. All of these happen due to enhanced electron transfer reactions on nitrogen containing carbons [23, 81]. We suggest that the oxidation of H_2S on nitrogen modified carbon occurs according to three steps (Figure 47). In step I gaseous H_2S diffuses into the water film, condenses in the micropores and dissociates. The mildly basic character of most of the cyclic amines can enhance this process. In step II hydrosulfide ion is primarily chemisorbed on the carbon adjacent to nitrogen in the aromatic ring. In step III the -SH extension is attacked by superoxide ion leading to the formation of oxidized species of sulfur and the regeneration of the catalyst. The rate of the proposed reaction is likely enhanced in small pores environment. When the reaction occurs in small pores, the heat is released which may also enhance the oxidation process and creation of sulfuric acid [19].

Step I

Step II

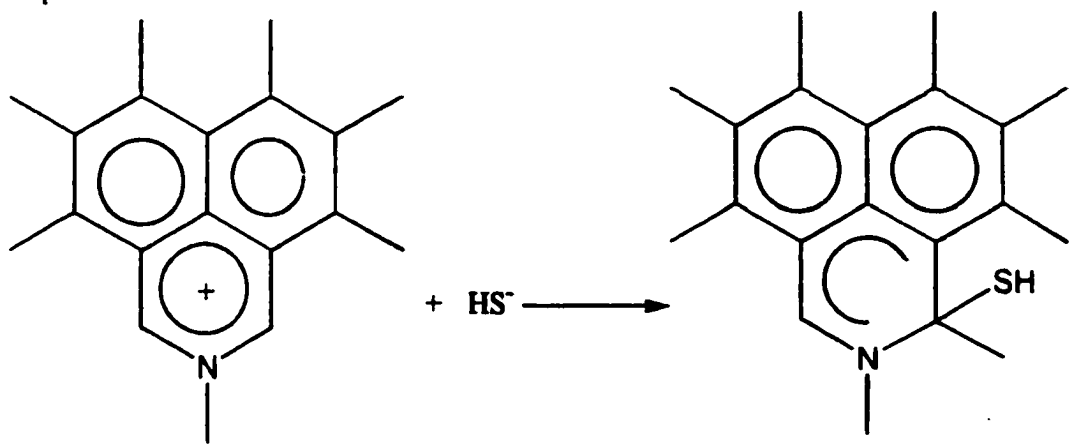

Step III

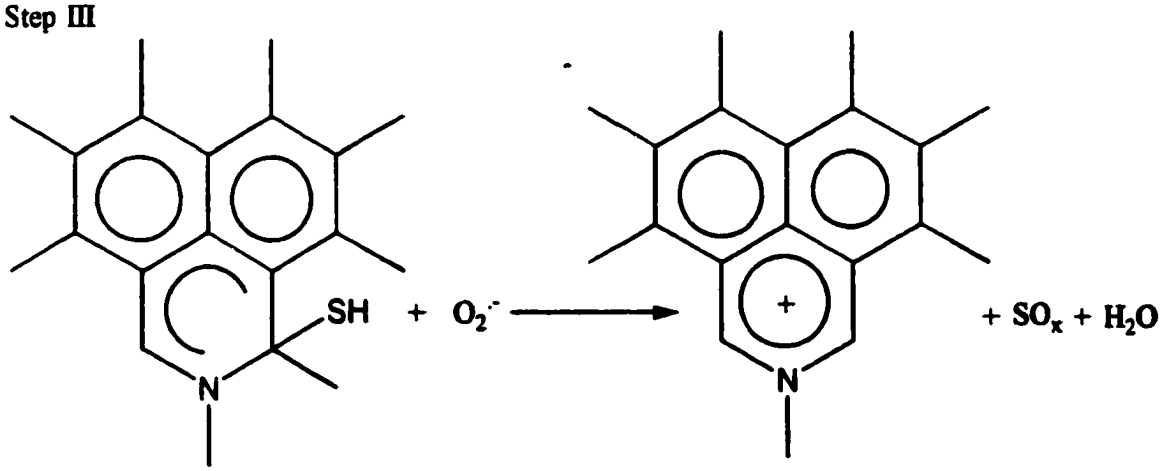

Figure 47. Mechanism of oxidation of hydrogen sulfide on nitrogen containing activated carbon.

Comparison of the results of W1Eu950 and oxidized samples in N and S series, despite their much smaller capacities, reveals similarity in selectivity of the oxidation products. In both cases the presence of an electron-withdrawing group (oxygen or nitrogen) has induced electron deficiency in the adjacent carbon atoms. These electron deficient sites can act as primary centers for chemisorption of hydrosulfide ion in the vicinity of small micropores, which can then promote their oxidation.

Hence, a proper combination of surface chemistry and pore structure can affect the selectivity of oxidation products for favorable results. In the case of Centaur®, when the smallest pores are filled with acid, the larger pores start to play a role. The distribution of nitrogen containing basic groups on the whole surface should be more or less the same, so the next portion of H_2S is oxidized in larger pores. The process proceeds until all pores are filled or the low pH represses the dissociation of H_2S. When all pores are filled the H_2S can be further oxidized to SO_2 via its reaction with sulfuric acid [26]. It is interesting to note that the capacity of Centaur® for removal of H_2S is relatively low compared to other carbons. This can be explained by its relatively smaller pore volume, which limits the deposition of oxidation products in this carbon. For example the total pore volume of W1u950 is 2.4 times that of Centaur® and its H_2S removal capacity is 2.65 times that of Centaur®.

CHAPTER 4

KINETICS OF HYDROGEN SULFIDE OXIDATION ON ACTIVATED CARBON AND DESIGN CRITERIA

One of the objectives of this research is the analysis of the kinetics of the surface reaction of oxidation of H_2S on activated carbon from engineering design point of view. For this purpose, providing an expression for rate is a fundamental task.

4.1. Conditions of the Process

As explained earlier, most of the existing research on this subject was carried out at temperatures higher than ambient in industrial applications where the effect of adsorbed water is either minimal or negligible and elemental sulfur is the main product of the process [22, 36, 37, 41, 43]. Hence, the role of surface chemistry of carbon -which is enhanced in the presence of water- is negligible in semi-dry conditions. It is agreed that the chemisorption of both hydrogen sulfide and oxygen on the catalyst surface are the first steps of the reaction. The surface reaction between these two adsorbed molecules is considered to be the next and rate-limiting step. Finally the produced sulfur will deposit on the active sites of catalyst, imposing a fouling effect on the process [11, 43].

Contradictory views on the role of water in the reaction mechanism have been expressed [36, 43]. It is concluded, however, that the mechanism of the reaction in the presence of water below 100 °C is not well established [43]. The findings of this research, at ambient temperature, confirm that the presence of humidity in the feed gas is

necessary for dissociation of H_2S and its oxidation. But the water content beyond a threshold value has a negative impact on the process. Nevertheless, the maximum amount of adsorbed water is in equilibrium with its pressure in the feed gas and it allows the promotion of the reaction. Hence, the steady (constant) water effect is not considered a fouling factor in the unsteady state of the reaction.

Another important factor is the formation of sulfur oxides and sulfuric acid. Their formation is reported to be negligible at high temperatures. The findings of this research indicate that sulfur oxides and sulfuric acid are among the products of oxidation of H_2S at ambient temperature. The dissociation and oxidation of H_2S on the carbon surface is impeded by the resulting very low pH. This can considerably decrease the rate. Two factors in the properties of carbon have controlling effect on this impact. As outlined in previous sections, a moderately low pH (around 4.5) can still facilitate the H_2S dissociation requirements to the extent that the effect of sulfuric acid formation is mitigated. Secondly, the formation of sulfuric acid is associated with the most energetic adsorption in small micropores. Upon formation, sulfuric acid is contained in those pores and does not contribute significantly to the overall reaction environment. For example, Centaur® carbon, with dominant microporous structure, was found to operate in a very low pH before exhaustion. The pH of the exhausted Centaur® was found to be 1.47 (Table 8). Other carbons have also operated until a very low pH (around 2.0) emerged. This can only happen if the formation of sulfuric acid is contained locally within the small micropores. Hence, we may conclude that unlike sulfur, which its deposition on the active sites does in fact deactivate these sites [82], the produced sulfuric acid does not immediately impose a fouling effect on the catalyst.

Finally a major deviation from the conditions of high temperature adsorption of H_2S is in the intra-particle or pore diffusion limitations at ambient temperature. Being a function of temperature, diffusion is much smaller at ambient temperature so that it can actually interfere with the adsorption process. Investigators, carrying experiments with two different particle sizes of carbons at high temperature, have found no significant difference in the rate of oxidation, which suggests no diffusion limitations [39, 43]. The findings of this research at low temperature indicate that major increases in the rate of reaction and the final capacity of carbon for H_2S removal appears upon crushing the grains into smaller particles. This is an indication that particle size at low temperature is an important factor in the process. The diffusion effect, however, is steady (constant) throughout an experiment and will be reflected on the size of the mass transfer unit, initial rate of reaction, and final capacity of carbon. Hence, it will not impose a fouling effect - like sulfur deposition - on the activity of the catalyst and cannot be considered the rate-limiting-step in the unsteady state.

In this research, a rate expression is developed for the breakthrough condition (unsteady state) following the approach of Ghosh and Tollefson [43] for H_2S oxidation at 125-200 °C. Necessary modifications are enacted to account for the different conditions of the process.

4.2. Development of the Rate Expression

The following assumptions are considered for the reaction conditions and rate development:

1. The sorption of oxygen and hydrogen sulfide on the catalyst surface are the initial steps of the reaction. Oxygen undergoes bond dissociation in water phase so that each atom of oxygen occupies one site (O-X). Hydrogen sulfide dissociates in the adsorbed water layer into hydrosulfide ion (HS^-) and proton. HS^- will be adsorbed [HS^--X] while proton controls the local pH.
2. Reaction occurs between the adsorbed species of oxygen and hydrogen sulfide in the water layer inside the pores of carbon. This surface reaction is the rate-limiting-step.
3. Emission of sulfur oxides (SO_x) and elemental sulfur into the effluent is negligible. This is justified by not finding any evidence of them in the effluent in any of the experiments. Hence, the desorption of the oxidation products is negligible and all of the products of sulfur oxidation deposit on the active sites causing the deactivation of these sites (catalyst fouling).

Following the Langmuir-Hinshelwood surface reaction model [83], the following mechanism scheme, illustrated in Figure 48, is proposed for the oxidation process:

Dissociation of H_2S

$$H_2S \rightarrow HS^- + H^+ \qquad (4.1)$$

Adsorption

$$O_2 + 2\,X \rightarrow 2O\text{—}X \qquad (4.2)$$

$$HS^- + X \rightarrow HS^-\text{—}X \qquad (4.3)$$

Surface oxidation reactions

$$HS^-\text{—}X + O\text{—}X \rightarrow S\text{—}X + X + OH^- \qquad (4.4)$$

$$S—X + O—X \rightarrow SO—X + X \quad (4.5)$$

$$SO—X + O—X \rightarrow SO_2—X + X \quad (4.6)$$

$$SO_2—X + O—X \rightarrow SO_3—X + X \quad (4.7)$$

Sulfur deposition is the result of progression up to Reaction 4.4 while sulfuric acid is the result of further progression to Reaction 4.7. Reactions 4.3 to 4.7 may be summed as:

$$HS^-—X + 4O—X \rightarrow SO_3—X + 4X + OH^- \quad (4.8)$$

X represents an available site for the reactions. OH^- will be balanced by proton from Reaction 4.1. Reactions leading to 4.8 can only take place in the small micropores where high adsorption energy exists and sulfuric acid is the final product.

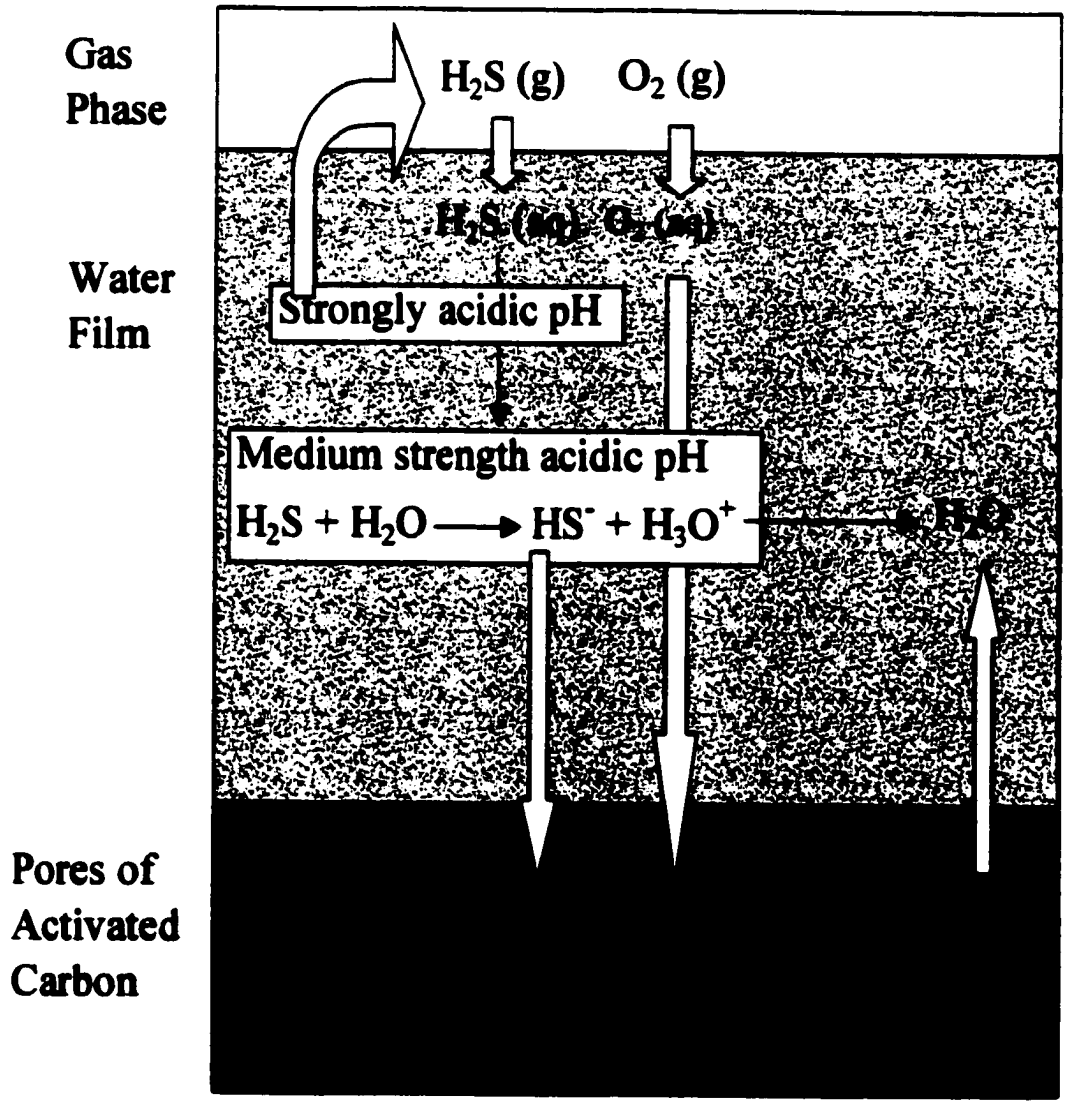

Figure 48. Schematics of the mechanism for oxidation of hydrogen sulfide on the surface of activated carbon.

An expression for the rate, R, based on Reaction 4.4 may be written as follows:

$$R = K\,[HS^{-}—X]\,[O—X] - K'\,[S—X]\,[X]\,[OH^{-}] \qquad (4.9)$$

The rate based on Reaction 4.8 may be written as:

$$R_1 = K_1\,[HS^{-}—X]\,[O—X]^4 - K_1'\,[SO_3—X]\,[X]^4[OH^{-}] \qquad (4.10)$$

K and K_1 are reaction rate constants. K' and K_1' are the reverse reaction rate constants.

It is noteworthy that progression of both surface reactions is pH dependent. According to the rate expressions a lower pH enhances the reaction rate as long as the requirement for the dissociation of hydrogen sulfide is observed. Another interesting aspect of the reactions is that formation of elemental sulfur or sulfur trioxide alone (Reactions 4.4 and 4.8) do not have a net effect on the surface pH of carbon.

Reaction 4.4 is irreversible since no evidence of its sulfur end products was found in the effluent. Based on this, it was assumed that the entire sulfur permanently deposits in the pores of carbon. It is so strongly adsorbed on the carbon surface that even upon heating of the exhausted carbons for removing adsorbed water at 120 °C for 24 hours, only negligible amount of physically adsorbed H_2S was removed. Table 6 shows that a reasonable mass balance existed in nearly all carbons between the amount of adsorbed H_2S-S and the total sulfur content of the exhausted carbons even after drying at 120 °C. Hence, we may assume that at ambient temperatures, the reverse reaction rate constant (K') is negligible and may be overlooked. The rate expression then simplifies to:

$$R = K\,[HS^{-}—X]\,[O—X] \qquad (4.11)$$

The case of Reaction 4.8 is somewhat more complicated although the reverse reaction rate constant (K_1') may be considered equal to zero for similar analysis as described above. The formation of sulfuric acid is thermodynamically irreversible but

unlike elemental sulfur, sulfuric acid is highly soluble and dissociates. The solubility and dissociation of sulfuric acid may have a double effect on the process. On the one hand it allows the formation of equilibrium between the liquid and the solid phase concentration of sulfuric acid, resulting in the transportation of some of the oxidation products to the liquid phase and therefore enhances the rate of process. On the other hand, the dissociation of sulfuric acid may strongly depress the pH below the threshold value required for H_2S dissociation. At the initial steps, when the amount of produced acid is low, the enhancing effect prevails. Upon the formation of more acid, the second effect will take over and impede the process. But the fouling of the catalyst due to sulfuric acid formation is secondary in most untreated activated carbons based on the reasons outlined earlier (Sections 3.8 and 4.1). The findings of this research indicate that elemental sulfur is the dominant product of the oxidation process (Table 6), responsible for the fouling of the catalyst. Hence, Equation 4.10 may be simplified as:

$$R_1 = K_1[HS^-—X]\,[O—X]^4 \qquad (4.12)$$

The factors [O—X], and [HS^-—X] result from Reactions 4.2 and 4.3. They represent the surface coverages due to oxygen and hydrosulfide ion and can be found from:

Pressure in influent gas phase P = K_H * concentration in adsorbed phase

$$[O—X]^2 = k\,[O_2]\,[X]^2$$

$$[O—X] = k_o^{0.5} P_o^{0.5} X = k_o^* X \qquad (4.13)$$

$$[HS^-—X] = k\,[HS^-]\,X = k_{H2S} P_{H2S} X = k_{H2S}^* X \qquad (4.14)$$

P_o and P_{H2S} are pressures of oxygen and hydrogen sulfide in the influent which are constant throughout the experiment. K_H is the heterogeneous equilibrium constant. k, k_o

and k_{H2S} are reaction equilibrium constants. k_o^* and k_{H2S}^* are constants associated with the product of k * P.

X represents the available sites, i.e. the sites yet uncovered by the products of oxidation. It may be written as:

$$X = 1 - \theta \qquad (4.15)$$

θ represents the fractional surface coverage. Hence, substituting Equations 4.13, 4.14 and 4.15 in Equations 4.11 and 4.12, more simplified expressions for rates may be written as:

$$R = K^* (1 - \theta)^2 \qquad (4.16)$$

$$R_1 = K_1^* (1 - \theta)^5 \qquad (4.17)$$

The fractional surface coverage, θ, is equal to zero at the beginning of the experiment. The rate R_0 at this time represents the maximum rate of the reaction and is equal to the constants K^* and K_1^* in Equations 4.16 and 4.17.

As described above, sulfur deposition constitutes the main fouling factor. The oxidation reaction is impeded when all of the active sites are covered with sulfur. At this situation, carbon is considered to be completely exhausted and the concentration of H_2S in the effluent is theoretically equal to that of the influent. In reality, however, owing to the fact that oxidation of H_2S in the presence of oxygen and humidity is a spontaneous process, such an effect will require an infinite time. The ultimate capacity of carbon to retain sulfur W_s^{ult}, thus, is only of theoretical value.

Hence, the values of the constants and θ in the rate expressions may be respectively substituted by R_0 and the ratio of W_s (the weight of deposited sulfur) to W_s^{ult} [43]:

$$R = R_0 \left(1 - \frac{W_s}{W_s^{ult}} \right)^2 \qquad (4.18)$$

$$R_1 = R_0 \left(1 - \frac{W_s \text{ from sulfuric acid}}{W_s^{ult} \text{ from sulfuric acid}} \right)^5 \qquad (4.19)$$

R is defined as the amount of sulfur adsorption per unit time. The rate expressions indicate that the rate is maximum at the beginning of the process and subsequently decreases according to a fouling factor associated with the deactivation of the catalyst due to deposition of oxidation products. As outlined earlier, Equation 4.18 is applicable to our results on unmodified activated carbons while Equation 4.19 can only be used where sulfuric acid is the only product of oxidation (i.e., Centaur®). Equation 4.18 may be written in a differential form as:

$$\frac{dW_s}{dt} = R_0 \left(1 - \frac{W_s}{W_s^{ult}} \right)^2 \qquad (4.20)$$

which upon integration yields [43]:

$$\frac{1}{W_s} = \frac{1}{R_0 t} + \frac{1}{W_s^{ult}} \qquad (4.21)$$

Time (t) represents the time from the beginning of the breakthrough condition. Equation 4.21 indicates that a linear relationship should exist between the reciprocal of time (t) and the reciprocal of the amount of adsorbed sulfur (W_s). The slope and the intercept of this straight line represent the values of $1/R_0$ and $1/W_s^{ult}$, respectively.

R_0 and W_s^{ult} are the characteristic values for describing the performance of a carbon under a certain condition. Once these two values are known the performance of

carbon and the shape of the breakthrough curve can be found using Equations 4.18 and 4.21.

Equation 4.19 upon integration yields the following non-linear equation that may not be used as Equation 4.21 for determination of the characteristic parameters:

$$\left(1 - \frac{W_s \text{ from sulfuric acid}}{W_s^{ult} \text{ from sulfuric acid}}\right)^{-4} = \frac{4 R_0 t}{W_s^{ult} \text{ from sulfuric acid}} + 1$$

4.3. Analysis of the Data

The ultimate test to any developed model is whether it can reasonably predict the experimental results. For this purpose series of experiments were carried out using variable weights of N, S, and W1 carbons with 900 ppm H_2S in the influent under controlled conditions outlined in Section 2.2. The weight of carbon was chosen so as to provide different conditions of the process, i. e., less than, equal to and more than the *Minimum Mass Transfer Unit (MMTU)*. MMTU is the minimum mass of carbon that can facilitate complete heterogeneous mass transfer. Consequently, breakthrough curves, with or without periods of *Zero Effluent Concentration (ZEC)* preceding the breakthrough condition, were observed. Figure 49 shows the plots of the reciprocal of time versus the reciprocal of mass of adsorbed sulfur (Equation 4.21) for two samples in each category. A perfectly linear relationship is observed in all samples. Since the model is only applicable to breakthrough condition, the latter was separated from the ZEC condition by subtracting the time and the amount of adsorption during the ZEC condition from the total amount. In this way, the beginning of the breakthrough period was considered as the

beginning of the experiment. Table 9 contains the calculated values of R_0 and Ws^{ult} from Figure 49 along with the weight of the tested carbons. It is evident that in most cases within a series, higher weight of carbon is associated with higher ultimate sulfur capacity and lower initial rate. The derived values are then used to predict the rate R using Equation 4.14. Figure 50 presents the model rate in comparison with the actual rate, which is calculated at any time using the breakthrough curve. It is evident that all carbons at the beginning of the process undergo a lag period in which the behavior of rate function is chaotic and may even sharply increase for a short time. This short period cannot be considered as part of the breakthrough condition since the latter is characterized by a decreasing rate due to gradual fouling of the catalyst. This period is actually associated with initial adsorption of the reactants and formation of intermediates. The model, hence, cannot predict the activity of carbon during this period. Good matching is observed for N carbons. As discussed in Chapter 3, this carbon was characterized by deposition of mostly elemental sulfur during adsorption (Table 6). S carbon on the other hand, contained more sulfuric acid than N. Since the amount of acid is still low, it may dissociate and release the active sites. As a result, a higher rate is observed at the initial steps of the process in S carbon. The result of a long test on S carbon confirms that the model prediction approaches the actual rate values in long run. Carbon W is characterized by a large capacity and considerable amount of elemental sulfur deposition. The model prediction is in good agreement with the actual results after the initial effect due to the presence of sulfuric acid.

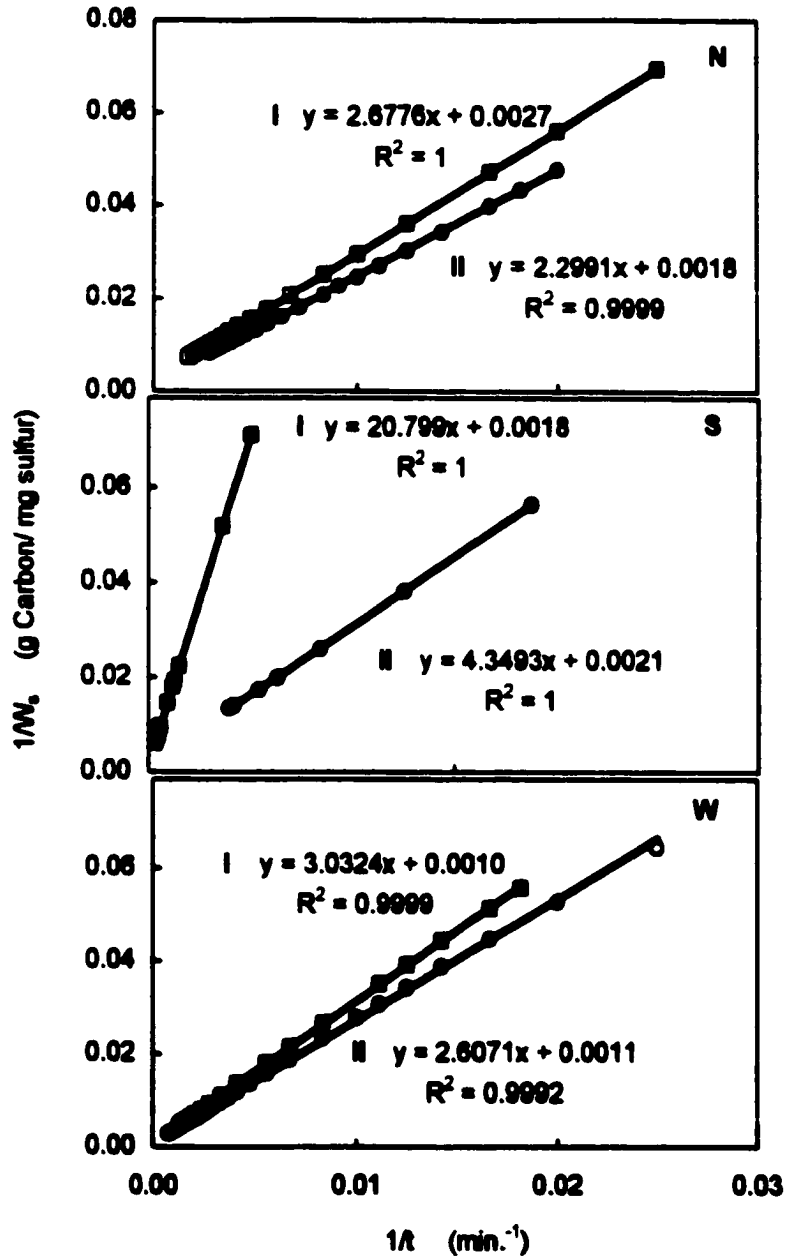

Figure 49. Plot of the reciprocals of Ws and Time (t) for determination of the Characteristic Parameters.

Table 9. Initial Rate (R_0) and Ultimate Sulfur Capacity (W_s^{ult}) of Tested Carbons

Sample	Number	Weight of Carbon g	W_s^{ult} mg/g	R_0 mg/g . min
N	I	0.3	370	0.37
	II	0.2	556	0.43
S	I	2.5	556	0.05
	II	0.5	476	0.23
W1	I	0.3	1000	0.33
	II	0.2	909	0.38

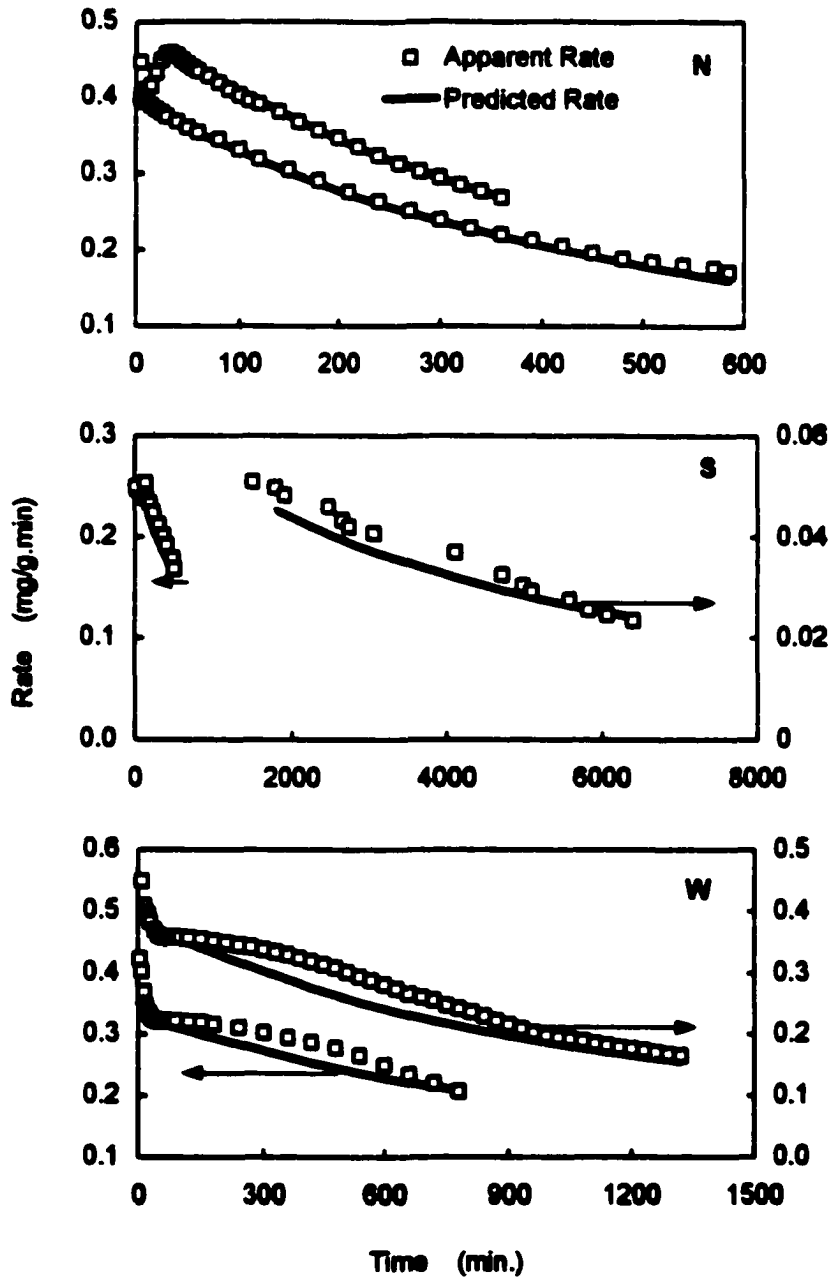

Figure 50. Comparison of the Apparent Rate and the Predicted Rate

4.4. Design of a Carbon Column

Figure 50 shows that the developed model can satisfactorily predict the performance of carbon in the breakthrough condition. But according to Figures 6-8 the breakthrough curve of a carbon sample is preceded by a long period of ZEC, to which the model may not be normally applied. To be able to design a bed for a real life performance, not only the performance during breakthrough period but also the duration of time required to reach the breakthrough under the applied flow rate and concentration is needed.

Figure 51 presents the translation pattern of the breakthrough curve within a bed of carbon under an applied concentration C_0 and flow rate Q. It shows that the breakthrough curve traverses the bed height from point O to point D beyond which actual breakthrough starts. During this time the effluent concentration at the top of the bed (point D) is steadily zero. If we hypothetically cut the bed at the cross section passing through any of the points A, B, or C at the time of the outreach of breakthrough, we will find that the concentration at those points is equal to zero. The rate R can then be calculated based on the weight of carbon participating in the process, while the rest of the carbon is still intact. Similarly, the bed could be hypothetically extended to point E to observe the same conditions despite the advent of breakthrough curve in the DE section. Using this simple analogy we conclude that despite the zero effluent concentration at the outreach points of the breakthrough curve, the actual rate is in fact decreasing owing to the increase in the weight of carbon (mass transfer unit). The apparent rate is defined as a function of the weight of carbon and is calculated from heterogeneous mass transfer as a result of adsorption:

$$R_a = \frac{\alpha\,(C_0 - C_e)\,Q\,.\,\text{Conversion for Units}}{\text{Weight of Carbon}} \qquad (4.22)$$

α is a correction factor typically ranging from 0.85 to 1.00, to account for error imposed by lag time, curve fitting, etc. It is determined empirically for the best curve fitting of the apparent and the predicted values for rate (Figure 50). The value of conversion is 1.331E-03 for concentration in ppm, flow rate in L/min, weight of carbon in grams, and rate in mg S/g C.min.

R_a in Equation 4.22 represents the mass of sulfur that is removed from air per gram of carbon per unit time whereas R in Equation 4.18 represents the mass of sulfur that deposits on the carbon per gram of carbon per unit time. Since the entire removed sulfur deposits on the carbon both values are equal at each step of the breakthrough period:

$R = R_a$

During the initial ZEC period, however, R_a is larger than R owing to smaller size of the mass transfer unit (the amount of carbon, which facilitates complete mass transfer). R remains constant throughout this period since all of the parameters of Equation 4.18 are constant during ZEC period. When C_e is set at zero, the numerator of Equation 4.22 is constant with weight of carbon more than MMTU, throughout the translation of the breakthrough curve along the bed. The denominator (weight of mass transfer unit), however, is increasing causing the apparent rate, R_a, to decrease until it equals the value of R at the beginning of the breakthrough. The two rates are equal beyond this point.

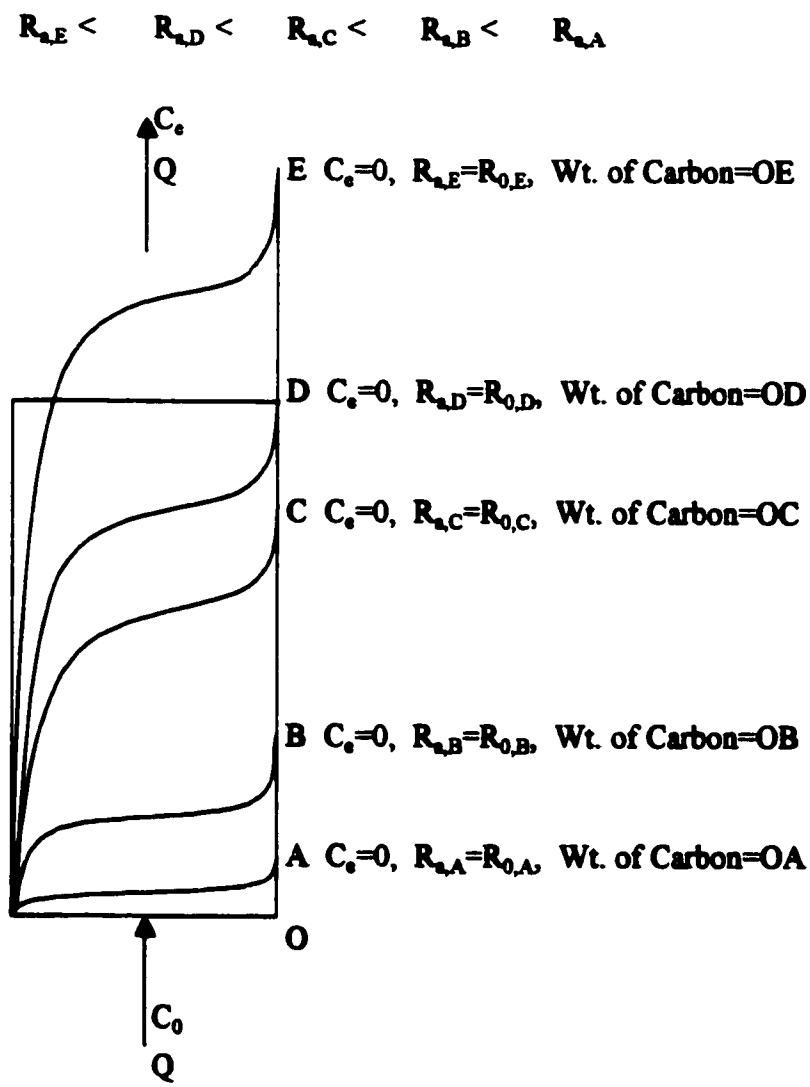

Figure 51. Movement of breakthrough curve along the bed of carbon.

Thus, what seems externally a steady state of zero effluent concentration (ZEC) is in fact unsteady (breaking through) in nature and can be conveniently analyzed by Equations 4.18 and 4.21.

Hence, the following steps can be taken to analyze the performance of an already existing bed:

1. The characteristic parameters of carbon, R_0 and W_s^{ult}, should be determined independently for the same conditions as the process, i. e., concentration, residence time, etc..
2. Since the weight of carbon is known, the value of apparent rate R_a at the beginning of breakthrough is calculated from Equation 4.22 by setting C_e at zero.
3. The apparent rate R_a is then equated with R in Equation 4.18 with R_0 and W_s^{ult} to calculate W_s at the beginning of the breakthrough.
4. W_s , R_0 and W_s^{ult} are then used in Equation 4.21 to calculate the time t required for the translational movement of the breakthrough curve to the top of the bed (time of zero concentration).
5. The performance during breakthrough period can be predicted using Equations 4.18 and 4.21 with the characteristic parameters. By arbitrarily decreasing the value of rate R, time t for each value is calculated from Equations 4.18 and 4.21 while the effluent concentration C_e is calculated using Equation 4.22 (weight of carbon is known).
6. Finally, the zero concentration time calculated in step 4 is added to the values of breakthrough time t found in step 5 and the breakthrough curve is constructed.

It is possible to substitute the expression found for W_s from Equation 4.14 into Equation 4.17 to find a direct relationship between rate R and time t.

$$\frac{1}{1-\sqrt{\frac{R}{R_0}}} = 1 + \frac{W_s^{ult}}{R_0 t}$$

Similar steps may be taken to design a bed of carbon for a certain working condition. For this purpose, initially a residence time is chosen based on the air flow rate which is then convertible (using the flow rate) to the volume and weight of carbon and can be handled as an existing bed.

The determination of the characteristic parameters, R_0 and W_s^{ult} (step 1), prior to measuring the breakthrough curve, might seem contradictory since to calculate these parameters one needs the breakthrough curve! Consequently, it will be convenient for the designer to be able to pick up these values from classified charts and curves with respect to another parameter such as residence time. These charts should be produced based on prior experiments. For this purpose, it is important to show that a reasonable relationship exists between the input parameter (i. e., residence time) and the outputs (characteristic parameters) and that the predicted performance is comparable with the actual (i. e., within acceptable error).

4.5. Preparation of the Design Charts and Determination of Minimum Mass Transfer Unit (MMTU)

According to Equation 4.18, actual rate R of the process decreases when weight of carbon increases beyond MMTU. Table 9 shows that a similar trend exists for R_0 whereas W_s^{ult}, on the contrary, increases with carbon weight. The weight of carbon is easily convertible to the volume of carbon and finally to the residence time. We may conclude that residence time is an important factor for determination of the characteristic parameters. Of course the role of other external factors (such as variations in concentration of H_2S in the influent or temperature) on the determination of characteristic parameters can not be neglected. Although these effects remain relatively constant throughout this study, their variations should be independently analyzed for in-the-field conditions.

To analyze the effect of residence time on the characteristic parameters of carbon, series of experiments were carried out using different masses of S carbon ranging from 0.05 to 2.50 g with 900 ppm H_2S in the influent under the conditions outlined in Section 2.2. The weight of carbon was chosen so as to provide condition of breakthrough curve in a mass of carbon less than or in excess of MMTU. The MMTU was determined empirically as the minimum mass of carbon that can facilitate complete removal of H_2S from air. Equation 4.14 was then used with the collected data to determine the characteristic parameters R_0 and W_s^{ult} in each case as outlined in Section 4.3. Table 10 shows, in each case, the values of these parameters with the weight, residence time, and the apparent rate for total removal calculated from Equation 4.18.

Table 10. Weight, Residence Time, Apparent Rate, and Characteristic Parameters (R_0 and W_s^{ult}) of Tested S Carbons

Sample	Weight	Residence Time*	R_0	W_s^{ult}	Apparent R**
	g	seconds	mg /g . min	mg /g	mg /g . min
1	0.05	0.06	0.944	43	2.300
2	0.10	0.12	0.652	128	1.150
3	0.50	0.60	0.199	159	0.230
4	0.75	0.90	0.145	286	0.153
5	1.00	1.20	0.126	345	0.115
6	1.50	1.80	0.083	389	0.077
7	2.00	2.40	0.067	472	0.058
8	2.50	3.00	0.050	532	0.046

* Flow rate = 0.1 L/min, density of carbon = 0.50 g/cm^3.

** At zero effluent concentration, $\alpha = 0.96$.

The weights of carbon were chosen so that the provided residence times are in the vicinity of the values used in the odor removal facilities of wastewater treatment plants (about 3 seconds). According to Table 10, the value for W_s^{ult} increases as the weight of carbon increases whereas the value for R_0 decreases with the same.

Since the apparent rate R is a linear function of the reciprocal of weight of carbon (Equation 4.18), similar relationship could be expected for R_0. Figure 51 provides plots of $1/R_0$ and W_s^{ult} against the residence time. It is evident that a linear relationship exists with acceptable error between $1/R_0$ and the residence time (Figure 52A). According to Figure 52B, for our experimental conditions, a second order decelerating relationship exists between the value of W_s^{ult} and the residence time. This is expected since lower rates are found for longer residence times. As a result a relatively flat plateau may be observed in Figure 52B in longer residence times beyond 3 seconds. This is an indication that the 3 seconds is an optimal choice for the residence time. Beyond this point, the ultimate capacity of carbon is fairly constant. Figures 51A and 51B may be considered as design charts since with their aid the designer can conveniently determine the values of the characteristic parameters needed for the design procedure (Section 4.4) for a chosen residence time without having to run any experiment.

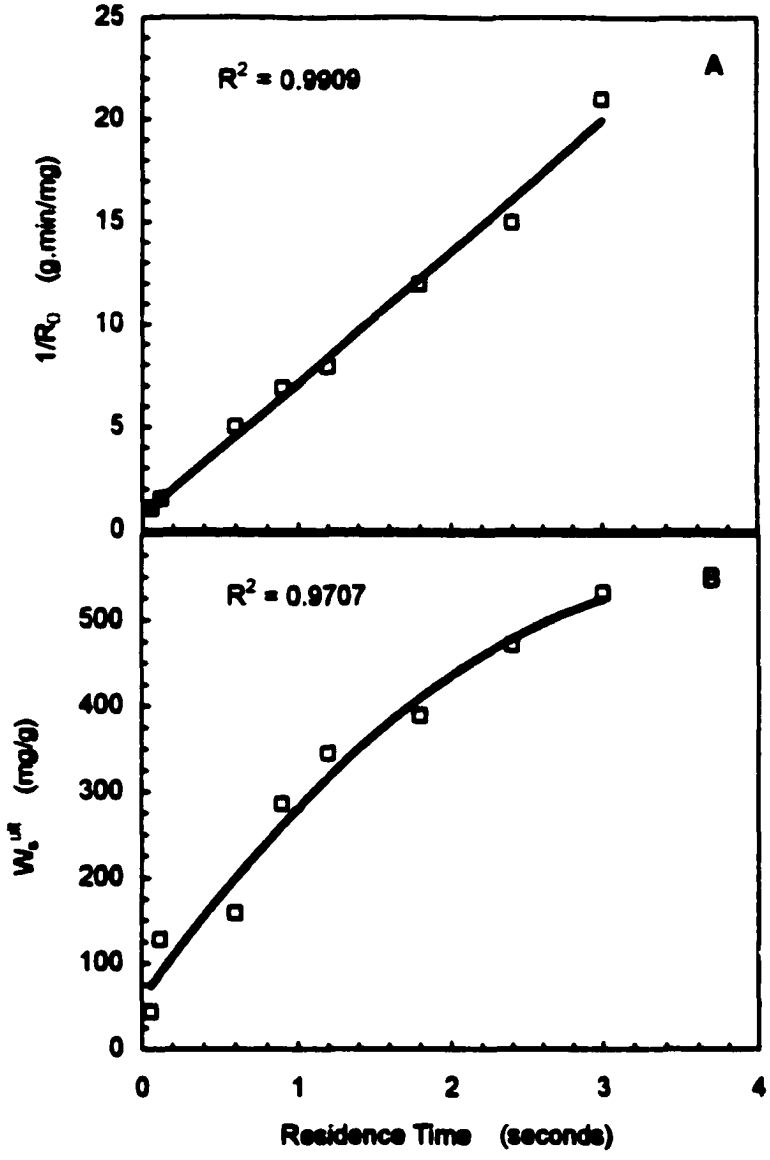

Figure 52. Change of characteristic parameters of carbon with residence time.

Before we turn our attention to the application of the model to predict the performance of carbons, we may re-examine the case of minimum mass transfer unit (MMTU). The determination of MMTU is important owing to the fact that it is the minimum mass of carbon that can facilitate complete removal of H_2S in the effluent at the beginning of the process and will immediately start the breakthrough thereafter. Since the mass of deposited sulfur is zero at the beginning of the process, the fouling term in Equation 4.17 vanishes and the rate R (for total removal) becomes equal to R_0. This only holds for MMTU since a higher mass generally starts the breakthrough with some prior sulfur deposition and a lower mass cannot facilitate total removal of H_2S. A review of the values of R_0 and R_e in Table 10 shows that R_e is much higher than R_0 in shorter residence times (1 and 2) whereas in longer times the opposite is true. The two values overlap somewhere between residence times equal to 0.90 and 1.20 seconds, closer to the former. Experimental results support this finding; at the beginning, a small concentration of H_2S breaks through the former (0.90 s) while the latter (1.20 s) shows a small period of ZEC. Figure 53 shows the plot of reciprocals of R_0 and R_e for determination of MMTU based on this analysis. The line representing $1/R_e$ in Figure 53 intersects $1/R_0$ line at the MMTU residence time equal to 1.00 seconds. Using this simple technique it is possible to easily determine the MMTU without having to carry out many random experiments.

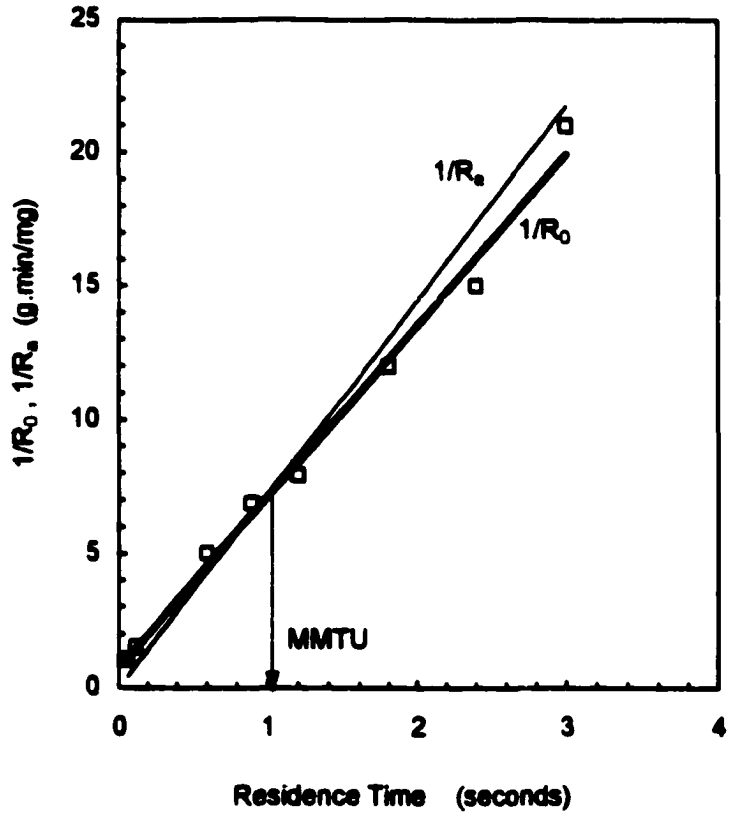

Figure 53. Determination of the Minimum Mass Transfer Unit (MMTU)

4.6. Application of the Model to Predict the Performance of Carbons (Constructing the Breakthrough Curve)

The primary aim of design is to find out when the effluent concentration of an existing bed will exceed the permitted limits. The duration time is composed of ZEC condition and breakthrough condition, which can be predicted independently using the developed method described in Section 4.2. The target concentration in this analysis was 500 ppm although permitted limits for H_2S are much lower (usually about 1 ppb).

The apparent rate and the characteristic parameters were used in Equations 4.18, 4.21 and 4.22 to predict the duration time for ZEC and breakthrough (up to 500 ppm) conditions of the process in each case according to the 6 steps outlined in Section 4.3. Tables 11 and 12 show the schematics of the spreadsheets used for calculations of the predicted and actual duration times for each condition. The values for MMTU are outputs of characteristic charts and are included in Table 11 to set the initial point.

Comparison of the actual and predicted duration times shows that despite differences, the predicted values are in good agreement with the actual values. The final step in application of the model is to construct the breakthrough curve based on the predicted duration times and concentrations. As outlined earlier (Section 4.3), for this purpose, the initial rate (R_o) is arbitrarily reduced at equal intervals to the value calculated for limit breakthrough concentration (apparent $R_{500\ ppm}$ in this study). The total time (ZEC + breakthrough) required at every step is calculated using Equations 4.18 and 4.21. $R_{500\ ppm}$ and effluent concentration at each step are calculated from Equation 4.22 with $\alpha = 1.00$. Table 13 shows the schematics of the spreadsheet used to carry out these operations for Sample 8 (Table 10).

Table 11. Determination of Duration Time for Zero Effluent Concentration (ZEC) Conditions of the Process

Sample	Residence Time	R_0	W_s^{ult}	Apparent R*	W_s/W_s^{ult}	Predicted Time	Experimental Time
	seconds	mg /g . min	mg /g	mg /g . min		min	min
1	0.06	0.944	43	2.037			
2	0.12	0.652	128	1.018			
3	0.60	0.199	159	0.204			
4	0.90	0.145	286	0.136			
MMTU	1.00	0.123	280	0.123	0.00	0	0
5	1.20	0.126	345	0.102	0.10	309	180
6	1.80	0.083	389	0.068	0.10	504	460
7	2.40	0.067	472	0.051	0.13	1021	1229
8	3.00	0.050	532	0.041	0.10	1149	1485

* At zero effluent concentration, $\alpha = 0.85$.

Table 12. Determination of Duration Time for Breakthrough Conditions* for Several S Samples

Sample	Residence Time	R_0	W_s^{ult}	Apparent R**	W_s/W_s^{ult}	Predicted Time	Experimental Time
	seconds	mg /g . min	mg /g	mg /g . min		min	min
1	0.06	0.944	43	1.065	-0.06	-3	1
2	0.12	0.652	128	0.532	0.10	21	6
3	0.60	0.199	159	0.106	0.27	293	323
4	0.90	0.145	286	0.071	0.30	847	800
5	1.20	0.126	345	0.053	0.35	1474	1410
6	1.80	0.083	389	0.035	0.35	2485	2840
7	2.40	0.067	472	0.027	0.37	4121	3828
8	3.00	0.050	532	0.021	0.35	5662	4915

* up to 500 ppm effluent concentration.

** At 500 ppm effluent concentration, $\alpha = 1.00$.

Table 13. Prediction of the Breakthrough Curve for Sample 8*

Rate mg/g.min	W_s/W_s^{ult}	Breakthrough Time min	Total Time min	H_2S Effluent Concentration ppm
$R_0 = 0.0500$	0.00	0	$T_{ZEC} = 1149$	0
0.0475	0.03	276	1425	8
0.0450	0.05	575	1724	55
0.0425	0.08	901	2050	102
0.0400	0.11	1256	2405	149
0.0375	0.13	1646	2795	196
0.0350	0.16	2077	3226	243
0.0325	0.19	2557	3706	290
0.0300	0.23	3096	4245	337
0.0275	0.26	3706	4855	383
0.0250	0.29	4407	5556	430
0.0225	0.33	5220	6369	477
$R_{500\ ppm} = 0.0213$	0.35	5661	6810	500

* Weight of carbon sample = 2.50 g, residence time = 3.00 s, $W_s^{ult} = 532$ mg/g.

Figure 54 shows the experimental and predicted breakthrough curves for Samples 7 and 8 (Table 10). A good agreement between experimental and forecast results was found for other samples where the mass of carbon was beyond MMTU. It indicates that the model can successfully predict the performance of the samples and hence, it can be used as a tool for designing purposes.

An interesting quantity collected in Tables 11 and 12 is the ratio W_s / W_s^{ult} that is calculated as an intermediate value for prediction of duration times from Equation 4.21. According to these values, beyond MMTU, carbons have shown equal values for W_s / W_s^{ult} at equal breakthrough concentrations independent of the residence time. The ratio is approximately 0.10 for zero ppm effluent concentration and 0.35 for 500 ppm. This may suggest that a more simplified model could be developed to predict the performance of a bed based on the relationship between W_s / W_s^{ult} and the effluent concentration.

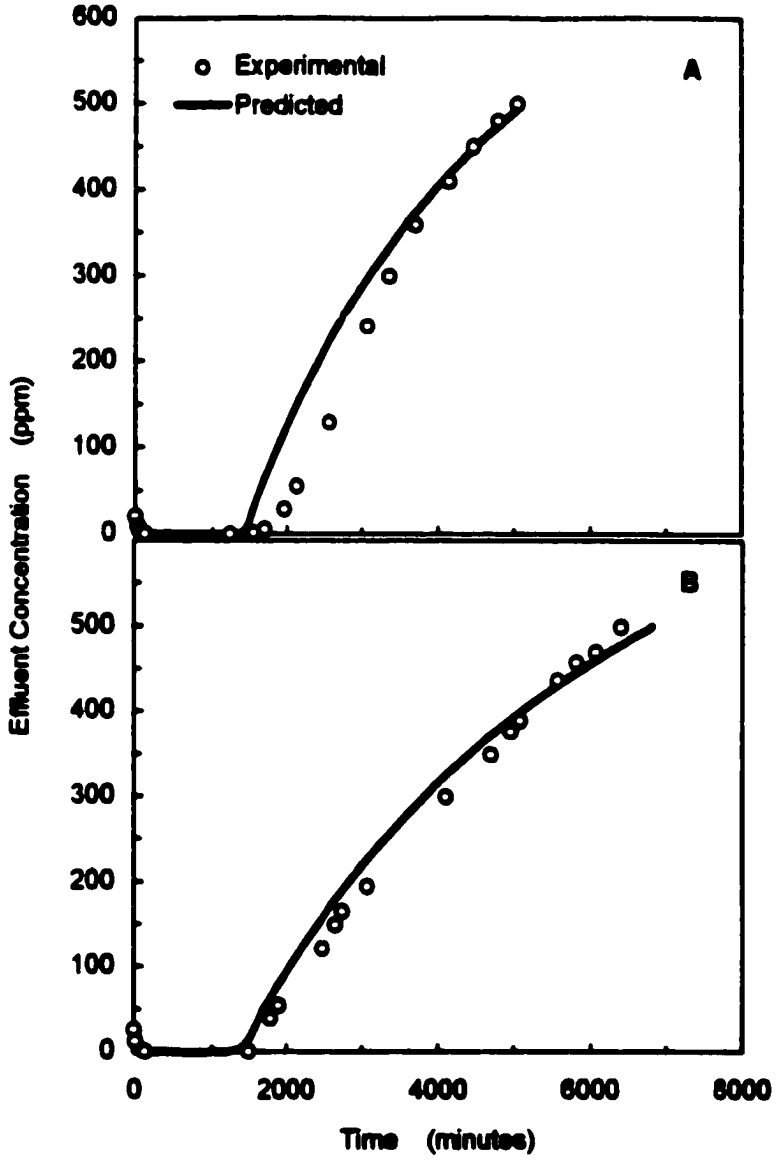

Figure 54. Experimental and Predicted breakthrough curves for Samples 7 and 8 (Table 10).

CHAPTER 5

FUTURE WORK

This research covered vast areas of scientific and engineering explorations related to the application of activated carbons for removal of H_2S. The fundamental aspects of the process were investigated and the findings were narrowed down to provide a practical, yet scientific, methodology and recommendation for analysis and design. The obtained results, however, are by no means claimed to be inclusive of every aspect of the work. Rather, they should be considered as an introduction, covering only one specific aspect of the process. Future work is necessary to bring about a comprehensive and practical insight for application of the outlined techniques. Followings are the proposed major vectors for future work. The findings of this research are mentioned in each section to provide a preliminary basis.

5.1. Conditions at Wastewater Treatment Plants (WWTPs)

Although the justification for this work is borrowed from odor removal facilities at the wastewater treatment plants (WWTP), this work is completely a laboratory-simulated research. Two major differences exist in the parameters of this work and actual field conditions.

Air streams at the WWTPs usually contain a large variety of other malodorous vapors such as mercaptans, amines and unsaturated carbonyl compounds in addition to H_2S [6]. The interaction of these compounds with H_2S oxidation is not investigated yet. It

is possible that some of these compounds will undergo similar oxidation process on the surface of carbon. The oxidized products can at least affect the surface pH which was found to be crucial. Larger molecules will be entrapped in the porous structure of carbon, affecting the pore volume available for sulfur deposition. Fortunately, results of carbon samples taken from NYC North River WWTP- where virgin carbon has been used for odor removal as a pilot project- are available and can be used for comparison. Figure 55 shows the TA results for aforementioned sample and NE and NS of this research. It suggests that similar products- in type and amount- have formed in WWTP and NE samples. This is especially noticeable for the peak around 250 °C, which is associated with sulfuric acid. The peak around 450 in WWTP is associated with elemental sulfur. This peak in laboratory samples only appears upon washing the sample (NS) as a result of polymerization of the sulfur radicals. In the WWTP sample, this same effect may result from intake of excessive moisture from the blower at the top of the preceding scrubber. In general we may conclude that H_2S oxidation pathways in the samples from laboratory simulated tests and actual field are similar and findings from the former can be extended to the latter.

Another major departure from the field conditions in simulated tests is the concentration of H_2S in the influent. Figure 2 shows that maximum ambient concentration of H_2S in a typical WWTP is in the order of 100 ppb. In simulated tests, however, due to time constraint an influent concentration in the order of 1000 ppm was used. The adopted concentration, although 10 times smaller than the recommendations for accelerated test (10000 ppm), is still much higher than the actual field values. Since the Langmuir-Hinshelwood surface reaction model [83] is based on availability of

reactants at the surface of the catalyst, extreme scarcity of one of the components will considerably affect the characteristic parameters (R_0, W_s^{ult}). To investigate the effect of concentration on these parameters, series of tests were carried out at similar conditions as kinetic studies (Section 2.2). For these tests 0.05 g of S carbon was subjected to four different concentrations of 100, 300, 600, and 900 ppm. Figure 56 shows the change in reciprocals of the characteristic parameters with influent concentration follows a straight line. The results indicate that lower concentration causes the values of characteristic parameters to markedly decrease. The finding on R_0 is in agreement with reported literature [82]. Additional work is necessary to determine the relationship between influent concentration at the field levels and characteristic parameters.

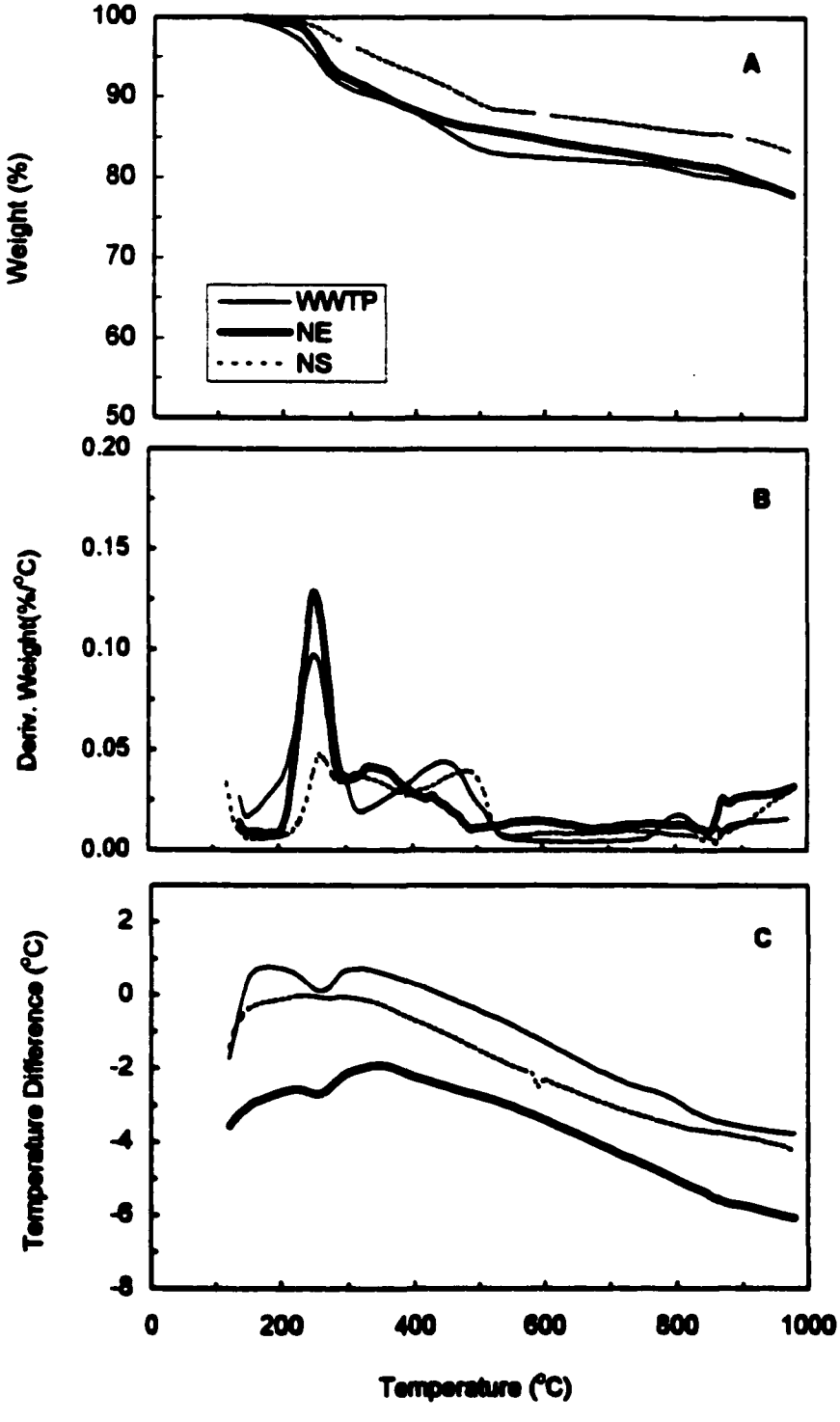

Figure 55. Thermal analysis results for NE, NS and a sample of used carbon from a wastewater treatment plant (WWTP). TG (A), DTG (B) and DTA (C).

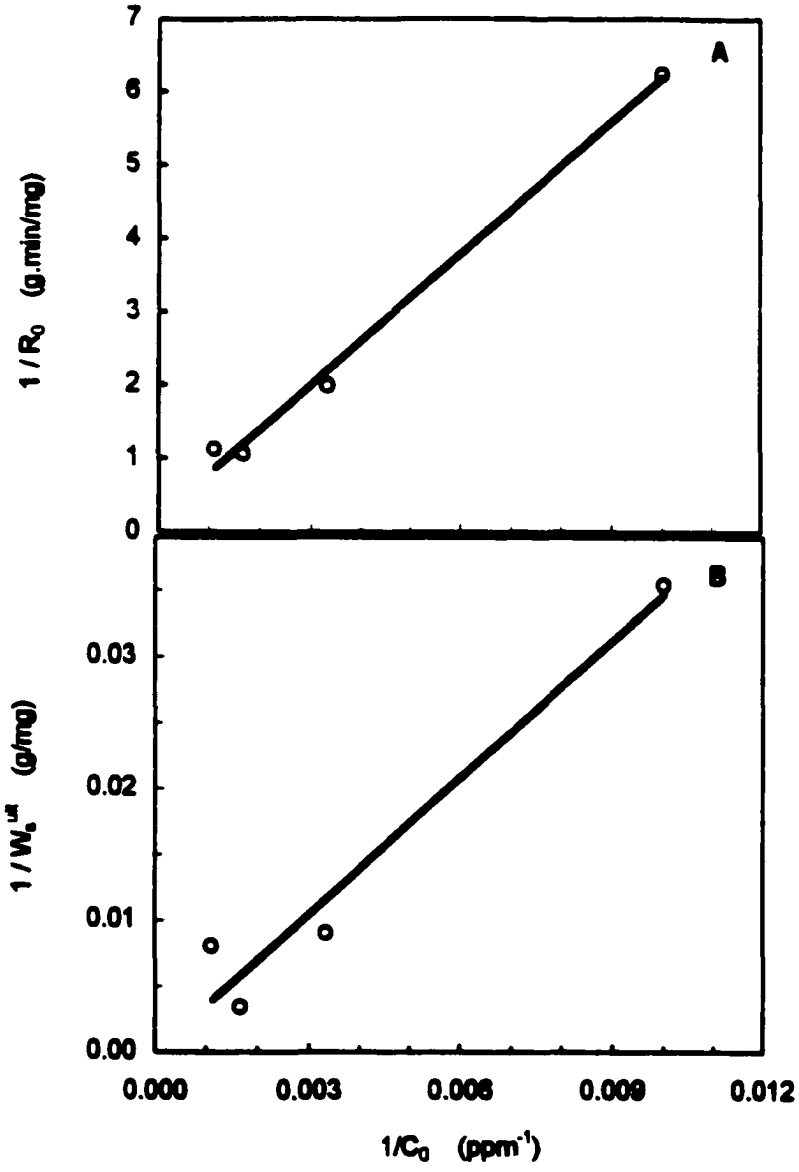

Figure 56. Changes of characteristic parameters of carbon with influent concentration.

5.2. The Role of Carbon Properties

From the standpoint of scientific analysis it would be of prime interest to conclude the performance of a carbon, not from introductory experiments to determine the characteristic parameters, but from the analysis of the surface properties of that carbon. This research provided a basis as to how the surface properties of carbons affect the adsorption/oxidation of H_2S. It was found that two most important surface properties that determine the performance of a carbon are surface pH and volume of micropores.

Series of experiments were performed under similar conditions described for concentration analysis (Sections 2.2 and 5.1) using different surface pH values while maintaining the concentration at 900 ppm. For this purpose samples of S carbon were impregnated with various amount of dilute sulfuric acid to mildly modify the surface pH. 0.05 g of each sample was ground and subjected to breakthrough test for determination of characteristic parameters. Figure 57 shows the dependence of the characteristic parameters on the surface pH. It verifies our previous findings that carbons with surface pH below 2 will demonstrate negligible capacity. The R_0 curve shows that the maximum rate occurs around pH of 4.5 whereas higher pH values observe a diminishing rate. This verifies our analysis of the role of pH on the rate of reaction (Section 4.1 and Equations 4.5 to 4.8).

Since these findings are the results of experiments on one type of carbon (S carbon), they can be observed as circumstantial and may not be directly extended to other carbons. The design criteria, however, should not be concluded from a special case and should be inclusive of all normal conditions. To investigate the general aspects of the surface properties that govern the adsorption of H_2S and are common among all of the

carbons, series of experiments were performed using a new collection of carbons. Six new carbons from different precursors in addition to the previously selected carbons (N, S, and W series = 9 carbons) were subjected to the dynamic breakthrough tests (Section 2.2). Since the initial (ZEC) H_2S removal capacity (before breakthrough starts) is a major indicator of performance of carbons, effort was made to relate the collected data with the aforementioned properties of carbons. It is reasonable to assume that initial capacity may depend on the properties in a relationship such as:

$$\text{Initial (ZEC) Capacity } W_{H2S}^{0} = K\,(pH)^{a} \cdot (\text{Volume of Micropores } V_{mic})^{b} \qquad (5.1)$$

K, a and b are constants associated with the equation constant and the order of dependence of initial capacity on each factor. Figure 58 shows the relationship between the components of Equation 5.1. Of the 15 samples used in the study, 13 showed an interesting linear correlation between the values of the initial capacity and the product of pH times the cube of the volume of micropores. Two samples fell outside the limits of the relationship and were abandoned. Both of the omitted samples possessed irregular properties not common among carbons. They were both exceptionally microporous (V_{mic} ~0.7 cm^3/g). One consisted of very fine grains, which as indicated earlier (Section 4) would undoubtedly produce large capacities owing to lowering the pore diffusion limitations. Considering the fact that the other tested carbons are random in size, shape, precursor and properties, we may conclude that in fact a linear relationship in the form of Equation 5.1 with the following constants exists between the initial capacity and the surface properties of carbon:

$$W_{H2S}^{0} = 297\,(pH \,.\, V_{mic}^{3}) - 20.5 \qquad (5.2)$$

The value of W_{H2S}^{0} can then be used to find other parameters of design. However, we still need to consider the effect of very low concentrations of H_2S in the influent since Equation 5.2 is derived at concentration equal to 900 ppm.

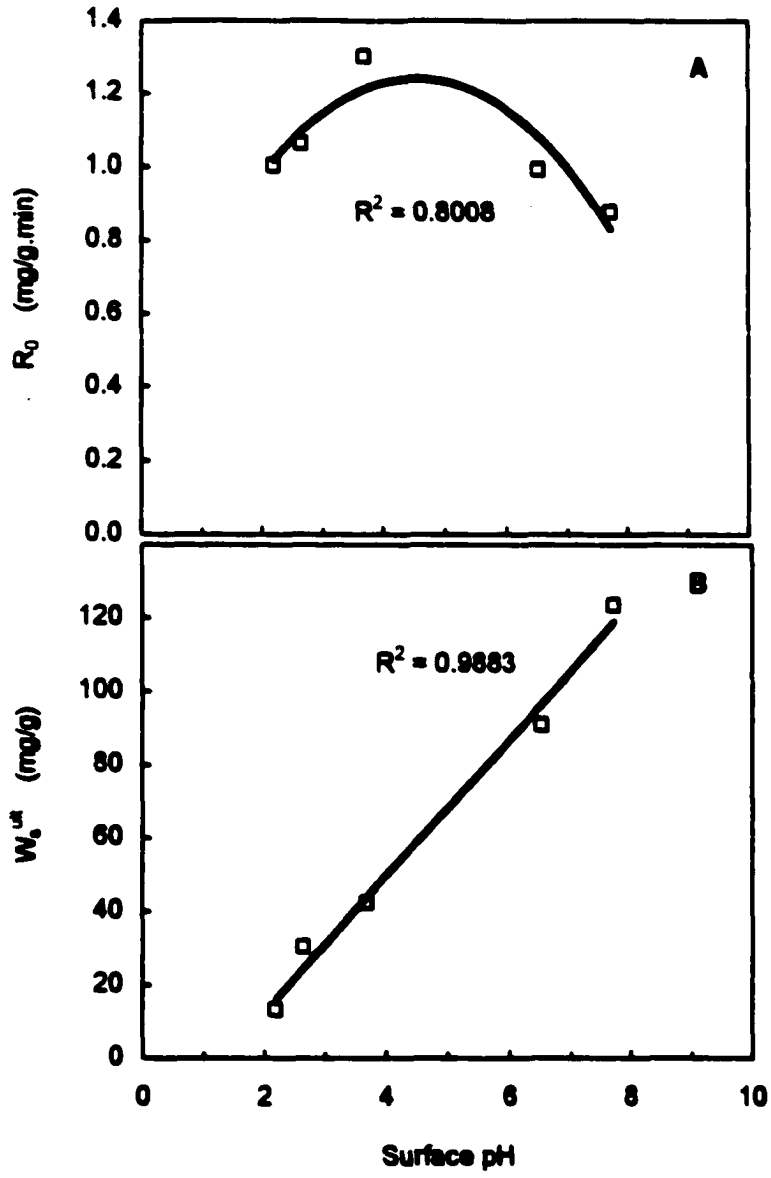

Figure 57. Changes of characteristic parameters of carbon with surface pH.

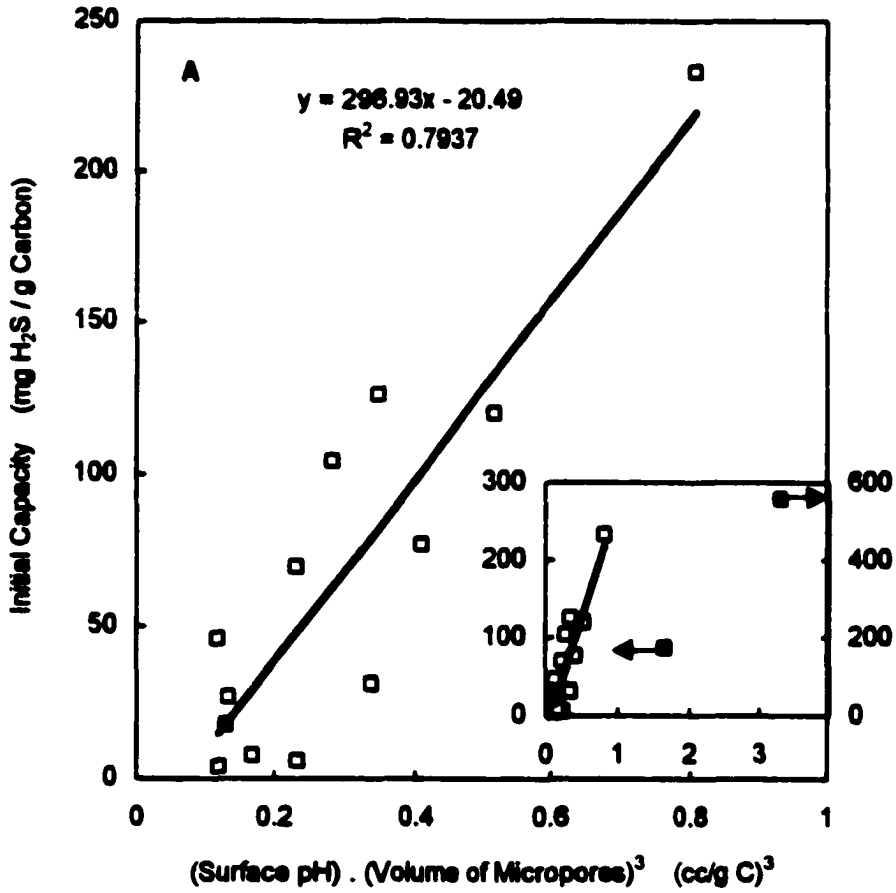

Figure 58. Changes of initial (ZEC) H_2S capacity with properties of carbon (A). The abandoned results are shown in the sub-figure (B) in solid black.

5.3. Regeneration of Exhausted Carbon

Another important area for investigation remains to be the regeneration of the exhausted carbons. In Section 3.10 it was shown that washing in Soxhlet apparatus (to represent the *in situ regeneration*) can remove considerable amount of sulfuric acid and sulfur radicals that are entrained in the pores of carbon (Figures 41-43). As a result the depressed surface pH and pore volume were largely recovered upon washing especially in oxidized samples. But the breakthrough tests on the regenerated carbons after a storage period of one year revealed small capacities for these carbons. A new measurement of the surface pH indicated much less values than those measured immediately after the regeneration process. A conclusion can be drawn that oxidation of the residual sulfur radicals during the storage period suppresses the surface pH and the H_2S removal capacity of the regenerated carbons. Although major recovery was observed in the capacity upon fresh washing of the carbons, the process may not be readily recommended since the storage time after regeneration can not be controlled. Another problem for regeneration was the deposition of polysulfides. It was found that some of the sulfur radicals can easily transform to polysulfides during washing, which are then resistant against washing and will permanently occupy some of the pore volume of carbon. This effect was common among unmodified carbons. To remedy this problem, a sample of W1E was alternatively heat-treated at 150 °C as outlined in Section 3.10 (Figure 40). Although heat-treatment removed considerable amount of sulfur radicals, the content of sulfuric acid remained intact. The removal of sulfuric acid is particularly problematic owing to its ability to form hydrogen bonding with surface functional groups.

Consequently, the regeneration of carbon with simple methods in general, and in situ regeneration in specific, remain subjects for future addressing.

CHAPTER 6

CONCLUSION

Hydrogen sulfide is one of the leading malodorants arising from sewage treatment facilities. Unmodified activated carbons (UAC) can be used to effectively remove H_2S from the air streams at the wastewater treatment plants and other odor generating facilities. Upon adsorption in pores of UAC, H_2S is immobilized through oxidation by oxygen to more stable elemental sulfur or sulfur oxides which deposit in the pores of carbon. The general mechanism for the process includes initial chemisorption of both oxygen and hydrogen sulfide on the surface of carbon and the following surface reaction between the adsorbed species.

Presence of a high level of humidity in the influent is a necessary condition for the process. Tests using relatively dry ambient air showed negligible H_2S removal by carbons. In some samples, the removal process did not develop until sufficient amount of moisture was established in the carbon through prehumidification. The removal ability disappeared shortly after cutting the influent humidity. The reactions take place in a thin film of water that can form inside the pores of carbon even at low relative pressures and serves as the reaction medium.

Surface properties of UAC including its surface chemistry and porosity play a pivotal role in the performance of a carbon as H_2S adsorbent. Among the parameters of surface chemistry, the surface pH has a dominant effect. This is owing to the fact that molecular H_2S is resistant against oxidation whereas its dissociated form, hydrosulfide

ion can be easily oxidized. Hence, for effective removal, H_2S should be dissociated upon chemisorption to hydrosulfide ion and proton. As a result, the dissociation of H_2S is a function of the surface pH of carbon. A pH value around 4.5, which is only high enough for mild dissociation of H_2S, is sufficient for its effective removal. The removal capacity will markedly decrease when the surface pH falls below this threshold value and chemisorption will eventually cease at values under 2.0.

The surface pH is a result of interaction among surface functional groups. When the density of acidic groups exceeds 1.2 $\mu eq/m^2$ the surface becomes too acidic to facilitate the dissociation of H_2S. Similar threshold values are observed in the affinity for water adsorption, UAC weight loss in 120-500 °C range, and the content of oxygen of the surface functional groups. All of these properties are closely related to the number of surface acidic groups.

Although the effect of pore structure is not as vivid as surface chemistry in the performance of carbons, the pore volume has to accommodate for the products of oxidation of H_2S. Carbons with higher pore volume, especially microporous volume, provide more removal capacity.

A common aspect among all of the exhausted carbons was their very low surface pH. A pH value measured around 2.0 is an indication that some of the sulfur is oxidized to sulfuric acid. Analysis of the exhausted carbons by various analytical methods revealed that while some sulfuric acid is produced in all of the UACs, the bulk of influent sulfur is transformed to sulfur radicals which can then form deposits of polysulfides on the surface of UAC. The selectivity of the oxidation products of H_2S is largely affected by the surface chemistry of carbon. Oxidized carbons, despite their lower capacities,

show a higher selectivity toward sulfuric acid than UACs. The effect is attributed to the electron withdrawing nature of surface oxygen. Similar effect is observed when nitrogen is incorporated into the carbon. In both cases the presence of an electron-withdrawing group (oxygen or nitrogen) induces electron deficiency in the adjacent carbon atoms. These electron deficient sites can act as primary centers for chemisorption of hydrosulfide ion in the vicinity of small micropores, which can then promote their oxidation. The presence of small micropores – pores under 10 Å, where adsorption energy is high- is another important factor in such selected transformations.

The selectivity of oxidation products may be utilized in regeneration of exhausted carbons using simple techniques such as *in situ* washing. Nearly all of sulfuric acid and a lot of sulfur radical content can be removed by washing at ambient temperature. Oxidized carbons provide a benefit of oxidation-during-washing of the sulfur radicals whereas UACs generally give way to the formation of bulky insoluble polysulfides. The latter will permanently deposit in the pores and can not be removed by simple methods.

A rate expression is provided primarily for the breakthrough condition of the process based on the Langmuir-Hinshelwood surface reaction model. The adsorption/oxidation process is considered irreversible based on the findings. Hence, sulfur deposition is introduced to the rate expression as the fouling factor and an expression is derived based on the initial rate of the reaction and the square of available sites. The model can effectively predict the value of falling rate at each stage of the reaction. Since sulfur deposition is the only fouling agent of the process the coverage may be substituted by the ratio of the deposited sulfur at any time to the ultimate capacity

of a carbon to retain sulfur. Eventually an expression is derived to relate the amount of deposited sulfur and the time.

The rate of the process is also a function of the weight of carbon. During the experiment, the breakthrough curve will travel along the carbon bed increasing the amount of carbon that is involved in the process. Thus, the initial zero concentration period of the reaction is in essence an unsteady process due to the diminishing value for rate. Consequently, the model can be confidently used to predict the performance of a carbon column in both states of the process. Although differences exist, the predicted values are in good agreement with the actual results. These findings can be used to design a bed of carbon to withstand a certain situation based on scientific and engineering analysis.

The Significance of this research is in clarification of some of the controversial issues in adsorption/oxidation of H_2S on the surface of UAC such as role of water and deposited sulfur in the process and products of oxidation. The new findings and accomplishments of this research can be summarized as:

- The significance of Surface Chemistry especially the surface pH in the performance of UAC.
- The effect of surface properties on the selectivity of the oxidation products.
- Modification of Langmuir-Hinshelwood surface reaction model to incorporate the experimental data.
- Application of the model to successfully predict the steady (ZEC) and the breakthrough condition of the process.

REFERENCES

1. Stuetz, R. M.; Fenner, R. M.; Engin, G. Assessment of Odours from Sewage Treatment Works by an Electronic Nose, H_2S Analysis and Olfactometry. *Wat. Res.* **1999**, 33, 453.

2. McGinley, C. M Sydney Water Board Tackles H_2S Odour Problems. *Water & Wastewater Intenational* **1993**, 8 (June), 13.

3. OSHA Regulations Standards - 29 CFR Standard Number: 1910.1000 TABLE Z-2, Z37.2-1966.

4. Bansal, R. C.; Donnet, J. B.; Stoeckli, F. *Active Carbon*; Marcel Dekker: New York, **1988**.

5. Leon y Leon D., Radovic, L. R. *Interfacial Chemistry and Electrochemistry of Carbon Surfaces* in Chemistry and Physics of Carbon; Marcel Dekker: New York, **1992**, 24, 213.

6. Turk, A.; Sakalis, S.; Lessuck, J.; Karamitsos, H.; Rago, O. Ammonia Injection Enhances Capacity of Activated Carbon for Hydrogen Sulfide and Methyl Mercaptan. *Environ. Sci. Technol.* **1989**, 23, 1242.

7. Turk, A.; Mahmood, K.; Mozaffari, J. Activated Carbon for Air Purification in New York City's Sewage Treatment Plants. *Wat. Sci. Tech.* **1993**, 27, 121.

8. Bandosz, T. J.; Le, Q. Evaluation of Surface Properties of Exhausted Carbons Used as H_2S Adsorbents in Sewage Treatment Plants. *Carbon* **1998**, 36, 39.

9. Matviya, T. M.; Hayden, R. A., Catalytic Carbon. *U.S. patent 5,356,849*, **1994**.

10. Bopart, S. A Comparison of Activated Carbons for the Adsorption of Sewage Odors. Published by *Norit Americas Inc.*.

11. Kaliva, A. N.; Smith, J. W. Oxidation of Low Concentration of Hydrogen Sulfide by Air on a Fixed Activated Carbon Bed. *Can. J. Chem. Eng.* **1983**, 61, 208.

12. Bandosz, T. J. Virgin Activated Carbons as Adsorbents of Hydrogen Sulfide in *Fundamentals of Adsorption 6*, Elsevier: Paris, **1998**, 635.

13. Turk, A., Sakalis, E., Rago, O., Karamitsos, H. Activated Carbon Systems for Removal of Light Gases *Annals New York Academy of Sciences* **1992**, 661, 221.

14. Adib, F.; Bagreev, A.; Bandosz, T. J. Effect of Surface Characteristics of Wood-Based Activated Carbons on Adsorption of Hydrogen Sulfide. *J. Coll. Interface Sci.* **1999**, 214, 407.

15. Adib, F.; Bagreev, A.; Bandosz, T. J. Analysis of the Relationship between H_2S Removal Capacity and Surface Properties of Unimpregnated Activated Carbons. *Environ. Sci. Technol.* **2000**, 34,686.

16. Puri, B. R. Surface Complexes on Carbon in *Chemistry and Physics of Carbon*; Marcel Dekker: New York, **1970**, 6, 191.

17. Boehm H. P. Some Aspects of the Surface Chemistry of Carbon Blacks and Other Carbons. *Carbon*, **1994**, 32,759.

18. Boehm, H. P., Chemical Identification of Surface Groups. in *Advances in Catalysis*, Academic Press: New York, **1966**, 16, 179.

19. Adib, F.; Bagreev, A.; Bandosz, T. J. Effect of pH and Surface Chemistry on the Mechanism of H_2S Removal by Activated Carbons. *J. Coll. Interface Sci.* **1999**, 216, 360.

20. Adib, F.; Bagreev, A.; Bandosz, T. J. On the Possibility of water Regeneration of Unimpregnated Activated Carbons Used as Hydrogen Sulfide Adsorbents. *J. Coll. Interface Sci.* in press.

21. Ghosh, T. K.; Tollefson, E. L. A Continuous Process for Recovery of Sulfur from Natural Gas Containing Low Concentrations of Hydrogen Sulfide. *Can. J. Chem. Eng.* **1986**, 64, 960.

22. Steijns, M.; Mars, P. The Role of Sulfur Trapped in Micropores in the Catalytic Partial Oxidation of Hydrogen Sulfide with Oxygen. *J. Catal.* **1974**, 35, 11.

23. Mikhalovsky, S. V.; Zaitsev, Y. P. Catalytic Properties of Activated Carbons I. Gas-Phase Oxidation of Hydrogen Sulfide. *Carbon* **1997**, 35, 1367.

24. Choi, J. J.; Hirai, M.; Shoda, M. Catalytic Oxidation of Hydrogen Sulfide by Air over an Activated Carbon Fiber. *Applied Catalysis A: General* **1991**, 79, 241.

25. Li, C. T. Process for Purifying Geothermal Steam. *U. S. Patent No. 4,196,183*, **1980**.

26. Klein, J., Henning, K-D. Catalytic Oxidation of Hydrogen Sulfide on Activated Carbon. *Fuel* **1984**, 63, 1064.

27. Hedden, K.; Humber, L; Rao, B. R. Adsorptive Reinigung von Schwefelwasserstoffhaltigen Abgasen. *VDI Bericht*, **1976**, 253, 37.

28. Meeyoo, V., Lee, J. H., Trimm, D. L., Cant, N. W. Hydrogen Sulfide Emission Control by Combined Adsorption and Catalytic Combustion. *Catalysis Today* **1998**, 44, 67.

29. Meeyoo, V., Trimm, D. L., Cant, N. W. Adsorption-Reaction Processes for the Removal of Hydrogen Sulphide from Gas Streams. *J. Chem. Tech. Biotechnol.* **1997**, 68, 411.

30. Grekel, H. H_2S to S by Direct Oxidation. *Oil and Gas J.* **1959**, 57 (July), 76.

31. Savage, P. R. Sulfur: 1980's Shortage or Glut? *Chem. Eng.* **1976**, 49(September).

32. Grekel, H.; Kunkel, L. V.; McGalliard, R. Package Plants for Sulfur Recovery. *Chem. Eng. Prog.* **1965**, 61(9), 70.

33. Barrer, R. M.; Whiteman, J. L. Intracrystalline Sorption of Sulphur and Phosphorous by Some Porous Crystals. *J. Chem. Soc.* **1967**, Ser. A 13.

34. Dudzik, Z.; Preston, K. F. Paramagnetism and Catalytic Activity of Sulfur-Impregnated Zeolite. *J. Colloid Interface Sci.* **1968**, 26, 374.

35. Swinarski, A.; Siedlewski, J. Effect of Pore Size on the Catalytic Power of Activated Carbon for Oxidation of Hydrogen Sulfide by Oxygen. *Annales du Genie Chemique* International Congress of Sulfur, Toulouse, **1961**, 102.

36. Sreeramamurthy, R.; Menon, P. G. Oxidation of H_2S on Active Carbon Catalyst. *J. Catal.* **1975**, 37, 287.

37. Steijns, M.; Derks, F.; Verloop, A.; Mars, P. The Mechanism of the Catalytic Oxidation of Hydrogen Sulfide.II. *J. Catal.* **1976**, 42, 87.

38. Steijns, M.; Koopman, P.; Nieuwenhuijse, B.; Mars, P. The Mechanism of the Catalytic Oxidation of Hydrogen Sulfide.III. *J. Catal.* **1976**, 42, 96.

39. Cariaso, O. C.; Walker, P. L. Oxidation of Hydrogen Sulfide over Microporous Carbons. *Carbons* **1975**, 13, 233.

40. Steijns, M.; Mars, P. Catalytic Oxidation of Hydrogen Sulfide. Influence of Pore Structure and Chemical Composition of Various Porous Substances. *Ind. Eng. Chem., Prod. Res. Dev.* 1977, 16(1), 35.

41. Coskun, I.; Tollefson, E. L. Oxidation of Low Concentrations of Hydrogen Sulfide over Activated Carbon. *Can. J. Chem. Eng.* **1980**, 58, 72.

42. Storp, K. Abluft-und Abgasentschwefelumg durch Adsorption und Katalyse an Aktivkohlen. DECHEMA-monographien. Wasser-Abfas-Abfall. Band 64, Nr. 1144-1176, Verlag Chemie GmbH, Frankfurt **1970**, 91.

43. Ghosh, T. K.; Tollefson, E. L. Kinetics and Reaction Mechanism of Hydrogen Sulfide Oxidation over Activated Carbon in the Temperature Range 125-200 °C. *Can. J. Chem. Eng.* **1986**, 64, 969.

44. Hayden, R. A. Process for Making Catalytic Carbon. *U.S. patent 5,444,031*, **1995**.

45. Brasquet, C.; Le Cloirec, P. Adsorption onto Activated Carbon Fibers: Application to Water and Air Treatments. *Carbon* **1997**, 35, 1307.

46. Hayden, R. A. Process for Regenerating Nitrogen-Treated Carbonaceous Chars Used for Hydrogen Sulfide Removal. *International patent Publication No. WO 95/26230* **1995**.

47. Lisovskii, A.; Semiat, R.; Aharoni, C. Adsorption of Sulfur Dioxide by Active Carbon Treated by Nitric Acid: I. Effect of the Treatment on Adsorption of SO_2 and Extractability of the Acid Formed. *Carbon* **1997**, 35, 1639.

48. Bandosz, T. J.; Bagreev, A.; Adib, F.; Turk, A. Unmodified versus Caustics-Impregnated Carbons for Control of Hydrogen Sulfide Emissions from Sewage Treatment Plants. *Environ. Sci. Technol.* **2000**, 34, 1069.

49. Bandosz, T. J. Effect of Pore Structure and Surface Chemistry of Virgin Activated Carbons on Removal of Hydrogen Sulfide. *Carbon* **1999**, 37, 483.

50. Bandosz, T. J.; Jagiełło, J.; Schwarz, A. Effect of Surface Chemistry on Sorption of Water and Methanol on Activated Carbons. *Langmuir* **1996**, 12, 6480.

51. Jagiełło, J. Stable Numerical Solution of the Adsorption Integral Equation Using Splines. *Langmuir* **1994**, 10, 2778.

52. Lastoskie, C. M.; Gubbins, K. E.; Quirke, N. Pore Size Distribution Analysis of Microporous Carbons: A Density Functional Theory Approach. *J. Phys. Chem.* **1993**, 97, 4786.

53. Olivier, J. P. Modeling Physical Adsorption on Porous and Nonporous Solids Using Density Functional Theory. *J. Porous Materials* **1995**, 2,9.

54. Salame, I.; Bandosz, T. J. Experimental Study of Water Adsorption on Activated Carbons. *Langmuir* **1999**, 15, 587.

55. Salame, I.; Bandosz, T. J. Study of Water Adsorption on Activated Carbons with Different Degrees of Surface Oxidation. *J. Coll. Interface Sci.* **1999**, 210, 367.

56. Papirer, E.; Dentzer, J.; Li, S; Donnet, J. B. Surface Groups on Nitric Acid Oxidized Carbon Black Samples Determined by Chemical and Thermodesorption Analyses. *Carbon* **1991**, 29, 69.

57. Jagiełło, J.; Bandosz, T. J.; Schwarz, A. Carbon Surface Characterization in Terms of its Acidity Constant Distribution. *Carbon* **1994**, 32, 1026.

58. Rodriguez-Reinoso, F.; Molina-Sabio, M.; Gonzalez, M. T. Effect of Oxygen Surface Groups on the Immersion Enthalpy of Activated Carbons in Liquids of Different Polarity. *Langmuir* **1997**, 13, 2354.

59. Otake, Y.; Jenkins, R. G. Characterization of Oxygen-Containing Surface Complexes Created on a Microporous Carbon by Air and Nitric Acid Treatment. *Carbon* **1993**, 31, 109.

60. Jagtoyen, M.; Derbyshire, F. Activated Carbon from Yellow Poplar and White Oak by H_3PO_4 Activation. *Carbon* **1998**, 36, 1083.

61. Benaddi, H.; Legras, D.; Rouzaud, J. N.; Beguin, F. Influence of the Atmosphere in the Chemical Activation of Wood by Phosphoric Acid. *Carbon* **1998**, 36, 306.

62. Dubinin, M. M.; Serpinsky, V. V. Isotherm Equation for Water Vapor Adsorption by Microporous Carbonaceous Adsorbents. *Carbon* **1981**, 19, 402.

63. Gregg, S. J.; Sing, K. S. W. *Adsorption, Surface Area, and Porosity;* Academic Press: New York, **1982**.

64. Gubbins, K. E. Theory and Simulation of Adsorption in Micropores. In *J. Fraissard (ed.)Physical Adsorption: Experiment, Theory and Applications.* Kluwer Academic Publishers, Netherlands **1997**, 65.

65. *Handbook of Chemistry and Physics*; CRC Press, 67th edition **1986-1987**.

66. Rodriguez-Mirasol, J.; Cordero, T.; Rodriguez, J. J. Effect of Oxygen on the Adsorption of SO_2 on Activated Carbon. *Extended Abstracts of 23rd Biennal Conference on Carbon, College Park, July 1997* p. 376.

67. Chang, C. H. Preparation and Characterization of Carbon-Sulfur Surface Compounds. *Carbon* **1981**, 19, 175.

68. Zumdahl, S. S. *Chemistry* Third Ed., D. C. Heath and Co., Lexington, MA, **1993**, 912.

69. Adib, F.; Bagreev, A.; Bandosz, T. J. Adsorption/Oxidation of Hydrogen Sulfide on Nitrogen Containing Activated Carbons. *Langmuir*, **2000**, 16, 1980.

70. Stohr, B.; Boehm, H. P. Enhancement of the Catalytic Activity of Activated Carbons in Oxidation Reactions by Thermal Treatment with Ammonia or Hydrogen Cyanide and Observation of a Superoxide Species as a Possible Intermediate. *Carbon*, **1991**, 29, 707.

71. Hoigne, J.; Bader, H. Ozonation of Water: Oxidation Competition Values for OH Radical Reactions in Different Types of Waters Used in Switzerland. *Ozone Sci. Engng.* **1979**, 1, 357.

72. Hoigne, J.; Bader, H. Rate Constants of Direct Reactions of Ozone with Organic and Inorganic Compounds in Water. *Wat. Res.* **1983**, 17, 185.

73. Walling, C. *Free Radicals in Solution*. Wiley: New York, **1957**.

74. Zawadzki, J. in *Chemistry and Physics of Carbon*. P.A. Thrower, Ed, Marcel Dekker: New York, Vol.21, **1989**, 21, 180.

75. Simons, W.W. *The Sandtler Handbook of Infrared Spectra*. E: Sandtler Research Laboratories, Inc., **1978**.

76. Dandekar, A.; Baker, R. T. K.; Vannice, M. A. Characterization of Activated Carbon, Graphitized Carbon Fibers and Synthetic Diamond Powder Using TPD and DRIFTS. *Carbon* **1998**, 36, 1821.

77. Biniak, S.; Szymanski, G.; Siedlewski, J.; Swiatkowski, A. The Characterization of Activated Carbons with Oxygen and Nitrogen Surface Groups. *Carbon* **1997**, 35, 1799.

78. Olivier ,J. P.; Conklin, W. B. Determination of Pore Size Distribution from Density Functional Theoretic Models of Adsorption and Condensation within Porous Solids. Presented at *The International Symposium on the Effects of Surface Heterogeneity in Adsorption and Catalysis on Solids*, Kazimierz Dolny, Poland, **1992**.

79. Repik, A. Two Stage Fluid Bed Regeneration of Spent Carbon. *U. S. Patent No. 4,248,706*, **1981**.

80. Kaneko, K.; Suzuki, T.; Fujiwara, Y; Nishikawa, K. In *Characterization of Porous Solids II* (Rodriquez-Reinoso et al. Eds.); Elsevier, Amsterdam **1991**, 389.

81. Matzner, R.; Boehm, H. P. Influence of Nitrogen Doping on the Adsorption and Reduction of Nitric Oxides by Activated Carbons. *Carbon* **1998**, 36, 1697.

82. Zhenglu, P.; Weng, H.; Han-Yu, F.; Smith, J. Kinetics of the Self-Fouling Oxidation of Hydrogen Sulfide on Activated Carbon. *AIChE J.* **1984**, 30, 1021.

83. Nix, R. Introduction to Surface Chemistry. Department of Chemistry, University of London, *www.chem.qmw.ac.uk/surface/scc/* Last updated 01/10/99.